The role of protein-tyrosine phosphatases for sensitivity and resistance of CML-cells to tyrosine-kinase inhibitors

Dissertation

zur Erlangung des akademischen Grades
„doctor rerum naturalium“ (Dr. rer. nat.)

vorgelegt dem Rat der Fakultät für Biowissenschaften
der Friedrich-Schiller-Universität Jena

von Diplom Biochemikerin Julia Drube

geboren am 23. November 1982 in Trier

Tag der öffentlichen Verteidigung

29.05.2018

Gutachter

1. apl. Prof. Dr. Frank-Dietmar Böhmer (Jena, Deutschland)
2. PD Dr. Christian Kosan (Jena, Deutschland)
3. Prof. Dr. Wiljan J. A. J. Hendriks (Nijmegen, Niederlande)

Zusammenfassung

Die Chronisch myeloische Leukämie (CML) ist eine Krankheit des hämatopoetischen Systems, welche durch die Expression von BCR-ABL1 ausgelöst wird. Dieses Onkoprotein ist eine konstitutiv aktive Protein-Tyrosinkinase (PTK), welche in Zellen Signalwege anschaltet, die unkontrolliertes Wachstum und Überleben steuern. Aus diesem Grund kann die CML mit spezifischen Tyrosinkinase-Inhibitoren (TKI) behandelt werden, die die Funktion von BCR-ABL1 hemmen. Imatinib, der erste TKI der in der Klinik Anwendung fand, hat die Therapie der CML revolutioniert: Die Patienten hatten gute Ansprechraten und viele ein gutes Langzeitüberleben mit vergleichsweise wenig Nebenwirkungen. Die Einführung von Nilotinib, eines noch potenteren Zweit-Generationen-TKI führte zu einem weiter verbesserten Wirkprofil mit schnellerem und tieferem Ansprechen. Ein Teil der Patienten wird voraussichtlich die Therapie absetzen können und trotzdem in therapiefreier Remission bleiben. Gegenstand aktueller klinischen Studien ist die Optimierung der Therapie und die genauere Untersuchung der Voraussetzungen für ein erfolgreiches Absetzen der TKI. Es ist bereits bekannt, dass ein besonders schnelles Erreichen einer anhaltenden, tiefen molekularen Remission sich günstig auf eine funktionelle Heilung auswirkt. Aus diesem Grund ist es von großem Interesse, die molekularen Mechanismen besser zu verstehen, welche das Erreichen der tiefen molekularen Remission beeinflussen.

Protein-Tyrosinphosphatasen (PTPs) sind die Gegenspieler der PTK, indem sie Phosphotyrosin-Reste hydrolysieren. Auch BCR-ABL1 wird durch PTPs reguliert. Entspechend können PTPs auch das Ansprechen auf TKI beeinflussen. Der Beitrag einzelner PTPs, insbesondere bei einer Therapie mit TKI der zweiten Generation, ist jedoch noch nicht bekannt, und sollte in dieser Arbeit untersucht werden.

Im ersten Teil der vorliegenden Arbeit wurde eine qRT-PCR Plattform etabliert und das mRNA-Expressionsniveau von 38 ausgewählten PTPs im peripheren Blut von 66 neu diagnostizierten CML Patienten bestimmt. Diese Expressionsspiegel wurden dann mit dem individuellen Nilotinib-Ansprechen der einzelnen Patienten korreliert. Dies erfolgte anhand von Daten, die in der regelmäßigen Kontrolle des Therapieverlaufs auf molekularer Ebene erhalten wurden: Die Menge an *BCR-ABL1* Gentranskript wird bestimmt und bezugnehmend auf eine „Internationale Skala“ (*BCR-ABL1*^{IS}) angegeben. Das Erreichen, oder Nicht-Erreichen der tiefen molekularen Remission (MR^4, *BCR-ABL1*^{IS} ≤ 0.01 %) nach 9 Monaten Nilotinib-Behandlung wurde mit dem individuellen Expressionsspiegel der PTPs verglichen. Patienten mit einem hohen Expressionsniveau von PTPRA, PTPRC, PTPRG, PTPRM und PTPN13 zu Beginn der Therapie hatten eine signifikant höhere Wahrscheinlichkeit, nach 9 Monaten eine MR^4 zu erreichen. Dies legte nahe, dass diese PTPs die Sensitivität der TKI Behandlung

positiv beeinflussen könnten. Aus diesem Grund, wurden im zweiten Teil der Arbeit ausgewählte PTPs, PTPRC und PTPRG, weiter in funktionellen Analysen untersucht. Zusätzlich haben wir auch PTPN6 tiefergehend untersucht, da für diese PTP bereits beschrieben wurde, dass sie die Empfindlichkeit für Imatinib beeinflussen kann. Es wurden Zelllinien hergestellt, in denen der PTP Expressionsspiegel durch Überexpression oder CRISRP/Cas9 vermittelten *„Knockout* (KO)" verändert wurde. Diese Zellen wurden zur Bestimmung des IC_{50} von Nilotinib, Imatinib und Dasatinib, eines weiteren Zweit-Generationen-TKI, genutzt. Für PTPN6 konnten wir weder durch Überexpression, noch durch KO eine nennenswerte Änderung des IC_{50} aller drei TKIs feststellen. Unsere Daten sprechen deutlich gegen einen, früher von anderen vorgeschlagenen, Einfluss von PTPN6 auf die TKI-Wirkung. Der KO von PTPRC und die Überexpression von PTPRG jedoch führten zu signifikante Änderungen im IC_{50} für die Inhibitoren Nilotinib und Imatinib. Für Dasatinib war der IC_{50} durch die Änderung der PTP-Spiegel jedoch zumeist nicht signifikant verändert.

Im dritten Teil der Arbeit wurden die molekularen Mechanismen der PTP-Wirkung weiter analysiert. Wir untersuchten zunächst den Einfluss der PTPs auf die BCR-ABL1-vermittelte Zell-Transformation mit Hilfe von Koloniebildungs-Experimenten. Die Bildung von Kolonien wurde durch den KO von PTPRC sowie die Überexpression von PTPRG signifikant reduziert. Diese Befunde identifizierten PTPRC als potenziellen Verstärker und PTPRG als hemmenden Faktor der Transformation durch BCR-ABL1. Die Analyse verschiedener Signalwege zeigte Gemeinsamkeiten zwischen der Änderung durch die Nilotinib Behandlung einerseits und dem KO von PTPRC, beziehungsweise der Überexpression von PTPRG andererseits. Wir beobachteten eine gleichsinnige verminderte Aktivierung von Kinasen der SRC-Familie (SFKs) und eine Erhöhung der Spiegel des Zellzyklus-Inhibitors p27. Es ist wahrscheinlich, dass diese beiden Signalwege an der Verminderung der TKI-Empfindlichkeit sowie der BCR-ABL1 vermittelten Transformation beteiligt sind. Konsistent mit einer Bedeutung dieser veränderten Signalereignisse, wurde die Sensitivität gegenüber dem dualen BCR-ABL1/SFK-Inhibitor Dasatinib durch PTPRC und PTPRG wenig beeinflusst. Weiterhin konnte eine Kombinations-Behandlung von Nilotinib mit dem Phosphoinositid-3-Kinase-Inhibitor Idelalisib, welcher einen Anstieg von p27 in den behandelten Zellen hervorruft, die Wirkung von Nilotinib verstärken.

Zusammengefasst konnte gezeigt werden, dass PTPs, im besonderen PTPRC und PTPRG, einen Beitrag zum Behandlungs-Erfolg auch in Nilotinib-behandelten Patienten leisten. Die Befunde zum Wirkungsmechanismus könnten genutzt werden, um die Therapie weiter zu verbessern. PTPs sollten weiterhin als mögliche prognostische Marker für das Therapieansprechen evaluiert werden.

Summary

Chronic myeloid leukemia (CML) is a disease of the hematopoietic system, caused by the expression of the constitutively active oncogenic fusion protein-tyrosine kinase (PTK) BCR-ABL1. This kinase triggers signaling cascades that lead to uncontrolled cell proliferation and survival. Therefore, treatment of CML is possible with specific tyrosine-kinase inhibitors (TKIs) targeting BCR-ABL1. Imatinib, the first TKI introduced in the clinic, has revolutionized CML therapy with excellent efficiency and long-term survival of responders with only little side-effects. The recent introduction of the more potent second-generation TKIs has led to even better therapeutic efficiency with faster and more complete responses, allowing some patients to stop treatment and remain in treatment-free remission. The optimization of the treatment regimens and the specific prerequisites to successfully stop treatment are currently addressed in several clinical studies. It is already known, that a fast and sustained deep molecular response is beneficial to achieve a functional cure. Therefore, molecular mechanisms promoting or delaying achievement of this state are of great interest and clinical relevance.

Protein-tyrosine phosphatases (PTPs) are counter-acting the activity of PTKs by hydrolyzing phospho-tyrosines. By antagonizing the activity of the oncogenic PTK BCR-ABL1, PTPs may have an effect on TKI sensitivity and treatment response. The potential impact of specific PTPs on therapeutic response in CML patients treated with second-generation TKIs is currently unknown but may be clinically relevant. This issue was therefore addressed in the current thesis.

In the first part of the thesis, we attempted to correlate the individual treatment response with the PTP-status in CML cells before the beginning of treatment. To this end, the mRNA expression levels of 38 selected PTPs were determined in total peripheral blood leukocytes in 66 newly diagnosed CML patients using a qRT-PCR platform that was newly developed in this project. The molecular response of the patients was regularly assessed during clinical monitoring by determination of *BCR-ABL1* transcript levels that are reported on an international scale (*BCR-ABL1*^{IS}). PTP mRNA-levels at the beginning of treatment were then correlated to whether or not the patient had reached a deep molecular response (MR^4, *BCR-ABL1*^{IS} ≤ 0.01 %) after 9 months of nilotinib treatment. We found mRNA expression of PTPRA, PTPRC, PTPRG, PTPRM, and PTPN13 to be positively associated with a particularly good nilotinib treatment outcome. This finding indicated that these PTPs may affect TKI-sensitivity at the cellular level. Therefore, in the second part of this thesis, PTPRC and PTPRG were selected for further functional analyses in cell line models. In addition, PTPN6, a PTP earlier reported as affecting imatinib treatment response, was included, although its expression was not found correlated with response in our patient dataset.

CRISPR/Cas9-mediated gene knockout (KO) or PTP over-expression were used to manipulate PTP expression levels in CML cell lines, and the impact on TKI response was measured by determination of potential changes of the IC_{50}s for nilotinib, imatinib, and another second-generation inhibitor, dasatinib. In case of PTPN6, neither gene KO nor over-expression led to substantial changes in the IC_{50}s of all tested TKIs, disproving a role of PTPN6 for the therapy response at least under our experimental conditions. In contrast, PTPRC and PTPRG had effects on TKI responses. A KO of PTPRC or the over-expression of PTPRG caused a significant reduction of the IC_{50}s for nilotinib and imatinib whereas the IC_{50} for dasatinib was not significantly affected.

In the third part of the thesis, the mechanisms potentially involved in the altered TKI responses in cells with genetically modified PTP levels were addressed. First, effects on BCR-ABL1 driven cell transformation were measured by analyzing colony forming capacity of the cell lines in methylcellulose. Indeed, both PTPRC and PTPRG had an impact. The colony-forming capacity was significantly reduced in PTPRC-KO cells as well as in PTPRG over-expressing cells, suggesting PTPRC as promoting, and PTPRG as attenuating BCR-ABL1 dependent transformation, respectively. Assessment of BCR-ABL1 signaling in immunoblotting experiments revealed common alterations in nilotinib-treated cells, and cells with PTPRC-KO or PTPRG over-expression. These comprised a reduction of SRC-family kinase (SFK)-activity and an elevation of the cell cycle inhibitor p27. It is possible that both events contribute to the observed phenotypes, namely promotion of TKI responses and attenuation of BCR-ABL1-mediated transformation. Consistent with this interpretation, altered PTPRC or PTPRG levels had little effect on response to dasatinib, a dual BCR-ABL1/SFK inhibitor. Moreover, co-treatment of cells with TKI and idelalisib, a phosphoinositide 3-kinase inhibitor which promotes p27 accumulation, showed enhanced efficiency.

Taken together, work presented in this thesis has shown that PTPs, especially PTPRC and PTPRG, contribute to treatment response to the second-generation TKI nilotinib, and that the knowledge of the mechanistic background may help to optimize therapeutic strategies. Expression of PTPs identified to be correlated with response may also be explored as possible prognostic markers in the future.

Inhaltsverzeichnis

1 Introduction

1.1 Chronic myeloid leukemia

Chronic myeloid leukemia (CML) is a malignant disease based on an aberrant clonal proliferation of hematopoietic stem cells (HSCs). It is characterized by an elevated level of cells of the myeloid differentiation line, mainly granulocytes and their precursors. Main symptoms of the disease are fatigue, anemia, splenomegaly, abdominal discomfort, and episodes of infections, but patients may also be asymptomatic. The disease is often discovered during routine checkups or unrelated medical examinations. The CML progresses in three phases: chronic phase (CP), accelerated phase (AP), and blast crisis (BC), with the latter appearing similar to an acute leukemia.

The first treatments were purely palliative, using arsenic (first reported in 1865), splenic irradiation, the cytostatic agents busulfan and hydroxyurea (HU), or combinations of different chemotherapeutics. It took more than one century to introduce the first curative therapy, the stem cell transplantation. In addition to that, the cytokine interferon-α (IFN-α), HU, the anti-metabolite cytarabine, or combinations of them were used as life-prolonging therapies (Hehlmann, 2005). Today, drugs are available that specifically target the molecular cause of CML: the BCR-ABL1 oncoprotein.

1.1.1 The Philadelphia chromosome and BCR-ABL1

A chromosomal abnormality associated with “chronic granulocytic leukemia” (a different name for CML) was first described by Peter C. Nowell and David A. Hungerford in 1960 (Nowell & Hungerford, 1960a; Nowell & Hungerford, 1960b) which was later named “Philadelphia Chromosome” after the city in which both scientists had made this observation. It took until 1973, when Janet D. Rowley identified this abnormality to be the consequence of a reciprocal chromosomal translocation, today referred to as t(9;22)(q34;q11). It is the fusion product of a shortened chromosome 22 and a part of the q-arm of chromosome 9 (Figure 1-1, A)(Rowley, 1973).

In 1982, de Klein *et al.* found ABL1 *(Abelson Murine Leukemia Viral Oncogene Homolog 1)* to be translocated from chromosome 9 to chromosome 22 (de Klein, 1982), and in 1984, Groffen *et al.* described the 5’ DNA region to which a major part of the *ABL1* gene is fused as the breakpoint cluster region (*BCR*). This designation was chosen because they found different breakpoints in individual patient samples (Groffen,

1984). Later on, the fusion protein encoded by *BCR* and *ABL1*, *BCR-ABL1*, was identified as a constitutively active tyrosine kinase (Naldini, 1986).

Not only the exact breakpoints of *BCR* but also those of the *ABL1* gene are variable, with the *ABL1* sequence usually breaking between exon 1 and 2, ("a2") and in rare cases between exon 2 and 3 ("a3"). The *BCR* breakpoints are more variable and can be categorized in *M-BCR* (major), *m-BCR* (minor), *μ-BCR* (micro), and *v-BCR* (nano) (Figure 1-1, B). The transcripts are named after the last exons of both genes that are included in the transcript. The most prevalent CML-associated transcripts are e13a2 (also named "b2a2") and e14a2 ("b3a2") (Figure 1-1, B). These transcripts encode proteins that have a molecular mass of about 210 kDa (p210). The protein encoded by the transcript e1a2 is a 190 kDa protein, associated with Philadelphia positive ALL (acute lymphoblastic leukemia), a distinct disease with features different to that of CML.

In the normal ABL1 protein, the N-terminus gets myristoylated. The myristoyl-moiety folds into a myristoyl-binding pocket close to the ABL1 C-terminus. This leads to an inactive kinase conformation and thereby autoinhibition of the ABL1-tyrosine kinase activity. In the BCR-ABL1 protein the N-terminus of ABL1 is replaced by the bulky BCR and consequently lacks myristoylation. Therefore the kinase cannot be autoinhibited and is constitutively active (Hantschel, 2003). This activity leads to transformation of cells: It causes growth factor-independent proliferation, and inhibits apoptosis. Expression of BCR-ABL1 in HSCs used for reconstitution of mouse bone marrow is sufficient to cause a CML-like phenotype, indicating that expression of BCR-ABL1 is the only lesion required for CML (Daley, 1990).

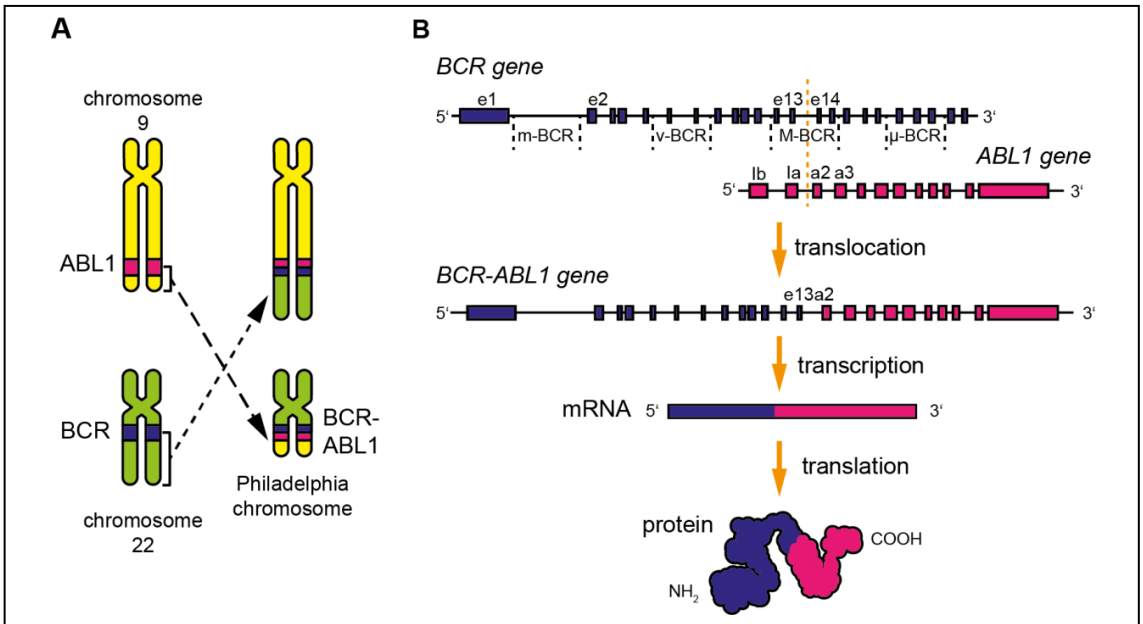

Figure 1-1. (**A**) Overview of the 9;22 translocation leading to formation of the Philadelphia chromosome. (**B**) Scheme of the *BCR* and the *ABL1* genes and the exemplary translocation leading to the e13a2 ("b2a2") transcript, and expression of the respective protein with the N-terminal BCR and the C-terminal ABL1 part. Figure layout adapted from "Grundkurs Hämatologie" (Hoffbrand, 2002), gene structures adapted from (Burmeister & Reinhardt, 2008), and BCR-ABL1 protein domain structure adapted from (Reckel, 2017).

1.1.2 BCR-ABL1 signaling

As indicated, the expression of BCR-ABL1 causes elevated cell proliferation, growth-factor-independent growth, and diminished apoptosis. This occurs via different signaling pathways. A simplified scheme of BCR-ABL1 signaling is provided in Figure 1-2.

BCR-ABL1 can activate the MEK (MAP- and ERK kinase) / ERK (extracellular signal-regulated kinase) pathway, via activation of membrane associated Ras / Raf molecules, leading to cell proliferation. The PI3K (phosphatidylinositol-3-kinase) / AKT (v-akt murine thymoma viral oncogene homolog, also known as PKB, protein kinase B) pathway inhibits apoptosis by regulating Bcl-2 (B-cell lymphoma 2) proteins. It also leads to phosphorylation of the cell cycle inhibitor p27 (CDKN1B, cyclin-dependent kinase inhibitor 1B, also referred to as $p27^{Kip1}$), causing its proteasomal degradation and thereby cell cycle progression (Roy & Banerjee, 2015). BCR-ABL1 can activate STAT5 (signal transducer and activator of transcription 5), either indirect via activation of Jak2 (Janus kinase 2) or SFK (SRC-family kinases) (Okutani, 2001; Weisberg, 2007; Schmidt & Wolf, 2009), or by direct phosphorylation (Hantschel, 2012). This leads to activation of STAT5 target genes, for example genes encoding anti-apoptotic proteins such as Bcl-2, promoting cell survival and proliferation. Also cytosolic SFK are

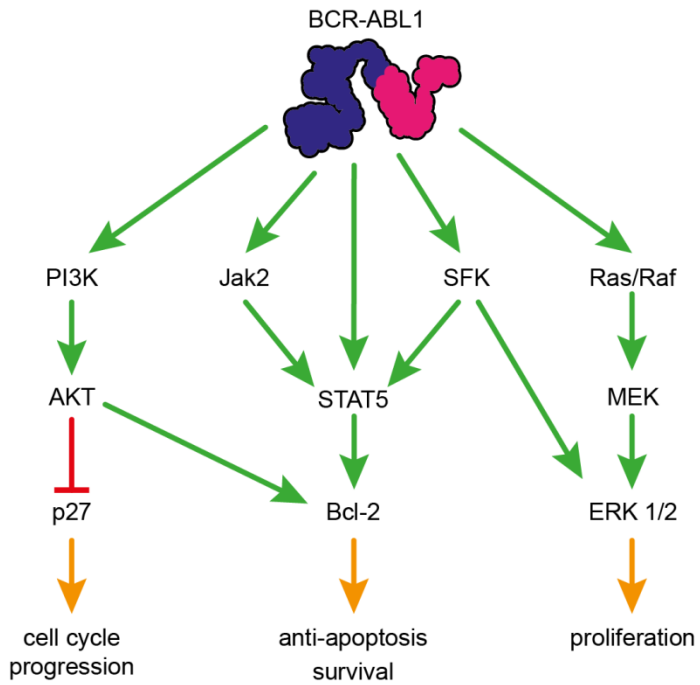

Figure 1-2. Simplified scheme of BCR-ABL1 signaling. Green arrows indicate activation, red mark indicates induction of degradation. Orange arrows show general consequences of signaling pathways. For details see text.
PI3K (phosphatidylinositol-3-kinase), AKT (v-akt murine thymoma viral oncogene homolog, also known as PKB, protein kinase B), p27 (CDKN1B, cyclin-dependent kinase inhibitor 1B, also referred to as $p27^{Kip1}$), Jak2 (Janus kinase 2), STAT5 (signal transducer and activator of transcription 5), Bcl-2 (B-cell lymphoma 2), SFK (SRC-family kinases), MEK (MAP- and ERK kinase), ERK 1/2 (extracellular signal-regulated kinase).

activated by BCR-ABL1. These kinases are involved in multiple signaling pathways promoting cell proliferation and anti-apoptotic processes (Danhauser-Riedl, 1996; Ptasznik, 2004).

Several key players that will be analyzed in some detail later in this thesis project are: ERK 1/2, STAT5, AKT, SFK, especially cSRC (cellular homologue to v-src expressed by Rous Sarcoma virus) and Lyn (Lck / Yes related novel tyrosine kinase), p27, and Bcl-2.

BCR-ABL1 was also reported to affect DNA repair response pathways, leading to accumulation of mutations and additional chromosomal alterations (Cramer, 2008) further promoting CML progression or therapy failure (see below). Many of these pathways can cross-interact with each other, building a signaling network triggered by BCR-ABL1 and resulting in the CML phenotype. In all described signaling cascades, phosphorylations of different signaling proteins by protein kinases play an important role.

The counter actors of protein-tyrosine kinases (PTKs), the protein-tyrosine phosphatases (PTPs), can de-phosphorylate target proteins of BCR-ABL1 (*e. g.* STAT5) or BCR-ABL1 itself and thereby interfere with the signaling cascades driven by the BCR-ABL1 oncogene (see chapter 1.2).

1.1.3 CML diagnostics and monitoring

The CML diagnostics are based on hematologic, cytogenetic, and molecular analyses. In the hematologic examination, peripheral blood is microscopically analyzed. The elevation of leukocytes with presence of immature precursors or even blasts can thereby be detected. To assure the CML diagnosis, cells of the bone marrow are also analyzed microscopically (criteria: higher cell density, elevation of leukocytes and their precursors, elevated levels of megakaryocytes) and with a chromosome banding or FISH (Fluorescence in situ hybridization) analysis of cell metaphases, assessing the presence of the characteristic Philadelphia chromosome or other chromosomal aberrations. In addition to these analyses, the presence and type of BCR-ABL1 transcript is determined by qualitative PCR (Polymerase-chain reaction). The knowledge of the specifically expressed BCR-ABL1 transcript is needed for correct disease monitoring under therapy. Therapy response can be observed directly in a blood or bone marrow sample, giving information on the hematologic or cytogenetic response. Once the complete cytogenetic remission (CCyR) is achieved (no Philadelphia chromosomes detectable in at least 20 analyzed bone marrow cell-metaphases), only more sensitive molecular detection methods can be used to further monitor treatment efficiency. Therefore, molecular monitoring in peripheral blood

samples after erythrocyte lysis has been established, using a standardized RT-qPCR (reverse transcription quantitative PCR) assay to determine the quantitative mRNA (messenger RNA) ratio of *BCR-ABL1* and *ABL1*. Today, this is the preferred method to monitor treatment response in CML patients since it is less invasive that bone marrow analysis and can detect even lower levels of residual disease. In the IRIS Study (International Randomized Study of Interferon and STI571 (Imatinib)), the RT-qPCR analysis was performed in 3 different laboratories, showing a high variability of results that needed to be standardized to be comparable. For this reason, the International Scale (IS) was developed, by analyzing a set of 30 individual patient samples in all three laboratories, and normalizing all subsequent results to this IRIS-baseline as "100 % *BCR-ABL1*^{IS}". This baseline is also the reference for the definitions of "major" and "deep" molecular response as outlined in Table 1-1 (Hughes, 2003).

Since the initially used 30 reference samples were limited, the use of a general laboratory-specific conversion factor was initiated. This factor is derived by regular re-analysis of 20 – 30 reference samples, and calculation of a laboratory specific conversion factor with the measured results to obtain comparable values in all different laboratories (Cross, 2015).

Evaluation of clinical trials using the *BCR-ABL1*^{IS} led to the definition of therapy milestones by the European LeukemiaNET (ELN) to give indications for optimal response, warning, or failure of treatment, according to the de- or increase of BCR-ABL1 of each individual patient under therapy (Baccarani, 2013).

Table 1-1. Stages of molecular responses to CML therapy on international scale (IS).

Response		***BCR-ABL1*^{IS}**
CML cells diagnosis		100 % *
Partial cytogenetic response	PCyR	10 % **
Complete cytogenetic response	CCyR	1 % **
Major molecular response	MMR	0.1 %
Deep molecular response	MR^{4}	0.01 %
Deep molecular response	MR$^{4.5}$	0.0032 %
Deep molecular response	MR^{5}	0.001 %
No detectable BCR-ABL1 transcripts		<0.001 %

*) 100 % is defined as the IRIS-standardized baseline (Hughes, 2003).
**) These *BCR-ABL1*^{IS} levels correspond to the indicated cytogenetic responses when measured in independent analyses.

1.1.4 Imatinib – the first targeted therapy in CML

The knowledge that the driver of CML cell proliferation, BCR-ABL1, is a constitutively active tyrosine kinase prompted the development of tyrosine-kinase inhibitors (TKIs) to specifically treat CML. The first TKI developed to target BCR-ABL1 was Imatinib (STI571, Gleevec, Novartis, Figure 1-3, A). Imatinib blocks the ATP binding-site of the ABL1 kinase by binding to the kinase in its inactive conformation. It was initially shown to effectively kill BCR-ABL1-positive cell lines and to reduce dose-dependently tumor formation of engineered 32D cells expressing BCR-ABL1 (p210) in syngenic C3H/HEJ mice (Druker, 1996).

Based on these promising preclinical findings, clinical trials started in 1998, showing the superiority of Imatinib over IFN-α treatment of CML in all clinical phases, leading to the approval by the US Food and Drug Administration (FDA) in May 2001, and shortly afterwards also in Germany (Hehlmann, 2005). Just recently, the long term analysis of the IRIS (International Randomized Study of IFN and STI571)-study has shown that the imatinib treatment-efficiency has persisted over more than 10 years, without cumulative or late toxic effects (Hochhaus, 2017). The median age of CML patients reported in this study was 50 years, with a survival rate of more than 80 % after 10-years follow up.

Despite the great success of imatinib treatment, not all CML patients benefit from treatment to the same extent. Some patients do not respond well to the TKI therapy from the beginning (primary resistance) or suffer from resistance development and disease progression under therapy (secondary resistance, relapse). There are two main scenarios leading to imatinib resistance: on the one hand, mutations in the BCR-

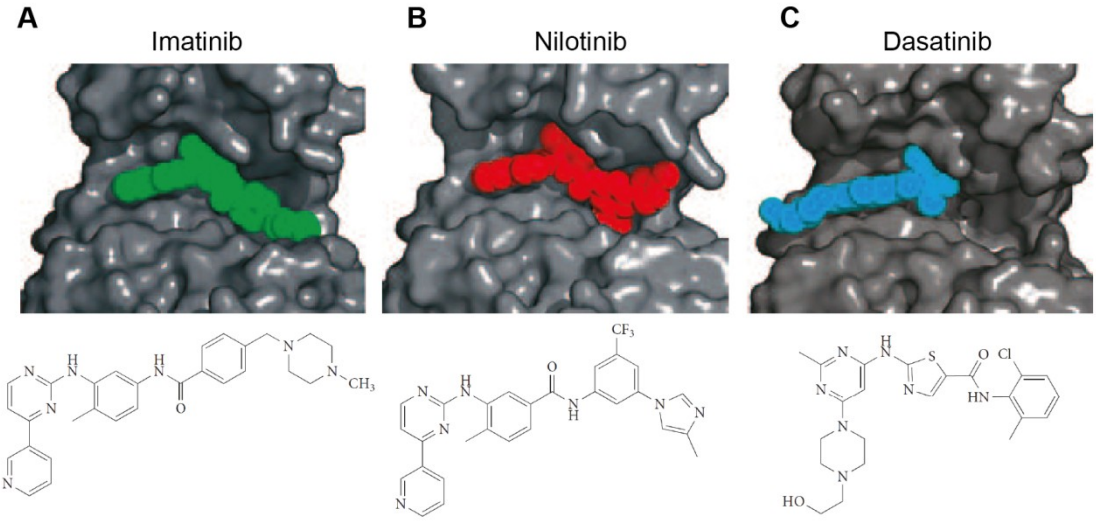

Figure 1-3. Three TKIs used in this thesis. Top: Surface representations of crystal structures of ABL1 kinase in complex with imatinib (**A**), nilotinib (**B**), or dasatinib (**C**). Residues from the nucleotide-binding loop (P-loop) and activation loop (A-loop) are omitted from the surface calculation for clarity. Below, the molecular structures of the TKIs. Adapted from (Weisberg, 2007).

ABL1 protein, leading to conformational changes that decrease the binding affinity of imatinib or destabilize the inactive conformation (*e. g.* mutations of Gly 250, Tyr 253, Met 351), or mutations that create direct steric hindrances that prevent binding of imatinib (*e. g.* Thr 315) are found. On the other hand, clonal evolution of leukemic stem cells with acquisition of additional mutations and activation of BCR-ABL1-independent pathways can lead to disease progression (Hehlmann, 2005; Weisberg, 2007).

1.1.5 Resistance mechanisms and new therapy options

As mentioned, the reasons for primary resistance or suboptimal therapy response can in some patients be directly linked to BCR-ABL1 mutations. In addition, genomic amplification or over-expression of *BCR-ABL1* can cause TKI resistance. In other patients, BCR-ABL1 independent mechanisms are the cause of refractory disease or relapse. These may involve the acquisition of additional chromosomal aberrations activating BCR-ABL1 independent signal transduction pathways, or general pharmacokinetic factors resulting in reduced drug availability (Hochhaus, 2002; Cross, 2015).

One way of overcoming BCR-ABL1-dependent resistance is the development of new drugs, targeting also imatinib resistant BCR-ABL1 mutants. Today, two more compounds are approved for first-line treatment of CML that can overcome imatinib resistance in many cases: nilotinib (AMN107, Tasigna, Novartis, Figure 1-3, B) and dasatinib (BMS-354825, Sprycel, Bristol-Myers Squibb, Figure 1-3, C). Nilotinib is a derivative of imatinib, developed by rational drug design. It is about 30-fold more potent in inhibiting ABL1 kinase, has improved specificity, and inhibits 32 of 33 mutant BCR-ABL1 forms *in vitro*, that are resistant to imatinib. Similar to imatinib, it also binds the inactive kinase conformation (Weisberg, 2007). Interestingly, formation of the inactive kinase conformation requires de-phosphorylation of BCR-ABL1. This may link the efficiency of imatinib and nilotinib to the status of PTPs, since they are responsible for the de-phosphorylation of BCR-ABL1, and thereby indirectly influence the TKI binding. Dasatinib is a highly potent inhibitor of cSRC and SFK, also targeting BCR-ABL1. It binds, in contrast to imatinib and nilotinib, to the active conformation of the ABL1 kinase. Dasatinib has been shown to inhibit 21 of 22 mutant forms, which are resistant to imatinib (Weisberg, 2007).

In addition to these first-line treatment options, the inhibitors bosutinib (AKI-606, Bosulif, Pfizer) and ponatinib (AP24534, Iclusig, Ariad Pharmaceuticals) are available as second-line treatment. Ponatinib is especially used for treatment of the Thr 315 Ile (T315I) mutation of BCR-ABL1 at any stage, since this mutation causes resistance to the four other inhibitors.

As mentioned above, wild type ABL1 kinase is autoinhibited by binding of a myristoyl-moiety to a myristoyl-pocket, inducing the formation of an inactive kinase conformation. This mechanism can be mimicked by administration of allosteric inhibitors that bind to this pocket, and induce the conformational change, leading to inhibition of the kinase. One such inhibitor is Asciminib (ABL001, Novartis). It was already tested in a phase I clinical trial, with first results published recently, showing activity in heavily pretreated CML patients (Wylie, 2017). ATP-competitive inhibitors and this allosteric inhibitor show distinct patterns of activity against BCR-ABL1 with resistance mutations, providing one more tool to overcome resistance if administered as single drug or in combination therapies.

Since more than 30 years, different CML risk scores based on clinical parameters have been established and improved to predict treatment outcome or prognosis of long-term survival by evaluating clinical parameters at diagnosis. These include the Sokal score (Sokal, 1984), Hasford score (Hasford, 1998), EUTOS score (Hasford, 2011), or ELTS score (Pfirrmann, 2016). Also, the specific BCR-ABL1 transcript expressed in the leukemic cells does have an influence on treatment response (Jain, 2016). In addition, the efficiency of the individual molecular and cytogenetic response after 3 and 6 months of TKI treatment can predict long-term progression-free and overall survival (Hanfstein, 2012; Hanfstein, 2014). Up to now, not many BCR-ABL1-independent resistance mechanisms are known (La Rosee & Deininger, 2010; Ernst & Hochhaus, 2012). To further elucidate such mechanisms, a number of genome wide expression analyses comparing well-responding to poor-responding patients were performed to identify genes and pathways potentially contributing to treatment outcome (reviewed by (Schmidt & Wolf, 2009)). These studies revealed interesting gene sets, that are associated with treatment response, but findings are inconsistent, and the types of analyzed patient samples are varying among the studies. A just recently published study presented a protein panel that was associated with molecular response of CML patients under imatinib treatment (Alaiya, 2016).

Almost all published studies on association of treatment response with gene expression so far are based on imatinib therapy. Therefore, there is a need for such studies in nilotinib-treated patients. In this thesis, I focused on the role of PTPs for nilotinib response.

1.1.6 Treatment-free remission and functional cure

For many years it was believed, that CML patients need to be treated lifelong with TKIs in order to control the disease. However, based on the continuous improvement of CML treatment and management, a newly emerged goal is to find patients eligible to stop treatment and still remain in treatment-free remission (TFR). Previous observations have suggested that this may be possible for a sub-set of patients. In 2002, some patients with undetectable disease after IFN-α treatment stopped the medication and remained in molecular remission (Mahon, 2002). In the STIM-study (Stop Imatinib), about 40 % of imatinib-treated patients stayed in TFR when treatment was stopped after 2 years of deep molecular response (Mahon, 2010). The initial studies showed that fast and durable deep molecular responses to TKI were associated with a higher probability of remaining in remission after discontinuation of TKIs. The second-generation TKI nilotinib is leading to much faster and deeper molecular remissions compared to imatinib (ENESTnd study)(Hochhaus, 2016), suggesting that a high fraction of patients may achieve a TFR. Therefore, one new study sponsored by the University of Jena, the TIGER study (Tasigna / Interferon in Germany, NCT01657604) is aiming to discontinue the TKI treatment after > 24 months of nilotinib treatment and > 12 months of MR^4 or better. In addition, the study is re-introducing the “classical” IFN-α treatment to find out, if the number of patients with a functional cure can be further enhanced by this combination treatment. The patients are randomized to either receive nilotinib alone, or nilotinib in combination with PEG-IFN-α2b (pegylated interferon α2b). All patient samples analyzed in this thesis are from participants of this study.

1.2 Protein-tyrosine phosphatases

1.2.1 The PTP families

PTPs are the counter-actors of PTKs, hydrolyzing phospho-tyrosines and thereby removing the tyrosine-phosphorylation from their target proteins. For a long time it was believed, that the PTPs are de-phosphorylating substrates constitutively with little regulation of activity, leaving the regulating part to the PTKs (Tonks, 2013). Later analyses revealed that the enzymatic activity of the PTPs is much higher than that of PTKs, causing the need to tightly regulate their catalytic activity, because otherwise no phosphorylation would occur in the cells. Indeed, the precise regulations of PTPs via many different mechanisms and their rather specific functions have meanwhile been established.

The human genome harbors 125 genes encoding the family of PTPs. The PTP proteins are determined by one of the following features: i) the presence of a PTP domain, ii) the presence of the CxxxxxR signature motif in a non-PTP domain, iii) the evidence of actual tyrosine phosphatase activity, or iiii) showing high sequence similarity to proteins with known tyrosine-phosphatase activity (Alonso & Pulido, 2016). Of these 125 proteins, only about 40 exclusively target phospho-tyrosines, while others target in addition, or exclusively *e. g.* phospho-serines, phospho-threonines, phosphatidyl-inositols, mRNA cap structures, or are even catalytically inactive (Alonso, 2004; Alonso & Pulido, 2016).

In 2004, Alonso *et al*. introduced a classification of the PTPs into 4 families according to the amino acid sequence of their catalytic domains. This classification was further adjusted in 2016, now proposing 3 main families to which the members were assigned according to their nucleophilic catalytic residue (Cys, Asp, or His) as summarized in Table 1-2. The cysteine based PTPs are the largest family (> 90 % of listed PTPs) and all 38 PTPs (chapter 3.1) analyzed in this thesis are members of this family. This large PTP family can again be sub-divided into 3 classes (Table 1-2). The class I cysteine-based PTP-family, that comprises the classical PTPs (sub-class I) and VH1-like (from vaccina virus) dual-specific PTPs (DUSPs, sub-class II). 35 of the 38 PTPs analyzed in this thesis are members of these two sub-classes (Alonso, 2004; Julien, 2011).

The class II cysteine-based PTP family has only two members, one of them is the LMW-PTP (ACP1, analyzed in this thesis). The three cell cycle regulators CDC25A, CDC25B, and CDC25C are the only members of the class III cysteine-based PTP family, with CDC25A and B being included in analyses in this thesis. Further details are outlined in Table 1-2.

Table 1-2. PTP classes (Alonso, 2004; Alonso & Pulido, 2016).

Main families				#	Sub-groups	#	Substrates
Cysteine-based	Class I	Sub-class I	Classic	37	RPTPs	20	pTyr, PIPs
					NRPTPs	17	
		Sub-class II	VH1-like	64	MKPs	11	pTyr, pSer, pThr, PIPs, other
					Atypical DSPs	20	
					Slingshots	3	
					PRLs	3	
					CDC14s	4	
					PTEN-like	8	
					MTMs	15	
		Sub-class III	SACs	5			PIPs
		Sub-class IV	PALD1	1			unknown substrate
		Sub-class V	INPP4s	2			PIPs
		Sub-class VI	TMEM55s	2			PIPs
	Class II		LMW-PTP	1			pTyr
			SSU72	1			pSer
	Class III		CDC25s	3			pTyr, pThr
Aspartate-based	HAD		EYAs	4			pTyr, pSer
Histidine-based	PGM		UBASH3s	2			pTyr
	Acid phosphatases		ACPs	3			pTyr, pSer, pThr, other

Abbreviations used: ACP (acid phosphatase), CDC (cell division cycle), DSP (dual-specific phosphatase), EYA (Eyes absent), HAD (haloacid dehalogenase), INPP (inositol polyphosphate phosphatases), LMW (Low molecular weight), MKP (MAPK phosphatases), MTM (myotubularin), NRPTP (non-receptor PTP), PALD (Paladin), PGM (phosphoglycerate mutase), PIP (phosphoinositide phosphate), PRL (Phosphatases of regenerating liver), PTEN (Phosphatase and Tensin homolog), RPTP (receptor-like phosphatase), SAC (from *Saccharomyces cerevisiae*), SSU72 (suppressors of sua7), TMEM (transmembrane protein), UBASH (ubiquitin-associated (UBA) and SRC homology 3 (SH3) domain-containing protein), VH (from vaccina virus).

1.2.2 Regulation of PTPs

As already mentioned above, PTPs are not just simple housekeeping enzymes. The regulation of PTPs occurs at different levels: by differential expression in organs, tissues, and cells, by regulation of the sub-cellular localization, and by regulation of activity at the molecular level by different mechanisms *e. g.* by posttranslational modifications.

Obviously, the differential expression can regulate the PTP function. There are PTPs which are ubiquitously expressed (*e. g.* SHP2 (PTPN11) or PTP1B (PTPN1)), and others which are selectively expressed and are induced (or silenced) upon differentiation of specific tissues, or as response to stimuli from outside of the cell. For example, the PTP DEP-1 (density enhanced phosphatase 1, PTPRJ) is up-regulated in some cell types when they reach high cell densities. In other cases, the expression of different PTP isoforms can be caused by the tissue-specific usage of different promoters for one PTP gene and, in case of the receptor like PTPs PTPRE and

PTPRR, that even results in the expression of either soluble, cytoplasmatic, or transmembranal PTP versions.

The specific localization of PTPs to the different compartments of the cell or their recruitment to other proteins (either adapter or target proteins) likewise influences the PTP activity. For example, PTPN6 and PTPN11 are targeted to the plasma membrane by their SH2 domains. The C-terminus of PTPN6 additionally harbors a recognition-site for acidic phospholipids, targeting it to lipid rafts in T-lymphocytes, where it regulates T-cell receptor signaling. Other domains like FERM, PDZ, or proline-rich domains can recruit cytoplasmatic PTPs to cell-cell or cell-matrix adhesion complexes. Likewise, the targeting to the ER, secretory vesicles, or to the nucleus is achieved by specific domains or targeting sequences. Alternative splicing may lead to PTP variants, that lack certain domains or targeting sequences, and thereby exhibit different specificity patterns (den Hertog, 2008).

Besides the influence of expression or localization, the PTP proteins can undergo post-translational modifications. Interestingly, the PTPs themselves can be phosphorylated (serine-, threonine-, and tyrosine-phosphorylation) leading to conformational changes that either activate or inhibit the activity, or serve as binding-sites for adapter molecules. This indicates that PTPs may also regulate each other's activity. An important regulatory mechanism is the reversible oxidation of the catalytic cysteine in the cysteine-based PTPs, leading to inhibition of the catalytic activity (Ostman, 2011). The involved reactive-oxygen-species (ROS) are often induced by surface receptors such as receptor PTKs, integrins or G-protein-coupled receptors, leading to temporal inhibition of PTPs counteracting the activated signaling events. This mechanism can also play a pathogenic role. For example, the oncogenic kinase FLT3-ITD (Fms-like tyrosine kinase 3 with internal tandem duplication) causes elevated ROS levels in the leukemic cells, leading to oxidation of PTPs like PTPRJ or PTPN6 which further enhances the leukemic phenotype (Godfrey, 2012; Jayavelu, 2016).

Similar to the ligand-binding to other receptors, the extracellular domain of RPTPs can also bind ligands. The ligand binding presumably leads to conformational changes within the PTP molecules, leading to either activation or inhibition of the phosphatase activity. Likewise, the dimerization of RPTPs can also regulate the activity. For PTPRC, the forced dimerization can inhibit the activity. However, the functional outcome of ligand induced dimerization is strongly dependent on the exact sterical layout of the RPTPs. This may be influenced differentially by different ligands or by post-translational modification of the PTP, so there is no general mechanism predicting activation or inhibition by dimerization (den Hertog, 2008).

1.2.3 PTPs in health and disease

PTPs can be dys-regulated in a pathological context. For example, PTP gene expression can be altered. Both, down-regulation of some PTPs *e. g.* by promoter methylation, or up-regulation of PTPs in diseases have been reported. In addition to epigenetic changes, also mutations (loss-of-function or gain-of-function) in the protein-coding sequence or in promoter regions and examples for the complete loss of genes are known (Ostman, 2006). These abnormalities can lead to hereditary diseases (Hendriks, 2013) or play a role in the development of malignancies. Interestingly, PTPs can not only appear as tumor suppressors in their role as counteractors of oncogenic kinases, but they can also act as oncogenes (Ostman, 2006; Julien, 2011). A well characterized example is PTPN11 (SHP-2), which is constitutively activated by mutations in some cancer entities, *e. g.* in 5 -10 % of acute myeloid leukemia (AML) patients. PTPN11 also activates the Ras / ERK signaling pathway and thereby contributes to cell transformation downstream of several oncogenic tyrosine kinases, including BCR-ABL1 (Gu, 2018). This highlights again the importance and differential function of PTPs in signaling networks. Therefore, the analysis of PTPs in oncogenic contexts may further help in understanding specific phenotypes.

In this thesis, I mainly focused on PTPN6, PTPRC, and PTPRG for the functional analyses, and therefore, some detailed information for these PTPs is provided in the following sections.

1.2.4 PTPN6 (SHP-1)

Figure 1-4. Domain structure of PTPN6. PTPN6 consists of two SH2 (SRC homology 2) domains, an active PTP domain (PTP) and a short C-terminal tail.

PTPN6 is a cytoplasmatic phosphatase, expressed as 4 different isoforms: 3 of them with variations in the N-terminus, and one “long” isoform with differences in the C-terminus due to alternative splicing resulting in a reading frame shift. All of them consist of N-terminal tandem SH2 (SRC homology 2) domains and one active PTP domain (Figure 1-4). The predominantly hematopoietic isoform is 595 amino acids long with the molecular mass of about 68 kDa. In the inactive state, the N-terminal SH2 (N-SH2) domain folds into the catalytic domain and thereby blocks access of substrates to the catalytic-site. An allosteric switch, opening the active-site is caused by binding of phosphopeptides to the N-SH2 domain. In addition, the activity of PTPN6 is modulated by tyrosine phosphorylation of the C-terminus (Hendriks & Böhmer, 2016).

In the hematopoietic compartment, PTPN6 may play a role as a tumor suppressor. Loss or reduction of PTPN6 expression, caused by promoter methylation, or allele loss is often found in leukemia, lymphoma, and multiple myeloma cases. Naturally occurring mouse strains with defects in the *Ptpn6* gene *e. g. motheaten* (no functional PTPN6) and *motheaten viable* (PTPN6 with 80 % reduced activity) have implicated hematological functions of PTPN6. Homozygous mice suffer from chronic inflammation and autoimmunity before they die at the age of 3 weeks (*motheaten*) or 6-9 weeks (*motheaten viable*). Heterozygous animals develop leukemia and lymphoma at higher age. These findings support the idea of PTPN6 as a tumor suppressor.

In contrast to that, there are also reports, that PTPN6 may act as an oncogene in some epithelial- and ovarian cancer types, where PTPN6 is rather over-expressed than down-regulated (Julien, 2011; Hendriks & Böhmer, 2016).

The PTPN6 mouse models implicate a possible role of PTPN6 in counteracting leukemia. Therefore several study groups already addressed the possible influence of PTPN6 in CML cell lines and patient samples: PTPN6 is reported to directly interact with BCR-ABL1 (Liedtke, 1998; Bruecher-Encke, 2001) and the down-regulation of PTPN6 is associated with CML disease progression from CP to AP and BC (Amin, 2007; Li, 2014). Most likely, this down-regulation is mediated by promoter methylation as shown in different publications (Oka, 2002; Li, 2014; Li, 2017). However, Amin *et al.* rather suggest post-transcriptional modifications of PTPN6 to be responsible for the decreased expression and not promoter methylation (Amin, 2007).

As described above (chapter 1.1.5), some CML patients are refractory to TKIs or relapse under TKI treatment, without detectable mutations or expression changes in BCR-ABL1. PTPN6 is a direct phosphorylation target of BCR-ABL1 (Tauchi, 1997), and may negatively regulate BCR-ABL1 and some of its downstream targets (Liedtke, 1998; Hendriks & Böhmer, 2016). Considering this, the direct impact of PTPN6 on imatinib resistance was analyzed by an Italian study group (Esposito, 2011). They analyzed bone marrow samples of CP-CML patients, and found the PTPN6 mRNA expression decreasing with sub-optimal response and treatment failure, compared to optimal responders. One other study reported a lower expression level of PTPN6 mRNA at diagnosis in a small group of CML patients not responding after 3 months of imatinib treatment, but could not show a significant difference (Papadopoulou, 2016).

Taken together, the currently available literature reports do not yet give a clear picture on the influence of the PTPN6 on CML treatment outcome. Therefore, I included PTPN6 in the functional analyses of TKI response in this thesis.

1.2.5 PTPRC (CD45)

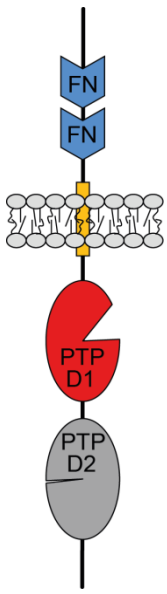

Figure 1-5. PTPRC domain structure. The C-terminal PTP domains are located in the cytoplasm of the cell. FN: fibronectin-like 3 domain, PTP D1: active phosphatase domain, PTP D2: inactive phosphatase domain.

The receptor-like tyrosine phosphatase PTPRC, also known as CD45, is commonly expressed on all nucleated cells of the hematopoietic system. Expression levels generally increase with hematopoietic differentiation. It consists of an extracellular domain harboring two or three fibronectin-like 3 sub-domains, a transmembrane domain, and two intracellular phosphatase domains. The membrane proximal PTP D1 domain is catalytically active, whereas the C-terminal PTP D2 domain is catalytically inactive (see Figure 1-5), but appears to be important for the phosphatase activity of D1. PTPRC is expressed as different N-terminal splice- and glycosylation variants, with molecular masses ranging from 180 to 240 kDa. The expression of different PTPRC isoforms can be used to distinguish sub-sets of cells and their activation status (Hermiston, 2009).

The most prominent PTPRC substrates are SFK. These membrane-associated non-receptor PTKs are key mediators of cellular proliferation, survival, migration, growth factor-, and cytokine signaling-pathways, including T- and B-cell antigen receptor signaling. The activity of SFKs is tightly regulated. In brief, an inhibitory tyrosine residue in the C-terminal tail gets phosphorylated by PTKs (*e. g.* Csk (C-terminal SRC kinase)), and this phospho-tyrosine (pY) binds in an intramolecular fashion to the SH2 domain of the SFK, thereby forming an inactive conformation. This inhibitory C-terminal phosphorylation (site pY530 in human cSRC) can be de-phosphorylated by PTPs, resulting in a “primed”, open conformation allowing auto-phosphorylation of a tyrosine residue in the kinase domain (site pY419 in human cSRC referred to as “pSFK” in immunoblots later in this thesis), which is needed for full activation of the kinase. PTPRC is known to activate SFKs by de-phosphorylation of the C-terminal inhibitory pY-site. Despite this activating role of PTPRC, there are also reports that PTPRC can regulate the phosphorylation of the SFK active-site tyrosine, resulting in a negative regulation of SFK activity, thereby providing a negative feedback mechanism (Hermiston, 2009; Rhee & Veillette, 2012). This regulatory role has been elaborately investigated for p56 (Lck), a prominent SFK in T-lymphocytes (McNeill, 2007).

Homozygous loss, or the expression of mutated PTPRC resulting in differentiation defects of lymphocytes, lead to a SCID (severe combined immunodeficiency)

phenotype in mice and humans, caused by a lack of peripheral T-lymphocytes (Cale, 1997; Kung, 2000; Tchilian, 2001). Polymorphisms of splicing-related bases in the *PTPRC* gene that change the expression pattern of the splice variants are linked to increased incidences of *e. g.* multiple sclerosis, autoimmune hepatitis, systemic sclerosis, and HIV (human immunodeficiency virus) infections, or are associated with a protective effect against hepatitis B infection (Hermiston, 2009).

Similar to the dual role that PTPRC can play in SFK activation, it can neither be clearly labeled as a tumor suppressor, nor as an oncogene related to leukemia development. PTPRC was reported to have tumor suppressive functions (Porcu, 2012), while others reported leukemia-promoting features (Kumar, 2016; Saint-Paul, 2016), or found low PTPRC expression correlated with increased treatment-free survival in CLL (chronic lymphocytic leukemia) (Rizzo, 2013).

Obviously, the role of PTPRC is cell-type dependent, but up to date, no reports addressing the role of PTPRC in CML patients or CML cell lines are published. This and the finding that PTPRC expression was correlated with treatment outcome in the study presented in this thesis (chapter 5.1) made PTPRC an interesting PTP to be followed up in more detail.

1.2.6 PTPRG (RPTPgamma)

PTPRG is a receptor-like classical PTP with an extracellular domain harboring a carbonic anhydrase-like (CA) and a fibronectin-like 3 (FN) sub-domain, a transmembrane domain, and an intracellular catalytically active D1- and a catalytically inactive D2-phosphatase domain (Figure 1-6), similar to PTPRC. PTPRG was reported having tumor suppressor functions in a variety of tissues. As reviewed by Stoker, there are reports on inactivating mutations, LOH (loss of heterozygosity), and promoter methylation of the PTPRG gene (Stoker, 2016). In Merkel-cell carcinoma (an aggressive rare skin cancer), nasopharyngeal carcinoma, as well as in ovary, lung, and renal tumor samples, a PTPRG down-regulation, gene disruption, or silencing were found. In gastric carcinoma studies, lymph-node metastases revealed a significantly higher rate of PTPRG silencing by promoter methylation than the primary tumors. Studies about nasopharyngeal carcinoma (Cheung, 2008) and breast cancer (Liu, 2004; Shu, 2010) provided experimental evidence that PTPRG negatively influences proliferation and anchorage-independent growth. In a study analyzing childhood ALL (Xiao, 2014), PTPRG was found down-regulated by promoter methylation, especially in samples with mutated *Ras* gene. The authors found PTPRG to counteract Ras signaling by de-phosphorylation of ERK, a downstream Ras target. In contrast to all these findings, PTPRG was found up-regulated in immunohistochemistry of frozen or

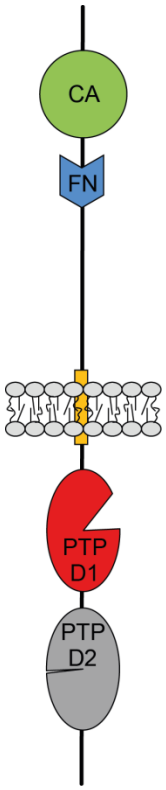

Figure 1-6. PTPRG domain structure. PTPRG consists of an extracellular N-terminal carbonic anhydrase like (CA) domain, a fibronectin-like 3 (FN) domain, a transmenbrane domain, and two intracellular PTP domains, one (D1) with phosphatase activity, the membrane distal domain (D2) lacking catalytic activitiy.

paraffin-embedded tissues of high-grade astrocytomas and subtypes of lymphomas (Vezzalini, 2007). However, this study completely lacks functional analyses, leaving the suspected tumor-promoting abilities of PTPRG unproven.

Of special interest for this thesis were reports addressing PTPRG in CML cell lines or patients. Two reports of the Italian working group headed by Claudio Sorio are published (Della Peruta, 2010; Vezzalini, 2017). They found PTPRG down-regulated in CML patient blood and bone marrow samples, and described a higher PTPRG level after imatinib treatment in patients responding to the therapy, but not in non-responding patients. In functional analyses, they found a direct interaction of PTPRG with BCR-ABL1, and showed that expression of PTPRG in K562 cells could diminish colony formation in methylcellulose, and decreased tumor size in xenografted nude mice.

In my patient analyses, I found a positive correlation of PTPRG mRNA expression levels before CML treatment with favorable treatment outcome after 9 months of nilotinib treatment (chapter 5.1). Taken together with the described tumor suppressor functions, I aimed to answer the question, whether PTPRG has a direct impact on the TKI treatment response and might therefore suit as a prognostic marker of CML treatment outcome.

2 Aim of the Study

The first aim of the study was to assess the potential influence of the PTP-status of CML patients for treatment response to the second-generation TKI nilotinib, and to identify PTPs that may be associated with the treatment response. To this end, a qPCR platform to analyze the mRNA expression level of 38 selected PTPs in primary CML patient samples should be set up and the PTP mRNA expression levels at timepoint of diagnosis should be correlated to the patient's individual nilotinib treatment response.

In the second part of the thesis, cell line models were to be established with manipulated expression levels of the candidate PTPs by either shRNA-mediated knockdown, CRISPR/Cas9-mediated knockout, or exogenous over-expression as applicable. These cell line models should then be used to study the direct influence of either PTP on the treatment response, by directly assessing the sensitivity to nilotinib, imatinib, and dasatinib treatment.

The third part of the thesis studies should focus on investigating mechanisms that cause the changed sensitivity to TKI, by analyses of selected signaling pathways. Using this information, new possible treatment options or reasonable combination-treatments should be identified.

3 Material

3.1 QPCR primers for PTP and control genes

Oligos were purchased from Sigma-Aldrich.

Gene name	Common name	Primer forward	Primer reverse	Size
PTPN1	PTP1B	CGTTAAAATGCGCACAATAC	GCTGTCGCACTGTATAATATG	120 bp
PTPN2	TC-PTP	GGCACCTTCTCTCTGGTAGA	TCTCAGTTGATCTGGGGTCT	129 bp
PTPN4	PTPMEG1	TACGATCAGTCAGAGAACTTG	GGAGATAAGCCTATGTGTTG	119 bp
PTPN6	SHP-1	CAAGAACATTCTCCCCTTTG	TCTTGATGTAGTTGGCATTG	98 bp
PTPN7	LC-PTP	AGGAGAAATGTGTCCACTAC	AAAGAGGATGTGCTTTACTG	155 bp
PTPN9	PTPMEG2	AGAAACTCGAAGGAAGGAAG	GATGGTGAATTTTCCACTGAG	88 bp
PTPN11	SHP2	CCTGAATTTGAAACCAAGTG	ACATTTACTCTTTCCTCTCTCC	168 bp
PTPN12	PTP-PEST	ATGAATCTCGTAGGCTGTATC	CCTCATTAAGCTTATCATGTCC	101 bp
PTPN13	FAP1, PTP-BAS	GAAGAACCAGTTCGAAGATAC	ACTTAAGGTTTCATCTACCCC	171 bp
PTPN14	PTP PEZ	CAGAATTGGAAGACAAGCGG	TAAAACTTGTGTCGTGTGGC	177 bp
PTPN18	PTP-HSCF	AGGAGAAGTGGCTGAATGAG	GTAGCTGGTACACAGAACGG	84 bp
PTPN21	PTPD1	ATTTAGGTGGCATGACATTG	CAACACAGAGTCTCCAAATG	137 bp
PTPN22	Lyp	GTGAAACTCGAACTATCTACC	TCTTGGTAACAACGTACATC	112 bp
PTPN23	HD-PTP	CTTTGAGGGCTGTAGTGTC	CGCTCCAAGGTTGTAGAGAA	187 bp
PTPRA	RPTPα	CAACAATGCTACCACAGT	AAGAGAAGTTAGTGAAGAAGTT	121 bp
PTPRB	VE-PTP	CTCTGTGGACATTTATGGAG	ACTGGATCTCTGTGATACTC	195 bp
PTPRC	CD45	CATATGACTATAACAGAGTGCC	ATGTATTTGCTTGGTTCCTC	118 bp
PTPRE	RPTPε	ATGACCATTCTAGGGTGATTC	CCATCTATGTAGGAAGCATTG	79 bp
PTPRG	RPTPγ	GACGAGAAGGAGAAGACGTT	AACAGGTAAAGGCTATCGGG	89 bp
PTPRJ	DEP-1	ATAGGCAATGAGACTTGGGG	CATGGCTTCCAATGCTTTCA	172 bp
PTPRK	RPTPκ	CTTGAAACTGATACTTCAGGTG	TTAGGCAGTGGATAATCGTC	80 bp
PTPRM	RPTPμ	GGCCAGATGACACAGAGATA	CATGCACACCTCTCTTTTCAA	111 bp
PTPRO	GLEPP1	ATTGAAAATCTGGTTCCTGG	ACAATAGCAAATGTCACAGG	101 bp
PTPRS	RPTPσ	CAGAGGATGAGTACCAGTTC	CTTTAGGTTGCATAGTGGTC	76 bp
PTPRT	RPTPρ	AGAGGAGCAATATGTGTTTG	GATATTGTAGTAGAGAGAACGG	103 bp
PTPRZ1	RPTPζ	TGAGGTGCTGGACAGTCATA	GCTCAGGAGCTGGAATTGTT	100 bp
DUSP1	MKP1	ACTACCAGTACAAGAGCATC	GATTAGTCCTCATAAGGTAAGC	183 bp
DUSP2	PAC1	CAACTTCAGTTTCATGGGG	CTGAAACTCTGAGGAGGTAG	184 bp
DUSP3	VHR	TTGGCTCAAAAGAATGGC	ATCATGAGGTAGGCGATAAC	86 bp
DUSP4	MKP2	TATCAGTACAAGTGCATCCC	ATCGATGTACTCTATGGCTTC	84 bp
DUSP6	MKP3	TGGTGTCTTGGTACATTGCT	CGTTCATCGACAGATTGAGC	92 bp
PTP4A1	PRL1	ACGAAGATGCAGTACAATTC	TCAAGTTCCACTTCCAGTAG	183 bp
PTP4A2	PRL2	TACGTTGCACATTTATGGCG	GCTCACTTGTCAGCGAAAAT	82 bp
PTP4A3	PRL3	AGCACCTTCATTGAGGAC	GCGTTTTGTCATAGGTCAC	79 bp
PTEN	TEP1	GGCTAAGTGAAGATGACAATC	GTTACTCCCTTTTTGTCTCTG	169 bp
ACP1	LMW-PTP	CTGTTTGTGTGTCTGGGTAAC	TGATCGGTTACAAGTTTCCTG	74 bp
CDC25A		AGAAGAATACATTCCCTACCTC	CAAGAGAATCAGAATGGCTC	76 bp
CDC25B		ATTGTAGACTGCAGATACCC	GAAAATGAGGATGACTCTCTTG	147 bp
GUSB		TAGAGCAGTACCATCTGGGT	GCTGCACTTTTTGGTTGTCT	160 bp
B2M		TACACTGAATTCACCCCCAC	GATGCTGCTTACATGTCTCG	110 bp

3.2 The shRNA sequences for PTP knockdown

Target Gene	Ordering number (Sigma-Aldrich)	Inserted shRNA sequence into pLKO.1 vector
Control	SHC002	CCGGCAACAAGATGAAGAGCACCAACTCGAGTTGGTG CTCTTCATCTTGTTGTTTTT
ACP1	TRCN0000002598	CCGGCTATGTATGGATGAAAGCAATCTCGAGATTGCTT TCATCCATACATAGTTTTT
	TRCN0000002599	CCGGGCCCATAAAGCAAGACAGATTCTCGAGAATCTGT CTTGCTTTATGGGCTTTTT
	TRCN0000002600	CCGGGAACTACTTGGGAGCTATGATCTCGAGATCATAG CTCCCAAGTAGTTCTTTTT
DUSP1	TRCN0000002514	CCGGAGTTTGTGAAGCAGAGGCGAACTCGAGTTCGCC TCTGCTTCACAAACTTTTTT
	TRCN0000002516	CCGGGCTCTGTCAACGTGCGCTTCACTCGAGTGAAGC GCACGTTGACAGAGCTTTTT
	TRCN0000002518	CCGGCTGCCGCTCCTTCTTCGCTTTCTCGAGAAAGCGA AGAAGGAGCGGCAGTTTTT
PTP4A2	TRCN0000002924	CCGGCTTCAGAGATACCAATGGGCACTCGAGTGCCCA TTGGTATCTCTGAAGTTTTT
	TRCN0000002926	CCGGATACCGACCTAAGATGCGATTCTCGAGAATCGCA TCTTAGGTCGGTATTTTTT
	TRCN0000002927	CCGGCAGATAGTAGATGATTGGTTACTCGAGTAACCAA TCATCTACTATCTGTTTTT
PTPN6	TRCN0000006885	CCGGCCCAGTTCATTGAAACCACTACTCGAGTAGTGGT TTCAATGAACTGGGTTTTT
	TRCN0000006886	CCGGGCATGACACAACCGAATACAACTCGAGTTGTATT CGGTTGTGTCATGCTTTTT
	TRCN0000011052	CCGGCCTCTCCCTGACCCTGTATATCTCGAGATATACA GGGTCAGGGAGAGGTTTTT
PTPN12	TRCN0000002830	CCGGCAGCCGAGTTAAATTGACATTCTCGAGAATGTCA ATTTAACTCGGCTGTTTTT
	TRCN0000002831	CCGGCCACCAGAAGAATCCCAGAATCTCGAGATTCTG GGATTCTTCTGGTGGTTTTT
	TRCN0000002832	CCGGGCTTTGCAGGTTATCAGAGATCTCGAGATCTCTG ATAACCTGCAAAGCTTTTT
PTPRC	TRCN0000002845	CCGGGCTGCACATCAAGGAGTAATTCTCGAGAATTACT CCTTGATGTGCAGCTTTTT
	TRCN0000002847	CCGGCCTTTCCTACAGACCCAGTTTCTCGAGAAACTGG GTCTGTAGGAAAGGTTTTT
	TRCN0000002848	CCGGGCAGGGTCAAACTACATAAATCTCGAGATTTATG TAGTTTGACCCTGCTTTTT
PTPRE	TRCN0000002893	CCGGCCGAGTGATCCTTTCCATGAACTCGAGTTCATGG AAAGGATCACTCGGTTTTT
	TRCN0000002894	CCGGGCTACCGACAGAAGGACTATTCTCGAGAATAGT CCTTCTGTCGGTAGCTTTTT
	TRCN0000002896	CCGGTGGACACATACAAGGAACTTTCTCGAGAAAGTTC CTTGTATGTGTCCATTTTT

3.3 Buffer list

RIPA lysis buffer	1 % NP-40 1 mM EDTA 50 mM Tris-HCl pH 7.4 150 mM NaCl 0.25 % Sodium-deoxycholate Add fresh: “PhosSTOP” tablet and “cOmplete” tablet diluted in RIPA according to manual
10x TBST pH 7.6	200 mM Tris 1.37 M NaCl 10 ml Tween 20 Adjust pH to 7.6 with HCl, then add Tween 20.
PBS pH 7.4	137 mM NaCl 2.7 mM KCl 10 mM Na_2HPO_4 2 mM KH_2PO_4 Adjust pH 7.4 with HCl
Stripping buffer	100 mM 2-mercaptoethanol 2 % SDS 62,5 mM Tris-HCl pH 6.7
6x Sample loading buffer	375 mM Tris-HCl pH 6.8 12 % SDS 30 % Glycerol 500 mM DTT Spatula tip Bromphenol blue
4x Separation gel buffer pH 8.8	1.5 M Tris-HCl pH 8.8 0.4 % SDS
4x Stacking gel buffer pH 6.8	0.5 M Tris-HCl pH 6.8 0.4 % SDS
10x SDS running buffer	250 mM Tris 2 M Glycine 1% SDS
1x Tank blot transfer buffer	25 mM Tris 192 mM Glycine 20 % Methanol
PEI	Dissolve PEI (10 µg/µl) in water and adjust pH to 7.2 with HCl. Sterilize by filtration, store at 4 °C.
10x Erythrocyte lysis buffer	1.55 M KH_4Cl 100 mM $KHCO_3$ 1.22 mM EDTA
PE-buffer	Add 2 mM EDTA to 1x PBS

3.4 Composition of polyacrylamide gels

	Stacking gel	**Separation gel**	
	5 %	**10 %**	**15 %**
Water	3.43 ml	4.1 ml	2.4 ml
Acrylamide	1 ml	3.3 ml	5 ml
4x Stacking gel buffer pH 6.8	1.5 ml	-	-
4x Separation gel buffer pH 8.8	-	2.5 ml	2.5 ml
10 % APS (in water)	60 µl	100 µl	100 µl
TEMED	6 µl	8 µl	8 µl

3.5 Immunoblotting antibodies

Protein	MW	Cat. no	Species	Dilution prim. antibody (in 1x TBST)	Blocking/ sec. antibody (in 1x TBST)
Sigma-Aldrich					
Actin	42 kDa	A5441	mouse	1:5 000 5 % BSA	5 % dry milk
Santa Cruz Biotechnology					
Bcl-2	26 kDa	sc-7382	mouse	1:250 5 % BSA	5 % dry milk
cSRC	60 kDa	sc-18	rabbit	1:1 000 5 % BSA	5 % dry milk
Lyn	53/56 kDa	sc-7274	mouse	1:1 000 5 % BSA	5 % dry milk
p27	27 kDa	sc-528	rabbit	1:1 000 5 % BSA	5 % dry milk
p27	27 kDa	sc-1641	mouse	1:250 5 % BSA	5 % dry milk
STAT5	90 kDa	sc-835	rabbit	1:1 000 5 % BSA	5 % dry milk
PTPN6	68 kDa	sc-287	rabbit	1:1 000 5 % BSA	5 % dry milk
PTPRC	155 kDa	sc-25590	rabbit	1:500 5 % dry milk	5 % dry milk
Cell Signaling Technology					
BCR-ABL1	135 kDa c-ABL1 210 kDa BCR-ABL1	# 2862	rabbit	1:1 000 5 % BSA	5 % dry milk
pBCR-ABL1	135 kDa c-ABL1 210 kDa BCR-ABL1	# 2861	rabbit	1:1 000 5 % BSA	5 % dry milk
pSFK	~50-60 kDa	# 6943	rabbit	1:1 000 5 % BSA	5 % dry milk
ERK	42/44 kDa	# 9107	mouse	1:1 000 5 % BSA	5 % dry milk
pERK 1/2	42/44 kDa	# 9106	mouse	1:1 000 5 % BSA	5 % dry milk
AKT	60 kDa	# 9272	rabbit	1:1 000 5 % BSA	5 % dry milk
pAkt	60 kDa	# 9271	rabbit	1:1 000 5 % BSA	5 % dry milk
BD Biosciences					
pSTAT5	90 kDa	BD611964	mouse	1:1 000 5 % BSA	5 % dry milk
Biozol					
Vinculin	124 kDa	BZL03106	mouse	1:1 000 5 % BSA	5 % dry milk
Custom made					
PTPRG	~160 kDa	Della Peruta (2010)	rabbit	1:1 000 1 % BSA	1% BSA

3.6 Reagents, media, enzymes, and drugs

Product		Company	Ordering number
Acrylamide	Rotiphorese Gel 30 (37,5:1)	Fa. Roth	3029.1
Blasticidin		Life Technologies	R21001
CellTiter-Blue reagent		Promega	G8081
cOmplete tablet	Protease inhibitor cocktail	Roche	04693132001
Dasatinib		Selleckchem	S1021
DMEM-F12	Dulbecco's Modified Eagle Medium: Nutrient Mixture F-12	Gibco	21041-025
ECL	Western Lightning Plus-ECL	Perkin Elmer	0RT2655
FCS	Fetal calf serum	Sigma-Aldrich	F7524
IBM	Iscove Basal Medium	Biochrom	FG0465
Idelalisib	CAL-101	Selleckchem	S2226
Imatinib	Obtained from Siavosh Mahboobi, University of Regensburg		
Iodonitrotetrazolium chloride		Sigma-Aldrich	I8377
Methylcellulose	3 % stock solution	R&D Systems	HSC001
Nilotinib		Selleckchem	S1033
Opti-MEM	Reduced Serum Medium	Gibco	31985-047
P/S	Penicillin/streptomycin	Sigma-Aldrich	P0781
PEI	Polyethylenimine (branched)	Sigma-Aldrich	408727
PeqGOLD Trifast		VWR Peqlab	30-2010
PhosSTOP tablet	Phosphatase inhibitor cocktail	Roche	04906845001
Polybrene	Hexadimethrine bromide	Sigma-Aldrich	H9268
Puromycin	Stock 2 mg/ml in water	Sigma-Aldrich	P8833
Restriction enzymes	*Avr*II, *Bam*HI-HF, *Bgl*II, *Bsm*BI, *Eco*RI, *Mfe*I-HF, *Sal*I, *Pvu*I, *Xba*I, *Xho*I	NEB	R0174, R3136, R0144, R0580, R0101, R3589 R0138, R0150 R0145, R0146
RPMI-1640	Roswell Park Memorial Institute - medium	Sigma-Aldrich	R8758
TEMED	N,N,N',N'-Tetramethyl-ethylenediamine	SERVA	35930.02
Trypsin-EDTA (0.05%)	Ready to use	Gibco	25300054

3.7 Plastic ware and kits

Product		Company	Ordering number
1 ml syringes	Inject-F	Braun	9166017V
10 ml syringes	Inject	Braun	4606108V
Amicon Ultra tube	Amicon Ultra-15 Ultracel – 30K	Merck Millipore	UFC903024
Black 96-well plates	with clear bottom	Greiner	655090
First strand cDNA synthesis kit		ThermoFisher Scientific	#K1612
Maxima SYBR Green/ROX qPCR Master Mix (2x)		ThermoFisher Scientific	#K0223
Nitrocellulose membrane	pore size 0.2µm	Biostep	01-14-101
qPCR plates		Sarstedt	72.1982.202
qPCR sealing foils		Sarstedt	95.1999
qPCR set	Contains plates & foils	Roche	04729692001
QuikChange XL Site-Directed Mutagenesis Kit		Agilent Technologies	200517
Syringe filter units	Filtropur S 0.2µm	Sarstedt	83.1826.001
Zymoclean Gel DNA recovery Kit		Zymoresearch	D4002

4 Methods

4.1 Patient studies

The cDNA samples and the corresponding *BCR-ABL1*^{IS} values of 66 patients participating in the TIGER (Tasigna / Interferon in Germany) study (NCT01657604) were kindly provided by Prof. Dr. Andreas Hochhaus and PD Dr. Thomas Ernst, Jena. The cDNA preparation and *BCR-ABL1*^{IS} determination was described in our joint publication (Drube, 2018). The prepared cDNA was then analyzed in this thesis for the mRNA expression pattern of 38 selected PTP genes (chapter 3.1) as described in chapter 4.4. All 66 patients were grouped according to whether or not they had a MR^4 or better (*BCR-ABL1*^{IS} ≤ 0.01 %) after 9 months of nilotinib study treatment. The mRNA levels of each PTP before study-treatment start was then compared between those two groups. Since the TIGER study protocol allowed some pretreatments, two sub-cohorts of patients were analyzed. For details see chapter 5.1.

4.2 Leukocyte cDNA of healthy donors

All donors have given written consent, and the analysis was approved by the local ethics committee (vote 4461-06/15). Primary leukocytes of healthy donors were isolated from 10 ml fresh blood sample by erythrocyte lysis. In brief, 40 ml of 1 x erythrocyte lysis buffer were added to the blood in a 50 ml tube and incubated on ice for 10 min. The mixture was inverted several times during the incubation. The cells were centrifuged at 400 g, 4°C, for 10 minutes. The supernatant was discarded, and the cells were again resuspended in 1 x erythrocyte lysis buffer, incubated for 10 minutes on ice and centrifuged as described before. The supernatant was discarded, and the cells were washed with 25 ml PE-buffer and centrifuged at 400 g, 4°C, for 5 minutes. Total RNA was isolated using 2 ml of PeqGOLD TriFast solution according to the manual of the manufacturer and cDNA was transcribed from 5 µg of total RNA with the First strand cDNA synthesis kit using random hexamer primers according to the protocol of the manufacturer. QPCR was performed as described in chapter 4.4.

4.3 RNA isolation and cDNA preparation of cell lines

Two million cells were centrifuged (500 g, 5 min), and the supernatant was discarded. Without washing, 1 ml of PeqGOLD TriFast solution was added, and the RNA was isolated according to the protocol of the manufacturer. The cDNA was transcribed from 5 µg of total RNA with the First strand cDNA synthesis kit using random hexamer primers according to the protocol of the manufacturer. QPCR was performed as described in chapter 4.4.

4.4 QPCR

QPCR primers for the 38 PTPs and the control genes (chapter 3.1) were designed using the NCBI primer-BLAST tool (https://www.ncbi.nlm.nih.gov/tools/primer-blast/). Care was taken to pick up all relevant transcript variants of each PTP with equally long PCR products in order to get a comprehensive coverage of isoforms for each PTP. PCR products were validated for correct size by agarose gel electrophoresis and for correct sequence by DNA sequencing (data not shown). The reverse transcribed cDNA was diluted to 480 µl with water. Primer stock solutions, containing 1.2 µM of respective forward and reverse primers were prepared and 5 µl were transferred to each well of the 96-well qPCR plate. A master mix containing 10 µl of 2 x Maxima SYBR Green/ROX qPCR Master Mix and 5 µl of the diluted cDNA per sample was added to the pre-set primers. The plate was sealed with the provided foil and carefully mixed by vortexing. After a short spin, the qPCRs were carried out in a Roche LightCycler480 system with an initial denaturation step of 10 min, 95°C, and 40 cycles with 15 sec, 95 °C; 30 sec, 55 °C; and 30 sec, 72 °C, followed by a melting curve analysis. *Beta-glucuronidase* (*GUSB*) and *Beta-2 microglobulin* (*B2M*) were used as control genes. Each PTP and housekeeping gene was analyzed in duplicates, relative mRNA expression was calculated as $2^{-\Delta CT}$ using the mean CT value of *GUSB* and *B2M*.

4.5 Statistical analyses

4.5.1 Statistical analysis of patient data

The statistical analysis of patient data was done by PD Dr. Markus Pfirrmann, Munich and colleagues. The following method description was provided by PD Dr. Markus Pfirrmann (Drube, 2018): To identify the prognostic influence of the candidate variables on achieving *BCR-ABL1*^{IS} ≤ 0.01 % (MR^4) status at 9 months (yes or no),

univariate logistic regression analyses were performed (Hosmer & Lemeshow, 1989). Significance was judged using the likelihood ratio test. Since the study has an exploratory character, multiplicity was not considered. For the two-sided P values, the unadjusted significance level was 0.05. All calculations were performed with the SAS software version 9.4 (SAS Institute, Cary, NC, USA).

4.5.2 Statistical analysis of *in vitro* experiments

For the *in vitro* experiments the Wilcoxon matched-pairs test was employed using GraphPad Prism 5. Note that comparison of 6 independent values is the minimum sample number for this test. This precluded analyses of data sets with less than 6 independent experiments.

4.6 Cell lines

K562 and KCL-22 were purchased from the German Collection of Microorganisms and Cell Cultures (DSMZ, Braunschweig, Germany). Cells were cultured in RPMI-1640 supplemented with 1 % penicillin/streptomycin (P/S), and 10 % heat-inactivated fetal calf serum (FCS). HEK293T cells were purchased from the DSMZ, and cultivated with DMEM-F12 medium, supplemented with 10 % FCS and 1 % P/S. During transfection, HEK293T cells were cultivated without P/S (see chapter 4.8).

4.7 The shRNA-mediated knockdown of PTPs

In order to down-regulate the gene expression level of selected PTPs, we decided to use the technique of RNA interference (RNAi). RNAi selectively decreases the mRNA level of the target proteins, leading to a decreased expression of the protein itself. All this is mediated by the presence of short double-stranded RNA (dsRNA) molecules, complementary to the target sequence. In order to exogenously introduce this dsRNA, *e. g.* synthetic small (less than 30 bp) double stranded siRNA (small interfering RNA) can directly be transfected into the cells. In the cells, the siRNA assembles with RISC (RNAi –induced silencing complex). RISC unwinds the dsRNA and binds one strand of the siRNA molecule, which is the template to bind the complementary mRNA strand. This strand gets cleaved by the endonuclease activity of RISC, leading to mRNA degradation.

This siRNA approach is only transient. In order to get a stable down-regulation, the dsRNA needs to be continuously expressed in the cell. This can be achieved by the

transfection of cells with plasmids encoding shRNAs (small hairpin RNAs). These RNAs are designed to fold to a dsRNA strand with a linking single stranded hairpin. These molecules are processed by the RNase Dicer that cleaves off the hairpin structure to form siRNAs and enter the pathway described above.

In our study, we used the pLKO.1 system of Sigma-Aldrich. It uses Lentiviral-mediated transduction of the shRNA encoding sequence to the CML cell lines. The target sequences are outlined in chapter 3.2. Transduction of target cells was carried out as described in chapter 4.8. The cells were selected using puromycin (2 µg/ml) for 5 days. After that, cells were analyzed for remaining mRNA expression of the target gene.

4.8 Viral transduction

1.5 million HEK293T cells were seeded in DMEM-F12 medium supplemented with 10 % FCS and 1 % P/S in a 10 cm cell culture dish. 16 hours later, the medium was replaced by DMEM-F12 with 10 % FCS, but without P/S, and the HEK293T cells were transfected using PEI reagent: For production of lentiviral particles, 10 µg pMDL, 5 µg pRSV, 2 µg VSVg (packaging plasmids were originally obtained from Dr. Carol Stocking, HPI, Hamburg, Germany) and 10 µg of the lentiviral vector were added to 0.5 ml of OptiMem medium, and to a second tube, 6.75 µl PEI stock (10 µg/µl) were added to 0.5 ml OptiMem. Then the 0.5 ml of PEI solution were added to the first tube, and mixed thoroughly by pipetting up and down several times. After an incubation period of 20 minutes at room temperature, the PEI / DNA mixture was added dropwise onto the HEK293T cells. For production of retroviral particles, 10 µg RV GagPol, 2 µg VSVg (packaging plasmids were originally obtained from Dr. Carol Stocking, HPI, Hamburg, Germany), 5 µg of retroviral vector, and 4.25 µl of PEI stock (10 µg/µl) were used. Six hours after adding the transfection mix to the cells, the supernatant of the HEK293T cells was carefully taken off, and was replaced by 10 ml of full DMEM-F12 containing P/S.

24 h after start of transfection, the virus containing supernatant of the HEK293T cells was transferred to an Amicon Ultra tube using a 10 ml syringe and a 0.2 µm syringe filter unit to remove any HEK293T cells. The viral supernatant was centrifuged for 15 minutes at 4 000 g. The HEK293T were again cultivated with 10 ml of fresh culture medium containing FCS and P/S for 24 h.

50 000 target cells were seeded in 2 ml of their respective growth medium in 6-well cell culture dishes, containing 22 µl of 0.8 µg/µl polybrene (Hexadimethrine bromide) solution. The concentrated virus was added dropwise to the target cells, and the culture

plate was centrifuged at 500 g for 1 hour. After the centrifugation, the cells were incubated at 37°C, 5 % CO_2 until the next infection. In total, 3 rounds of infections (24 h, 48 h, and 72 h after start of transfection) were carried out. 24 h after the last infection, the target cells were washed with their respective growth medium.

4.9 Expression constructs

4.9.1 PTPN6

The human PTPN6-WT expression construct was originally obtained from Dr. Axel Ullrich (Max-Planck Institute of Biochemistry, Martinsried, Germany). The phosphatase-dead PTPN6-C453S mutant was generated by Annette Böhmer.

The two PTPN6 coding sequences (WT and CS) were amplified using the following primers: GCA GAA TTC ACG ATG GTG AGG TGG TTT CAC C, and GCA CTC GAG GCT TCA CTT CCT CTT GAG G. After gel extraction with the Zymoclean DNA recovery kit, the fragments were inserted into the pMSCV-IRES-mCherry (gift from Dario Vignali, Addgene # 52114) vector using EcoRI and XhoI restriction enzymes. The resulting plasmids (8 083 bp) were analyzed by control digest and sequencing (not shown).

4.9.2 PTPRG

A lentiviral human PTPRG-WT expression construct (coding sequence from NM_002841.3) containing a mCherry/Blasticidin expression cassette (pLV-PTPRG-WT-mCherry/Bsd) was custom made by Vector builder (Cyagen Biosciences Inc., Santa Clara, CA, USA). The encoded sequence corresponds to the 1445 aa long splice version of PTPRG (Ensembl ENST00000474889.5). The expression efficiency was not very high using this lentiviral system, and the sorting for mCherry expression also did not result in high expression levels, since this construct expresses mCherry independently of the insert, and therefore, the fluorescence signal does not directly reflect the expression of PTPRG. The direct sorting for PTPRG expression was not possible, since there are no reliable FACS antibodies commercially available. To overcome this, we decided to switch to the retroviral system pMSCV-IRES-mCherry. In this system, mCherry and the inserted protein are translated from the identical mRNA strand. The vector pLV-PTPRG-WT-mCherry/Bsd was cut with BglII, EcoRI, and AvrII in NEB buffer 3.1, and the resulting 5 013 bp fragment with the coding PTPRG-WT sequence was isolated and ligated into the BamHI-HF and MfeI-HF cut MSCV-IRES-mCherry vector (NEB cut smart buffer, 6 313 bp). The final MSCV-PTPRG-WT-IRES-

mCherry vector (11 326 bp) was analyzed by control digestion and sequencing. In order to study the influence of the phosphatase activity itself, we mutated the PTPRG-WT construct to the phosphatase-dead PTPRG-C1060S (CS) mutant. In this construct, the catalytically active cysteine in the membrane proximal PTP domain (PTP D1) is replaced by a serine, leading to a catalytically inactive enzyme. The site directed mutagenesis resulting in this amino acid change was carried out using the QuikChange XL Site-Directed Mutagenesis Kit according to instructions of the manufacturer with the following primers: CTG TGT TGG TGC ACT CCA GTG CTG GTG TGG and CCA CAC CAG CAC TGG AGT GCA CCA ACA CAG (the mutated base underlined).

Viral transduction of K562 cells with pMSCV-PTPRG-WT-IRES-mCherry, pMSCV-PTPRG-CS-IRES-mCherry, or respective empty vector pMSCV-IRES-mCherry was done as described in chaper 4.8. Since the vector does not encode any selection marker, the cells were sorted for equally high mCherry expression by the colleagues of the CF Flow Cytometry of the Fritz-Lipmann-Institute (FLI) Jena.

4.9.3 PTPRC

The PTPRC expression construct was obtained from Dr. Reiner Lammers (University Hospital Tübingen, Germany). It encodes the PTPRC isoform 2 (NP_563578.2). The coding sequence was subcloned into the lentiviral expression vector pLV-MCS-mCherry/Bsd (Vector Builder, Cyagen Biosciences Inc., Santa Clara, CA, USA).

Therefore, the PTPRC vector was cut with SalI, AvrII, and PvuI in NEB Buffer 3.1, the 4 620 bp fragment was isolated, and ligated into the gel extracted (Zymogen Gel DNA recovery kit, according to manual of the manufacturer) pLV-MCS-mCherry/Bsd vector fragment cut with SalI and XbaI (NEB Buffer 3.1). The identity of the resulting vector was confirmed by control digestion and DNA sequencing (not shown).

This expression vector was used to rescue the phenotype of K562 PTPRC knockout cell clone A. Therefore, the PTPRC-KO cells were infected with freshly produced viral particles made with pLV-PTPRC-mCherry/Bsd or corresponding empty vector (pLV-MCS-mCherry/Bsd) (chapter 4.8), selected with blasticidin (7.5 µg/µl for 10 days) and subsequently sorted for PTPRC expression (PTPRC expression construct) or mCherry expression (empty vector) respectively (CF Flow Cytometry of the Fritz-Lipmann-Institute (FLI) Jena).

4.10 CRISPR/Cas 9

The CRISPR/Cas (Clustered regularly interspaced short palindromic repeats/CRISPR-associated protein) system was originally discovered in bacteria and archaea, as an acquired immune defense system against viruses and phages: Upon infection with foreign DNA (*e. g.* phage DNA), this DNA is cleaved by the Cas nuclease and the resulting small pieces get incorporated into the bacteria or archaea genome itself. These pieces are transcribed to crRNA (CRISPR RNA) and serve as guiding sequences in case of re-infection: the Cas nuclease is guided to the invading DNA by these RNA pieces, and the nuclease in turn destroys the foreign DNA, leading to an efficient immune defense.

Since this system allows a targeted (by the guide RNA, gRNA) cutting of DNA by the nuclease, it provides a new tool to edit the genome of cell lines. To achieve this, a gene-specific gRNA gets co-expressed with the Cas 9 enzyme (consisting of two different nuclease domains), leading to a targeted double-strand DNA break (DSB), that is repaired by the error prone NHEJ (non-homologous end-joining) or HDR (homology-directed repair). NHEJ usually leads to small insertions or deletions, resulting in reading frame shifts and premature stop codons. Thereby the gene is functionally inactivated: a gene knockout. HDR uses a template to repair the DSB – giving also the opportunity to insert specific mutations or deletions by providing the desired sequence template (all reviewed by (Zhang, 2014)), a technique which was not applied in this thesis.

We used the lentiCRISPRv2 system (Addgene # 52961 (Sanjana, 2014)) to knockout different PTP genes in our cell models.

4.10.1 *PTPRC* knockout in K562

Since the shRNA-mediated knockdown of PTPRC gave only poor knockdown efficiencies, stable *PTPRC* knockout cells were generated by infecting the parental cells with viral particles (chapter 4.8) freshly made from lentiCRISPR v2 plasmid (Addgene #52961,(Sanjana, 2014)) encoding target specific gRNA (two different target sequences, A and B) or lentiCRISPR v2 vector without an inserted gRNA (control).

The final knockout vectors were made as follows:

Two different guide sequences were used and the vector insert was made by annealing of two complementary DNA oligos (Sigma-Aldrich), that already comprise the sticky ends (underlined) needed for ligation into the target vector.

“A”: oligo A1: <u>CACCG</u>TTACCACATGTTGGCTTAGA

oligo A2: <u>AAAC</u>TCTAAGCCAACATGTGGTAA<u>C</u>

"B": oligo B1: CACCGTTAATATTAGATGTGCCACC

oligo B2: AAACGGTGGCACATCTAATATTAAC

The annealed oligos were ligated into the empty lentiCRISPR v2 vector opened with *BsmBI*. The identity of the resulting vector was checked by control digest and sequencing (not shown).

Infected cells were selected using 2 µg/ml puromycin, single cell clones were established by limited dilution, and clones were analyzed for absence of the target protein by flow cytometric analysis (chapter 4.11) and immunoblotting (chapter 4.13). Two independent knockout clones (A and B) were selected for further analysis.

4.10.2 *PTPN6* knockout in KCL-22

Stable PTPN6 knockout cells were generated as described for PTPRC (chapter 4.10.1). For PTPN6, only one guide sequence was used with success, obtained by annealing of the following oligos:

Oligo 1: CACCGGAAGAACTTGCACCAGCGTC

Oligo 2: AAACGACGCTGGTGCAAGTTCTTCC

Infected cells were selected using puromycin (2 µg/µl), single cell clones were established by limited dilution, and clones were analyzed for absence of the target protein by immunoblotting (chapter 4.13). Two knockout clones (A and B) were selected for further analysis.

4.11 Flow cytometric analysis of PTPRC

Approximately 0.5 million cells were washed with 1 x cold PBS, and after taking the PBS off quantitatively, incubated with a solution of 39 µl PBS and 1 µl PTPRC-APC/Cy7 (Biolegend, # 304014) on a turning wheel, at 4 °C for 30 min. After washing the cells twice with 1x PBS, the cells were suspended in 500 µl PBS and analyzed using BD FACS Canto II or BD Fortessa.

4.12 IC_{50} assay

A cell suspension with 100 000 cells/ml in full growth medium was prepared, and 100 µl of this suspension were transferred to each well of rows A-G of black 96-well plates with clear bottom. For each inhibitor concentration, 995 µl RPMI medium were transferred into a 2 ml tube, and 5 µl of 1 000 x DMSO – inhibitor – stock (nilotinib [µM]: 2 000, 500, 100, 20, 5, 1, 0.2; imatinib [mM]: 50, 10, 2, 0.5, 0.1, 0.02, 0.005; dasatinib

[µM]: 100, 20, 5, 1, 0.2, 0.05, 0.01) were added and mixed well. 300 µl of the resulting 200 x inhibitor dilutions were transferred to one well of a standard 96 well cell culture plate, with the highest concentration in row A, and lowest in row G. Using an 8-channel-pipette, 100 µl of respective dilution was taken up, and 4 times 25 µl were added to 4 wells (quadruplicates) each containing the 100 µl cell suspension. This results in 125 µl cell suspension with 10 000 cells, containing final concentrations of 0.1 % DMSO and dose ranges of 0.2 nM to 2 µM nilotinib, 5 nM to 50 µM imatinib, and 10 pM to 100 nM dasatinib. All wells of row H were filled with 125 µl full growth medium. Selected experiments were carried out with 11 different final nilotinib concentrations (0.2, 1, 2.5, 5, 7.5, 10, 15, 20, 50, 100, 2 000 nM).

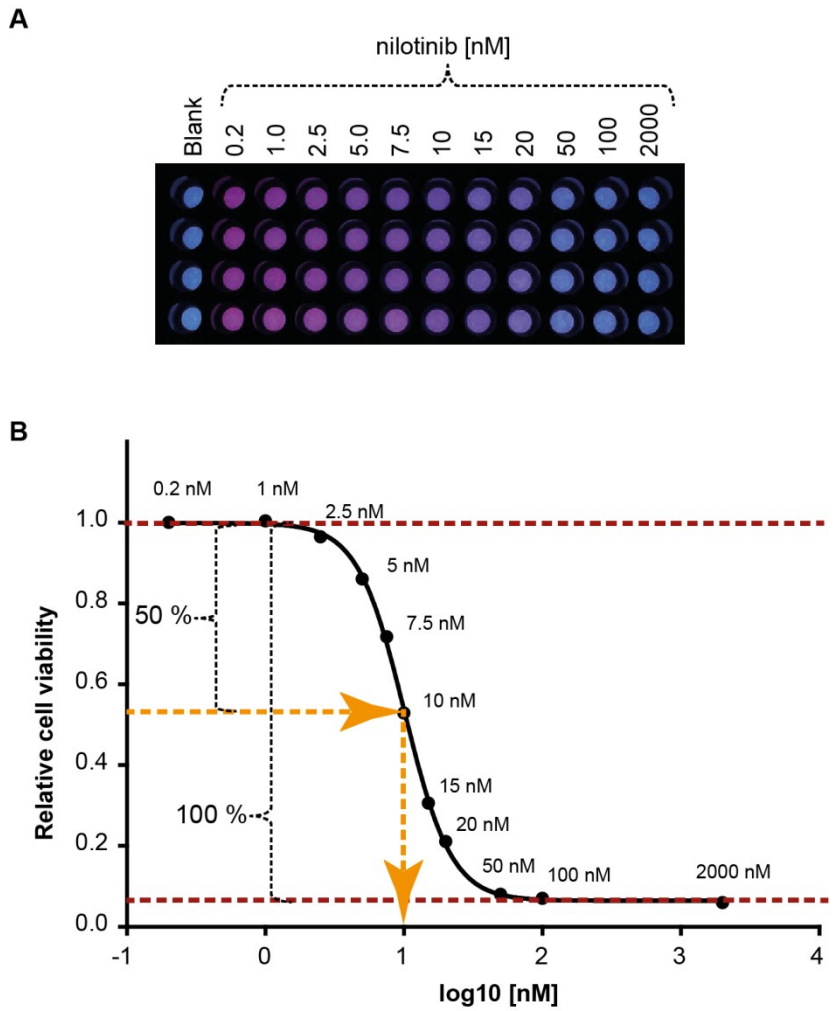

Figure 4-1. (**A**) Photograph of a 96-well plate section 2 hours after CellTiter -Blue addition. Cells were seeded as described in the text, and treated with nilotinib in the indicated concentrations. Shown are quadruplicates of each condition. (**B**) Graphical view of fitted dose response curve and IC_{50} calculation. Values of a representative experiment with 11 different nilotinib concentrations were used for IC_{50} calculation by Sigma Plot. The software fits the dose response curve and calculates the difference of maximum and minimum cell viability (difference between the two red dotted lines), and the inhibitor concentration, where 50 % of this are reached is reported as the IC_{50} (yellow arrows).

After incubation at 37°C for 72 h, 25 µl of CellTiter-Blue reagent were added to each well containing cells, and to 4 wells containing 125 µl medium (blank), the plate was incubated at 37°C for 2 hours in the dark. Then, fluorescence (E_x 540 nm, E_m 610 nm, Gain 35, top reading) was measured using a TECAN Infinite 200 (Tecan, Crailsheim, Germany) plate reader. The measurement is based on the reduction of the component resazurin (dark blue, little intrinsic fluorescence) to resorufin (pink, high fluorescence) by metabolically active cells. The mean blank value was subtracted from each of the quadruplicates, and a mean fluorescence value was calculated. A photograph of an example plate showing the visible color shift from blue (blank and high nilotinib concentrations) to pink (lowest nilotinib concentration, most viable cells) in the wells with living cells is shown in Figure 4-1, A.

IC_{50} values were calculated using Sigma Plot 13.0. Log10 of the respective inhibitor concentration was plotted against the corresponding mean fluorescence value, and the IC_{50} was calculated using the macro “ligand binding” with “sigmoidal dose-response (variable slope)” fitting. Figure 4-1, B shows an example of a fitted curve obtained from an experiment carried out with 11 different nilotinib concentrations and indicates the basis of the IC_{50} calculation.

For the combination-treatment with idelalisib, a cell suspension containing 125 000 cells/ml in full growth medium was prepared and 80 µl of this suspension were transferred into the black 96-well plate. For the samples containing a final concentration of 10 µM idelalisib, a dilution containing 62.5 µM idelalisib (with a DMSO concentration of 0.625 %) was prepared in full growth medium, and 20 µl of this was added to the cells. For the samples containing a final concentration of 1 µM idelalisib, a dilution containing 6.25 µM idelalisib was prepared, and 20 µl were added to the respective cells. Care was taken to have identical DMSO concentrations in all samples. Likewise, a growth medium solution containing only DMSO was prepared for the DMSO controls. To these 100 µl cell suspensions, 25 µl of the nilotinib dilutions (7 concentrations, prepared as described above) were added, and the plate was treated exactly as described for the nilotinib-alone treatment.

4.13 Immunoblotting

Cells were washed with ice-cold PBS and lysed on ice in RIPA lysis buffer containing “PhosSTOP” phosphatase inhibitor cocktail and “cOmplete” protease inhibitor cocktail diluted in RIPA lysis buffer according to the instructions of the manufacturer. The extracts were sonicated, and the cleared lysates were subjected to SDS-PAGE, using self made 10 % or 15 % gels (chapter 3.4), transferred to nitrocellulose membranes by tank blot (12 V over night), washed once in cold TBST, and blocked for 1 h at room temperature in the indicated blocking buffer (chapter 3.5). After washing 3 times for 10 minutes in cold TBST, membranes were incubated over night with the indicated primary antibodies at 4 °C. The membranes were incubated with the respective secondary antibody for 1 h at room temperature after washing off the primary antibody (3 x, 10 minutes, cold TBST). Detection was done using ECL solution and a LAS4000 system (Fujifilm). Membranes used to detect phospho-proteins were stripped for detection of respective total proteins by shaking the blots in stripping buffer at 55 °C for 25 min. After stripping, the blots were washed several times in water and TBST. The membranes were processed again as described above.

4.14 Colony formation assay

To prepare the methylcellulose master mix, 5 ml of 3 % methylcellulose stock were diluted with 5 ml IBM, 1.2 ml of heat inactivated FCS, and 120 µl P/S. All was mixed well using a 10 ml syringe. A cell suspension of 1 950 K562 cells in 50 µl of full growth medium was prepared in a 2 ml tube. After the bubbles had disappeared from the methylcellulose master mix, 1.2 ml of it were added to the prepared tube containing the cells, and everything was carefully resuspended using a 1 ml syringe. 500 µl of this cell suspension were added to two wells of a 24-well-plate each. After six days of cultivation at 37°C, 5 % CO_2, in a humid chamber, 40 µl of a 4 mg/ml Iodonitrotetrazolium chloride solution were added dropwise onto the methylcellulose. The stained colonies were scanned using a HP Scanjet G4050 scanner with 1 200 dpi resolution after additional incubation over night at 37°C, 5 % CO_2. Colony counting was done using NIH ImageJ 1.47v software. In general, colonies with a pixel size from 15-100 and circularity from 0.5-1.0 were counted. Different cell types shown in one experiment were always processed in parallel.

5 Results

5.1 PTP mRNA expression in patient leukocytes at start of treatment is associated with molecular response to nilotinib

The total leukocytes of 66 CML patients before start of nilotinib study treatment were isolated, and the mRNA levels of 38 PTPs and two control genes were analyzed by qPCR (chapter 4.4). In addition, total leukocytes of 15 healthy donors were analyzed for PTP expression on mRNA level. Patient and healthy donor characteristics are shown in Table 5-1.

To find out more about the influence of PTP expression status on nilotinib treatment outcome, we divided the CML patients in two groups according to whether or not the individual patient had reached a *BCR-ABL1*^{IS} lower than 0.01 % (MR^4 or better) after 9 months of study treatment. Using these criteria, n=30 patients were in the *BCR-ABL1*^{IS} ≤ 0.01 % group, and n=36 in the *BCR-ABL1*^{IS} > 0.01 % group respectively. The relative PTP mRNA levels of the analyses of all 66 patients (divided into these two groups) and 15 healthy donors are summarized in Figure 5-1. The PTPs are differentially expressed among healthy individuals and CML patients. Some of the PTPs show similar expression in healthy donors and CML patients (*e. g.* PTPN1, PTPN6, or DUSP2) and others show prominent differences (*e. g.* PTPN7, PTPN14, or CDC25A). After finishing the mRNA analysis of all 66 patient samples, the differences between the two CML patient groups were statistically evaluated by PD Dr. Markus Pfirrmann (Munich) and colleagues using univariate logistic regression analyses.

Table 5-1. Patient and healthy donor characteristics.

	Patients	**Healthy donors**
Total number	66	15
Age	Median 50 [19 – 72] IQR: [36 – 57]	Median 54 [23 – 66] IQR [33 – 60]
Gender	female n=18 (27.3 %)	female n=6 (40 %)
EUTOS-Score	low risk n= 56 (84.8 %)	not applicable
WBC x10^9/L	Median 48.45 [3.5 – 555] IQR: [18.95 – 160.55]*)	not determined
Platelets x10^9/L	Median 405.5 [93 – 3255] IQR: [256 – 670.5]*)	not determined
Hb g/dL	Median 12.25 [8.3 – 16.2] IQR: [10.3 – 14]**)	not determined

*) 2 values missing; **) 4 values missing, IQR: interquartile range

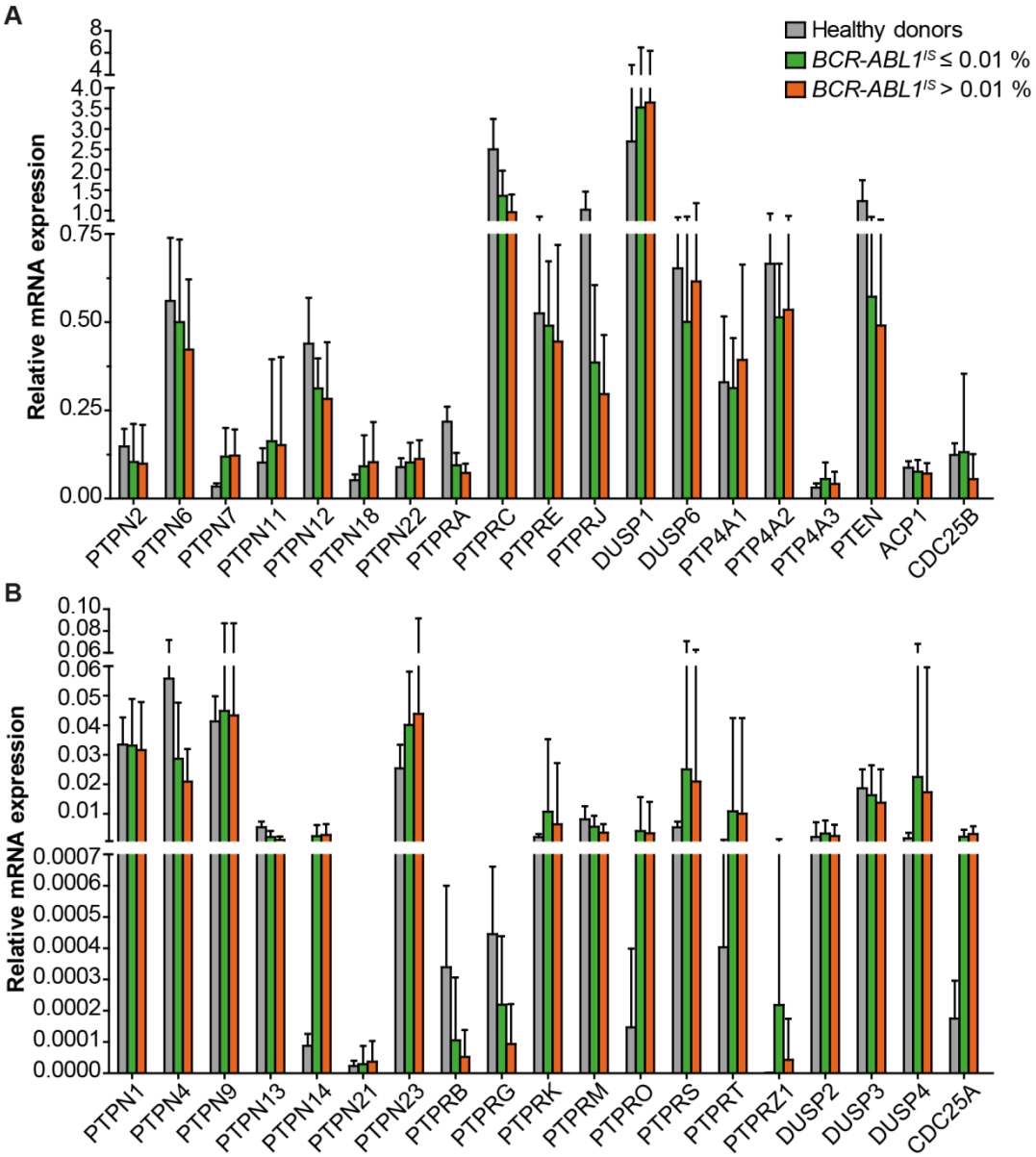

Figure 5-1. PTPs are differentially expressed in healthy donors and CML patients. Total leukocytes of healthy donors (n=15) or 66 newly diagnosed CML patients (n=30 *BCR-ABL1*^{IS} ≤ 0.01 %, n=36 *BCR-ABL1*^{IS} > 0.01 % after 9 months of study treatment) were isolated and mRNA levels of 38 PTPs were analyzed using RT-qPCR. *GUSB* and *B2M* were used as control genes. Shown here are the mean relative mRNA levels of all 38 PTPs + standard deviation with technical duplicates for each PTP per individual. For more clarity, the PTPs with higher mRNA expression levels are shown in (**A**), and the PTPs with lower mRNA expression levels are shown in (**B**).

Significant differences in the probability to reach MR^4 or better after 9 months of nilotinib treatment were found in patients with higher mRNA levels of PTPRG and PTPRC (Figure 5-2, Table 5-2) as well as for PTPN13, PTPRA, and PTPRM (Table 5-2). For all other PTPs, no significant differences were found in the final evaluation. Since the TIGER study protocol allowed inclusion of patients pretreated with imatinib or nilotinib for up to six weeks, and up to 6 months with hydroxyurea, we reassessed the actual treatment schedule of all 66 patients after unblinding and defined two sub-cohorts of patients: in one cohort we excluded 12 of 66 patients that had been TKI pretreated, or discontinued nilotinib within the first 9 months of treatment (cohort size n=54), in the second cohort, we additionally excluded all patients pretreated with hydroxyurea for more than 2 days, and patients that reduced nilotinib dose for more than 3 weeks (cohort size n=35). These two patient cohorts were used to validate the statistical significance of the 5 PTPs found in the 66 patient screen: significances for PTPRA, PTPRC, and PTPRG were still found in the two more stringently defined cohorts, but were lost for PTPRM in the n=54 patient group, and for PTPN13 in both newly defined sub-groups (Figure 5-2, Table 5-2).

Table 5-2. Odds ratios in univariate logistic regression on the probability to be in MR^4 (*BCR-ABL1*^{IS} ≤ 0.01 %) 9 months after start of nilotinib therapy.

Patient cohorts, number of patients (n)	PTP	Odds ratio	Lower 95% confidence limit for odds ratio	Upper 95% confidence limit for odds ratio	P value likelihood ratio test
n=66	*PTPN13*	1.045	1.009	1.092	0.0122
	PTPRA	1.275	1.073	1.561	0.0047
	PTPRC	1.015	1.005	1.028	0.0024
	PTPRG	1.046	1.013	1.088	0.0039
	PTPRM	1.019	1.004	1.038	0.0154
n=54	*PTPN13*	1.040	0.995	1.093	0.0834
	PTPRA	1.287	1.056	1.628	0.0112
	PTPRC	1.013	1.001	1.027	0.0389
	PTPRG	1.059	1.015	1.116	0.0064
	PTPRM	1.012	0.995	1.031	0.1748
n=35	*PTPN13*	1.039	0.990	1.103	0.1242
	PTPRA	1.344	1.060	1.826	0.0123
	PTPRC	1.014	1.000	1.031	0.0430
	PTPRG	1.087	1.026	1.175	0.0023
	PTPRM	1.032	1.005	1.069	0.0168

PTPs analyzed in cell based assays are highlighted.
For cohort details see legend Figure 5-2 and text chapter 5.1.

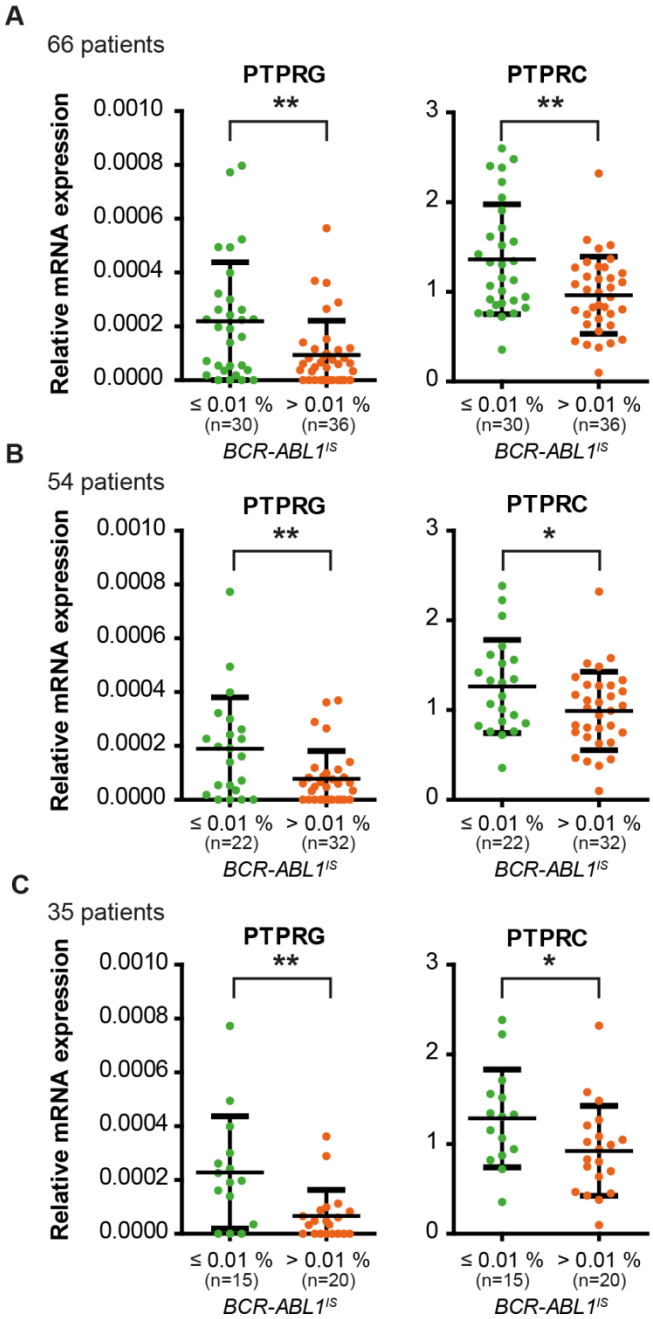

Figure 5-2. Expression levels of PTPRG and PTPRC are associated with response after 9 months of nilotinib treatment. The RNA of total, peripheral blood leukocytes of CML patients in chronic phase was isolated and mRNA expression levels of 38 PTPs were analyzed. *GUSB* and *B2M* were used as control genes.
(**A**) 66 patients were grouped according to their individual *BCR-ABL1*^{IS} (MR^4, yes or no) after 9 months of nilotinib treatment. The mRNA levels for PTPRG and PTPRC are shown. Since the TIGER study protocol allowed pretreatments with TKI and HU, we reassessed the actual treatment schedule of all 66 patients after unblinding. We defined two sub-cohorts of patients: (**B**) in one cohort we excluded 12 of 66 patients that had TKI pretreatments or discontinued the study treatment (total n=54), (**C**) In the second cohort, we additionally excluded 19 patients (total n=35), resulting in a cohort of patients with no TKI pretreatment, with no more than 2 days of HU pretreatment, and no nilotinib dose reductions for more than 3 weeks.
Each point represents the relative PTP expression value of one patient, bars show mean values +/- standard deviation. Differences in PTP mRNA expression between the patient groups were statistically tested. * if $p < 0.05$; ** if $p < 0.01$. P values were calculated using the likelihood ratio test. For details and confidence limits see Table 5-2.
*** This and other figures, as well as some parts of the text of this thesis were already published in (Drube, 2018).**

5.2 Functional analysis of PTP knockdown CML cell lines

In order to start functional analyses as early as possible, I performed preliminary statistical analyses (not shown) comparing PTP expression levels of patients before all 66 patient samples were available. Based on these preliminary analyses and literature reports, PTPN6, PTPN12, PTPRC, PTPRE, PTPRG, DUSP1, PTP4A2, and ACP1 were chosen for an initial functional analysis in CML cell lines. As cell line models, we chose the widely used CML cell lines K562 and KCL-22 for our assays. Similar to the PTP expression pattern of the healthy individuals and CML patients, the CML cell lines show a distinct individual expression pattern (Figure 5-3). For example PTPN6, PTPN13, PTPRE, and PTPRG are higher expressed, but PTPRB is much lower expressed in KCL-22 compared to K562 cells. PTPN12, PTPRC, DUSP1, PTP4A2, and ACP1 are similarly expressed in both cell lines.

To directly assess the influence of single PTPs on treatment outcome, stable shRNA-mediated knockdown cell lines or PTP over-expressing cell lines were created. In the patient samples, PTPRG was only expressed at a very low level. To further analyze this PTP, we chose to establish a PTPRG over-expressing K562 cell-model (see chapter 5.4). For the other seven selected PTPs, three different shRNA constructs were used to generate stable knockdown cell lines, and the remaining PTP levels were determined on mRNA level. Since in the K562 cells, PTPN6 and PTPRE are only lowly expressed (Figure 5-3, Figure 5-9, A), these two PTPs were only knocked down in KCL-22. Table 5-3 summarizes the used constructs and the remaining PTP expression levels after stable transduction of the shRNAs. For PTPRE, DUSP1, and PTP4A2, no more analysis was carried out, since the knockdown efficiency could not be improved in subsequent experiments (data not shown). For PTPN6, PTPN12, PTPRC, and ACP1, the cell pools highlighted in Table 5-3 were analyzed for the change in the IC_{50}s of nilotinib, imatinib, and dasatinib compared to control cell lines. The results of the two experiments carried out with K562-ACP1 (Figure 5-4, A) and KCL-22-PTPN12 (Figure 5-4, B) knockdowns did not show consistent IC_{50} changes. These PTPs were not further analyzed. In contrast, the knockdown of PTPRC in K562 cells resulted in IC_{50} reductions in all tested TKI in both experiments (Figure 5-5). Since this result was obtained with PTPRC mRNA reductions of only about 40 %, that could not be further improved by new transductions, we decided to carry out CRISPR/Cas9-mediated knockout of PTPRC to analyze the influence of this PTP on TKI susceptibility (see chapter 5.5). Following up PTPRC was also prompted, because it was one of the phosphatases with a significant correlation of mRNA level to reaching an MR^4 after 9 months of nilotinib treatment in the final patient-analysis.

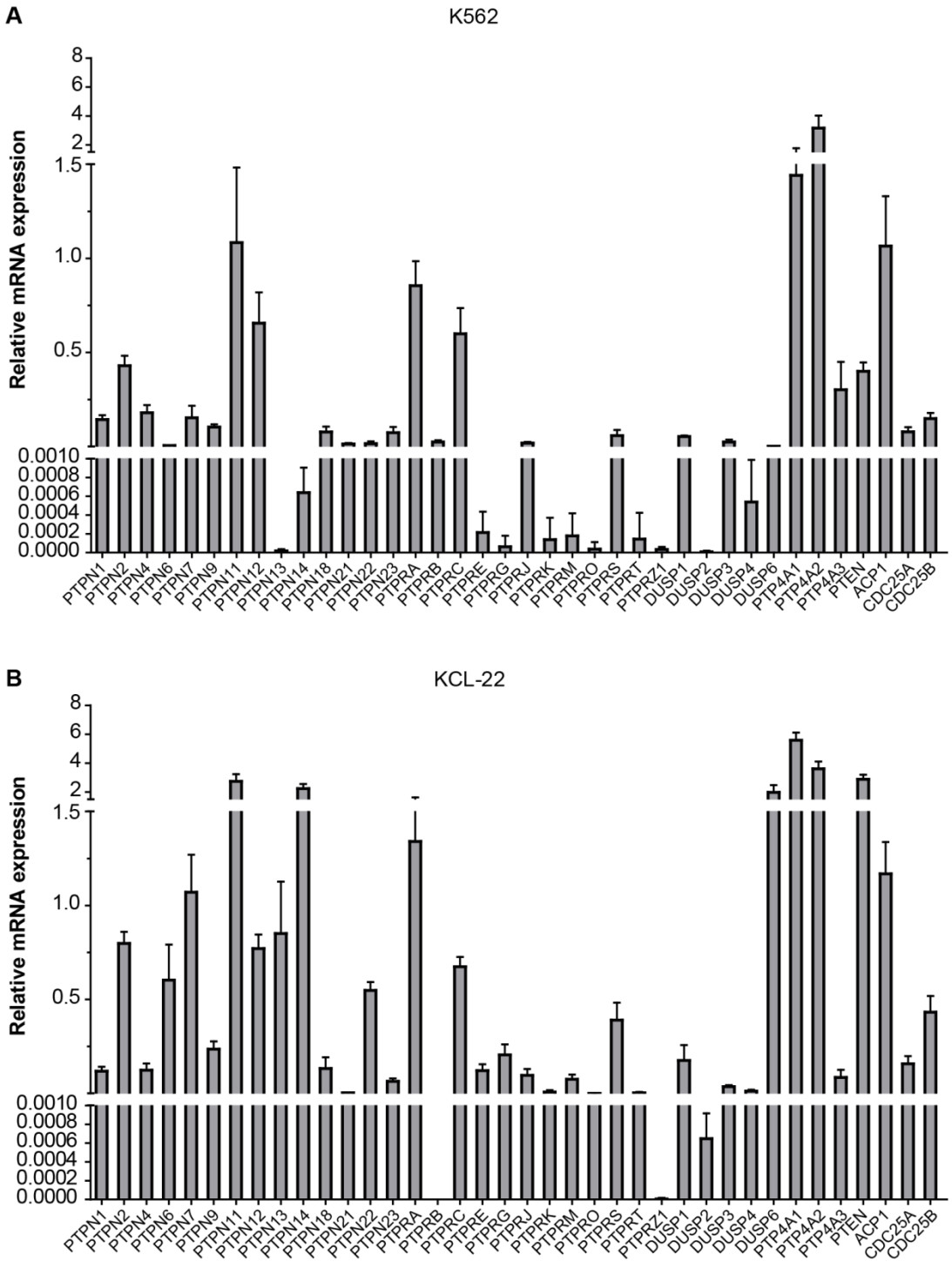

Figure 5-3. PTPs are differentially expressed in CML cell lines.
(**A**) The PTP mRNA expression status of the Ph^+ (BCR-ABL1, "b3a2") CML cell line K562 (derived from a 53-year-old female at CML blast crisis) was analyzed. *GUSB* and *B2M* were used as control genes. Shown are the mean relative expression values of n=4 independent measurements with technical duplicates + standard deviation (SD).
(**B**) The PTP mRNA expression status of the Ph^+ (BCR-ABL1, "b2a2") CML cell line KCL-22 (derived from a 32-year-old female at CML blast crisis) was analyzed. *GUSB* and *B2M* were used as control genes. Shown are the mean relative expression values of n=4 independent measurements with technical duplicates + standard deviation.

Table 5-3. Knockdown efficiencies of PTP genes in K562 and KCL-22 cells.

Gene	shRNA pLKO.1 construct number (only last digits)	Remaining relative expression	
		K562	KCL-22
PTPN6	6885	-	0.30
	6886	-	0.48
	11052	-	0.73
PTPN12	2830	0.67	0.33
	2831	0.77	0.31
	2832	0.87	0.39
PTPRC	2845	0.64	0.57
	2847	0.92	0.71
	2848	0.59	1.06
PTPRE	2893	-	0.92
	2894	-	0.63
	2896	-	0.61
DUSP1	2514	1.15	1.03
	2516	0.79	0.61
	2518	1.34	1.15
PTP4A2	2924	1.15	0.62
	2926	0.72	0.55
	2927	0.86	0.65
ACP1	2598	0.56	0.81
	2599	1.07	1.20
	2600	0.20	0.91

The cell pools highlighted were used for IC_{50} analyses in cell based assays (Figures 5-4, 5-5, and 5-6).

Using PTPN6 knockdown in KCL-22 cells, no clear answer to the question of whether or not it plays a role for treatment sensitivity was found. In nilotinib-treated cells, we saw a reduction of the IC_{50} in 5 of 6 experiments (with two different shRNAs), in imatinib-treated cells, we saw an increase in one cell pool, and a decrease in a cell pool generated using a different shRNA. Dasatinib-treated cells did also not seem to show any clear difference (Figure 5-6). Given these ambiguous first results, and the literature reports claiming a role of PTPN6 in imatinib treatment response, we chose to further analyze the influence of this PTP in more detail (chapter 5.3).

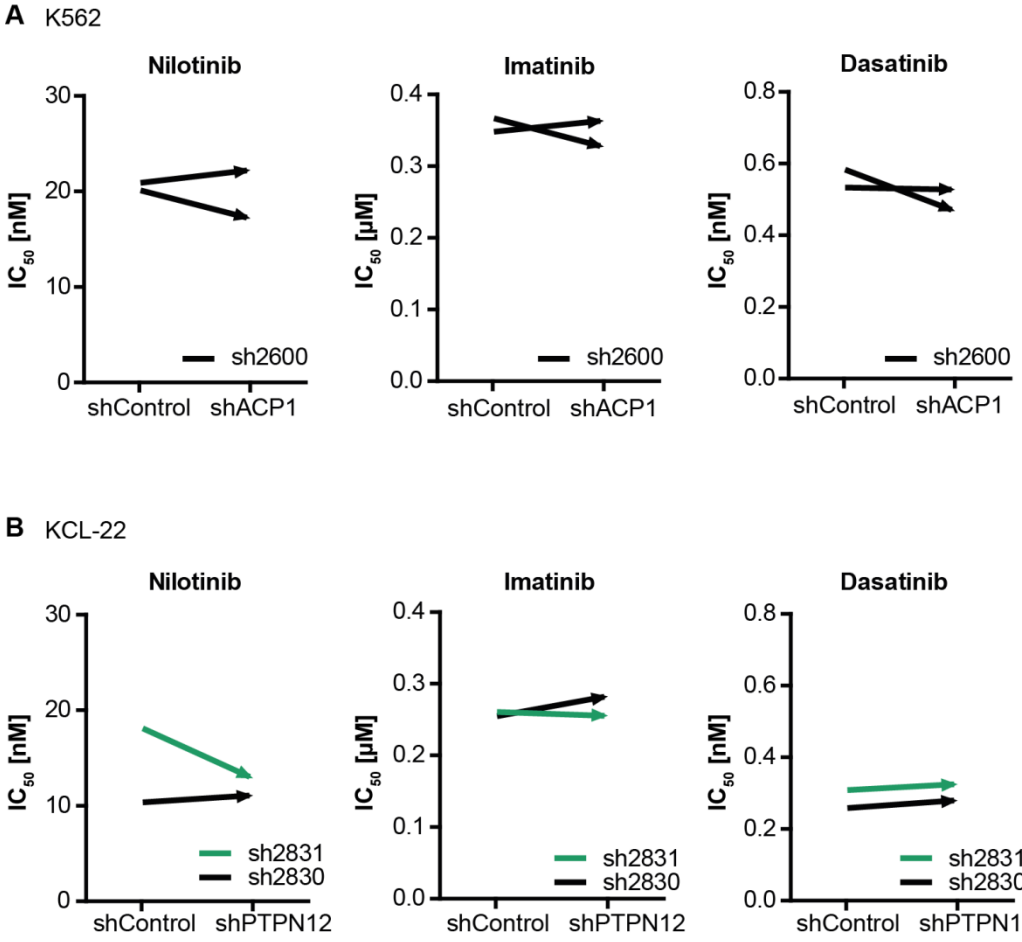

Figure 5-4. Knockdown of ACP1 or PTPN12 did not influence the TKI sensitivity in CML cell lines. (**A**) K562 cells with ACP1 knockdown (Table 5-3) were analyzed for the IC_{50} of nilotinib, imatinib, and dasatinib. Two independent experiments with quadruplicate technical replicas were carried out. One arrow represents one experiment.
(**B**) Two different cell pools of KCL-22 cells with PTPN12 knockdown (Table 5-3) were analyzed for the IC_{50} of nilotinib, imatinib, and dasatinib. One independent experiment of each cell pool (distinguished by color) with quadruplicate technical replicas was carried out. One arrow represents one experiment.

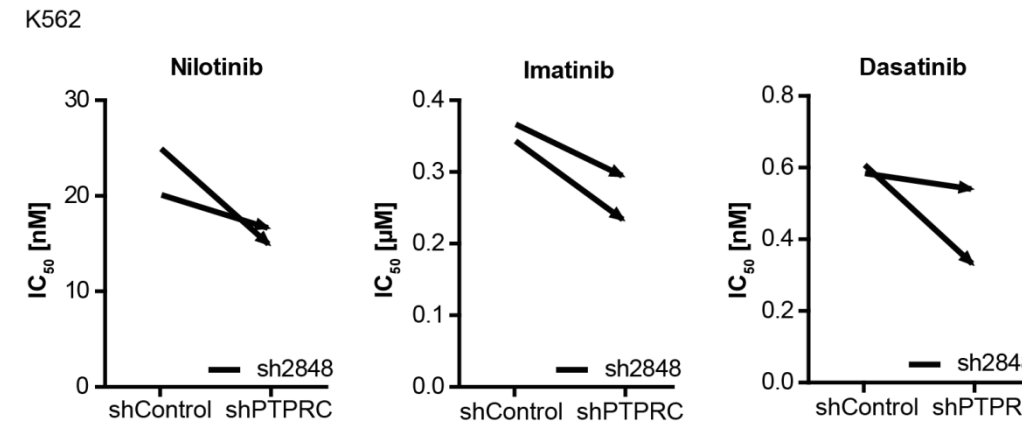

Figure 5-5. Knockdown of PTPRC did increase the TKI sensitivity in CML cell lines. K562 cells with PTPRC knockdown (Table 5-3) were analyzed for the IC_{50} of nilotinib, imatinib, and dasatinib. Two independent experiments with quadruplicate technical replicas were carried out. One arrow represents one experiment.

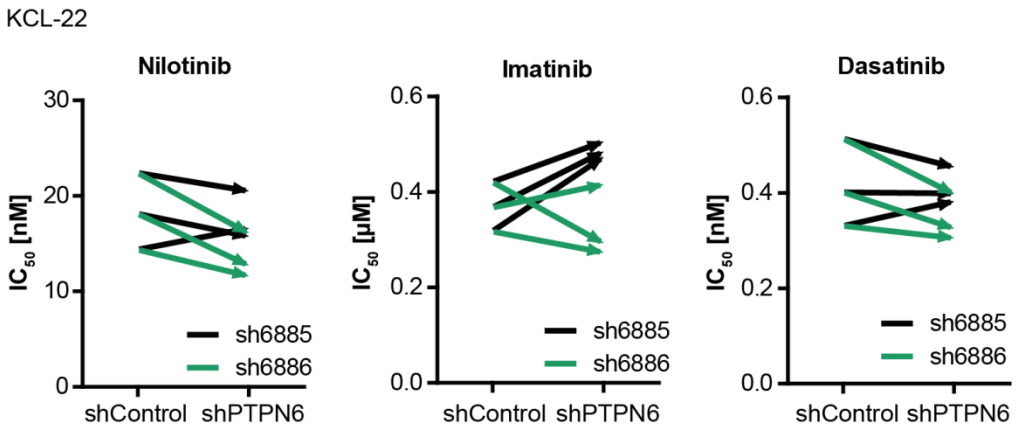

Figure 5-6. PTPN6 might influence the sensitivity of CML cells to TKI inhibitors.
Two different cell pools of KCL-22 cells with PTPN6 knockdown (Table 5-3) were analyzed for the IC_{50} of nilotinib, imatinib, and dasatinib. Three independent experiments of each cell pool (distinguished by color) with quadruplicate technical replicas were carried out. One arrow represents one experiment.

5.3 The role of PTPN6 for TKI treatment response

PTPN6 was not found to be associated with treatment outcome in our patient cohort (Figure 5-7) and the PTPN6-shRNA knockdown approach did neither clearly support, nor disagree with the literature reports on the influence of this PTP on the IC_{50} of the three tested TKI (see chapter 5.2). We therefore chose to include PTPN6 in a CRISPR/Cas9 knockout approach, to further clarify the role of PTPN6 on treatment response. Two CRISPR/Cas9 knockout cell clones (PTPN6-KO A and B) of KCL-22 cells were created and the knockout was confirmed by western blot (Figure 5-8, A). These cells and control cells transduced with the CRISPR/Cas9 vector lacking a guide RNA were analyzed for their IC_{50} of nilotinib, imatinib, and dasatinib (Figure 5-8, B). Again, comparable to the results in the shRNA knockdown experiments, no consistant change in the IC_{50} values was found in the knockout cell clones. In addition to the knockdown/knockout approaches, PTPN6 was over-expressed in K562 cells. These

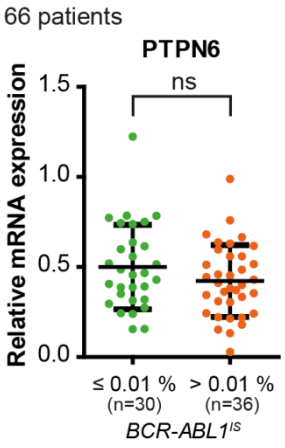

Figure 5-7: Expression level of PTPN6 is not associated with response after 9 months of nilotinib treatment. The RNA of total, peripheral blood leukocytes of CML patients in chronic phase was isolated and mRNA expression levels of 38 PTPs were analyzed. *GUSB* and *B2M* were used as control genes. Shown here is the PTPN6 mRNA level of 66 patients grouped according to their individual *BCR-ABL1*^{IS} (MR^4 yes or no) after 9 months of nilotinib treatment. Each point represents the relative PTP expression value of one patient, bars show mean values +/- standard deviation (SD). Differences in PTP mRNA expression between the patient groups were statistically tested. Not significant (ns), if $p > 0.05$. P values were calculated using the likelihood ratio test.

cells do express only very little endogenous PTPN6 (Figure 5-3, A; Figure 5-9, A).

We transduced the cells with either the empty vector (EV), or PTPN6 wild type (WT), or the catalytically inactive PTPN6-C453S (CS) mutant constructs. The expression level of both PTPN6 constructs was similar (Figure 5-9, A). These three cell pools were also analyzed for their IC_{50} of the three TKI (Figure 5-9, B). The over-expression of PTPN6 did not alter the IC_{50} of the analyzed K562 cells.

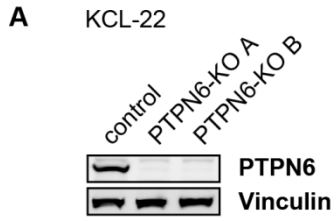

Figure 5-8. PTPN6 expression and response of CML cells to TKI. KCL-22 cells were subjected to CRISPR/Cas9-mediated knockout of the *PTPN6* gene. (**A**) Two individual single cell clones were analyzed for PTPN6 expression using western blot. (**B**) The engineered cells were analyzed for IC_{50} of nilotinib, imatinib, and dasatinib. Each dot represents the IC_{50} value determined in one independent experiment with quadruplicate technical replicas, black bars show the median of n=3 independent experiments.

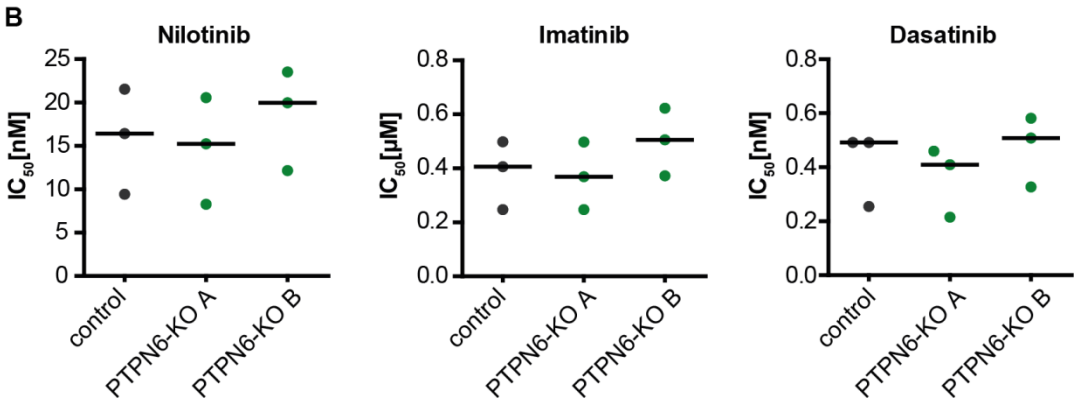

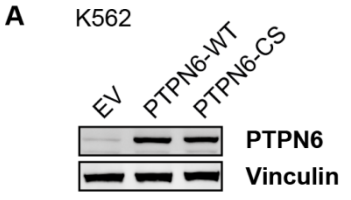

Figure 5-9. PTPN6 expression and response of CML cells to TKI. K562 cells with low endogenous PTPN6 expression were stably transduced with either empty vector (EV), wild type PTPN6 (WT), or the catalytically inactive PTPN6-C453S (CS) mutant. (**A**) Protein expression was analyzed by western blot. (**B**) The engineered cells were analyzed for IC_{50} of nilotinib, imatinib, and dasatinib. Each dot represents the IC_{50} value determined in one independent experiment with quadruplicate technical replicas, black bars show the median of n=3 independent experiments.

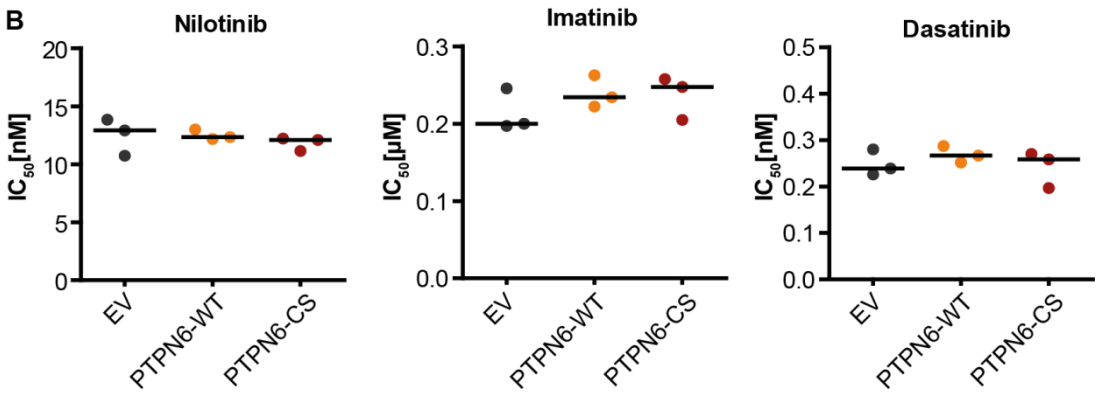

5.4 PTPRG increases nilotinib and imatinib treatment response, decreases clonogenic capacity, and modulates signal transduction of CML cells

In order to study the influence of PTPRG on treatment response, cells over-expressing either PTPRG wild type (WT), or the catalytically inactive PTPRG – C1060S (CS) mutant, or the respective empty vector (EV) were established. To initially characterize the PTPRG constructs, HEK293 cells were transiently transfected with PTPRG-WT or PTPRG-CS in combination with EGFR (Epidermal growth factor receptor), a PTPRG target (den Hertog, 2008). PTPRG-WT expressing cells showed prominent de-phosphorylation of EGFR, whereas PTPRG-CS cells did not show this activity, confirming the functionality of both constructs (data by B. V. Albert, a M.Sc. student in our lab (Albert, 2017), not shown).

I engineered K562 cells to obtain cell pools stably expressing empty vector (EV), or similar levels of PTPRG-WT or PTPRG-CS (Figure 5-10). They were subjected to IC_{50} assays with nilotinib, imatinib, and dasatinib. Fitted curves of one representative nilotinib experiment are shown in Figure 5-11, A. Note that only the concentration range from 2.5 nM to 50 nM is shown. IC_{50} values of n=6 independent experiments are shown for nilotinib (Figure 5-11, B), imatinib (Figure 5-11, C), and dasatinib (Figure 5-11, D). In case of nilotinib and imatinib, PTPRG-WT reduced the IC_{50} significantly compared to EV-cells, but in dasatinib-treated cells, no significant change of the IC_{50} was detectable. For two experiments carried out with 11 different nilotinib concentrations, the 95 % confidence intervals of the IC_{50} values were determined and are reported in Table 5-4. The 95 % confidence intervals of the PTPRG-WT IC_{50}s are not overlapping with the confidence intervals of EV or PTPRG-CS. The mean reduction of the IC_{50} for nilotinib compared to EV cells of the 6 experiments shown in Figure 5-11, B was 21.3 % in PTPRG-WT- and only 4 % in the PTPRG-CS-expressing cells, indicating a PTP activity dependent mechanism (Table 5-5).

Next, we wanted to analyze, whether PTPRG over-expression can also interfere with the BCR-ABL1 driven transforming capacity. Therefore colony formation assays were performed. We analyzed our engineered K562 cells for their ability to form colonies in methylcellulose. The cells were grown in methylcellulose in presence of 10 % serum for 7 days and colony numbers were counted. I performed six independent

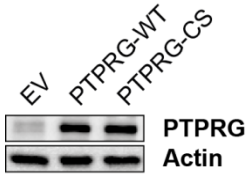

Figure 5-10. Stable over-expression of PTPRG-wild type (WT) and the phosphatase-dead mutant PTPRG-C1060S (CS) result in similar PTPRG expression levels. K562 cells were transduced with viral particles, resulting in the over-expression of PTPRG-WT or PTPRG-CS, or with viral particles made from respective empty vector (EV).

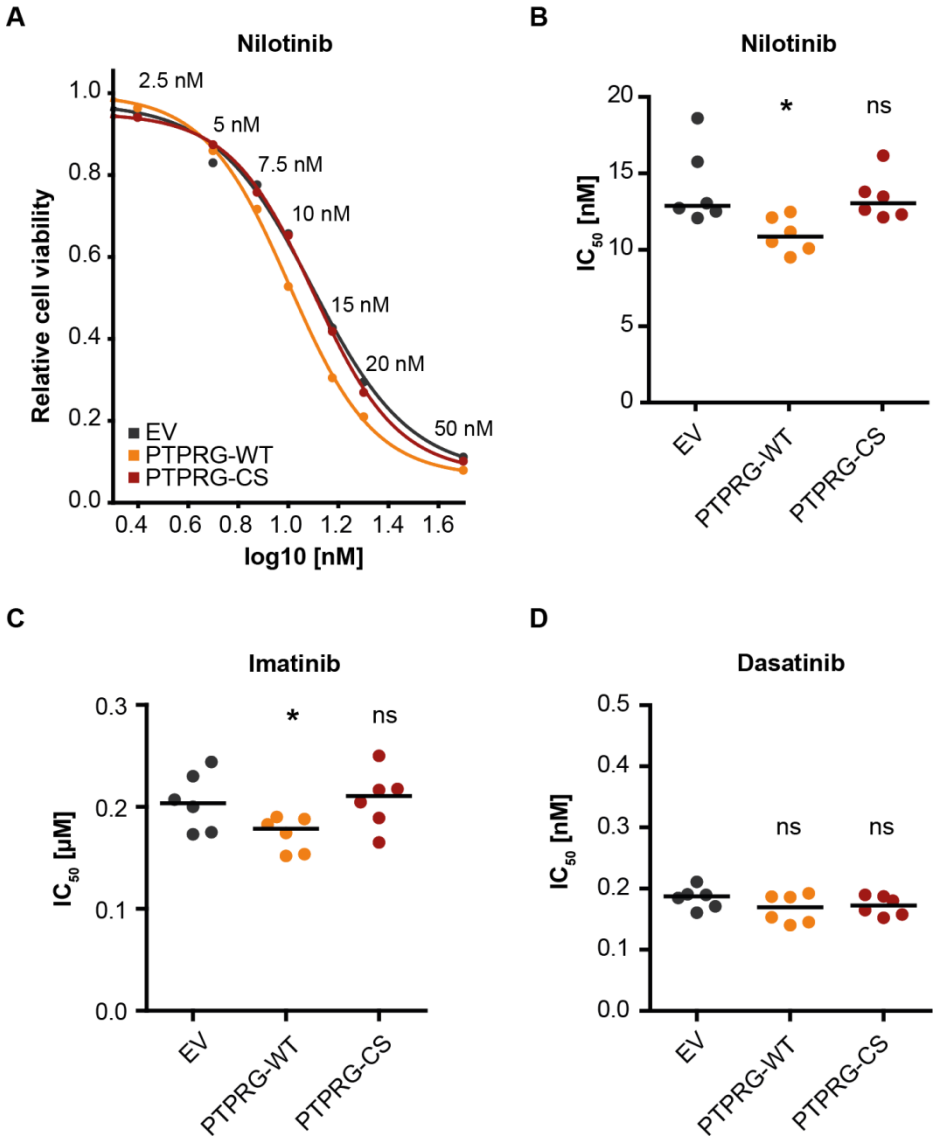

Figure 5-11. PTPRG modulates nilotinib and imatinib response in cell lines. (**A**) Fitted curves of one representative IC_{50} analysis carried out with 11 different nilotinib concentrations are shown. For more clarity, only dose ranges from 2.5 nM to 50 nM are presented.
IC_{50} analyses for nilotinib (**B**), imatinib (**C**), and dasatinib (**D**) were carried out with K562 cells stably expressing wild type PTPRG (WT) or catalytically inactive PTPRG-C1060S mutant (CS). PTPRG protein levels of engineered cells are shown in Figure 5-10. Each dot represents the IC_{50} value determined in one independent experiment with quadruplicate technical replicas, black bars show the median of n=6 independent experiments. Not significant (ns), if $p > 0.05$; * if $p < 0.05$. Comparison with the EV expressing cells was performed with the Wilcoxon matched-pairs test.

Table 5-4. IC_{50}s for nilotinib of K562 cells transduced with empty vector, PTPRG-WT, or PTPRG-CS, and respective 95 % confidence intervals of two representative experiments carried out with 11 nilotinib concentrations.

Nilotinib	Experiment A		Experiment B	
	IC_{50} [nM]	95 % confidence intervals	IC_{50} [nM]	95 % confidence intervals
EV	12.5	11.49 to 13.59	12.07	11.18 to 13.03
PTPRG-WT	10.09	9.785 to 10.41	9.515	8.614 to 10.51
PTPRG-CS	12.62	11.54 to 13.8	12.13	11.17 to 13.17

Table 5-5. Relative reductions of IC_{50}s for nilotinib compared to EV expressing K562 cells for the experiments shown in Figure 5-11 (B).

Nilotinib	IC_{50} % reduction EV vs.	
	PTPRG-WT	PTPRG-CS
Experiment 1	33.0	13.2
Experiment 2	12.1	-5.9
Experiment 3	23.2	12.5
Experiment 4	19.3	-1.0
Experiment 5	21.2	-0.5
Experiment 6	19.2	5.7
Mean % reduction compared to EV	**21.3**	**4.0**

experiments, and found a significant decrease in colony numbers of cells expressing PTPRG-WT compared to EV transduced cells, but no significant change when comparing control cells with cells expressing the mutant PTPRG-CS (Figure 5-12).

To get more information on the signaling cascades that might be involved in modulation of IC_{50} and colony formation, a screen for possible signaling molecules was done (data not shown). We decided to analyze BCR-ABL1 auto-phosphorylation, phosphorylation of SFK (especially cSRC and Lyn), STAT5, and ERK 1/2, and expression of p27 and Bcl-2 in more detail.

We followed two different approaches: First, the cells were analyzed after 4 h starvation from serum (4 h SFM, serum-free medium) in order to see effects that might otherwise be covered up by serum induced signaling (Figure 5-13). Second, cells were analyzed after 24 h of treatment with nilotinib or DMSO in presence of full growth medium, similar to the treatment in the IC_{50} assays (Figure 5-14). In the absence of serum (Figure 5-13), a decreased BCR-ABL1 auto-phosphorylation is visible in cells over-expressing PTPRG-WT, but not in cells expressing PTPRG-CS. The phosphorylation of SFK was analyzed and membranes were reprobed with specific antibodies for cSRC and Lyn, two SFK-members fitting to the molecular weights of the

detected phospho-SFK signals. A reduction of the pLyn signal was again found in the PTPRG-WT expressing cells, but not in PTPRG-CS expressing cells. The phosphorylation of ERK 1/2 tended to be affected in the same direction. In presence of serum (Figure 5-14, DMSO treatment), most of the described signaling modulations by PTPRG are not visible. They are possibly covered up by serum stimulation. Only the phosphorylation of ERK 1/2 appears moderately diminished in presence of PTPRG-WT. In presence of nilotinib (Figure 5-14, nilotinib treatment), the activation of most signaling mediators was eliminated; only the inhibition of SFK phosphorylation was partial. The signal for p27 strongly increased with the nilotinib treatment.

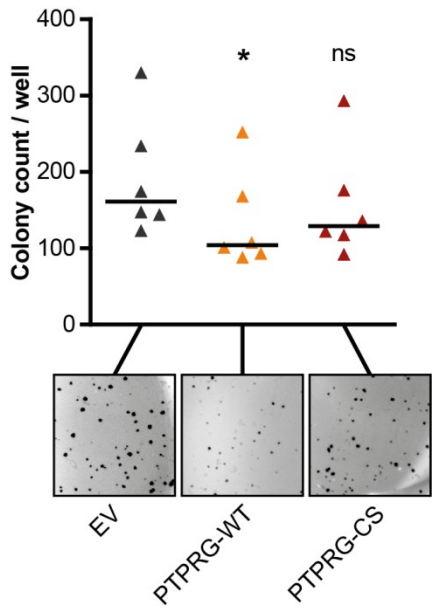

Figure 5-12. PTPRG attenuates BCR-ABL1 dependent cell transformation. K562 over-expressing PTPRG-WT or PTPRG-CS were analyzed for colony formation in methyl cellulose. Representative images of colonies are shown. Each triangle represents colony count per well (mean of duplicates of an individual experiment). Black bars represent the median of n=6 independent experiments. Not significant (ns), if $p > 0.05$; * if $p < 0.05$. Comparison with EV cells was performed with the Wilcoxon matched-pairs test.

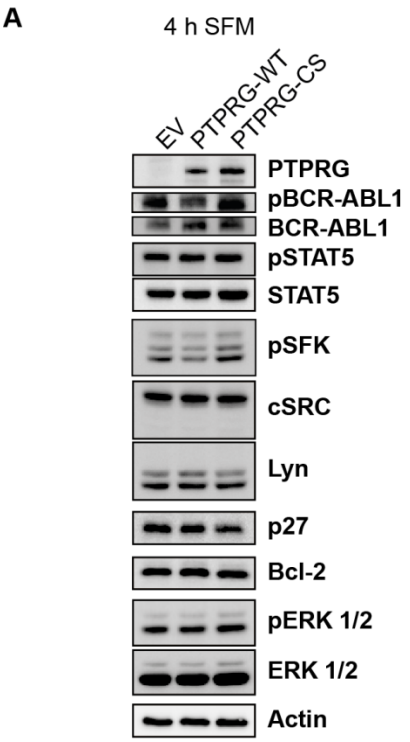

Figure 5-13. PTPRG over-expression attenuates BCR-ABL1 signal transduction. K562 cells over-expressing PTPRG-WT or PTPRG-CS were starved from serum for 4h (SFM). (**A**) Cell lysates were prepared and subjected to SDS-PAGE and immunoblotting with the indicated antibodies. Total protein was detected after stripping off the respective phospho-specific antibodies. Representative blots of n=3 independent experiments are shown.
(**B**) Quantification of blots from n=3 independent experiments: For BCR-ABL1, cSRC, Lyn, STAT5, and ERK 1/2, the phospho-signal was divided by the respective total protein signal. For p27 and Bcl-2, the specific signal was divided by the actin signal. The signals for PTPRG-WT and PTPRG-CS are reported relative to the EV cell signals of each experiment. Shown is the mean relative intensity of n=3 independent experiments +/- standard deviation.

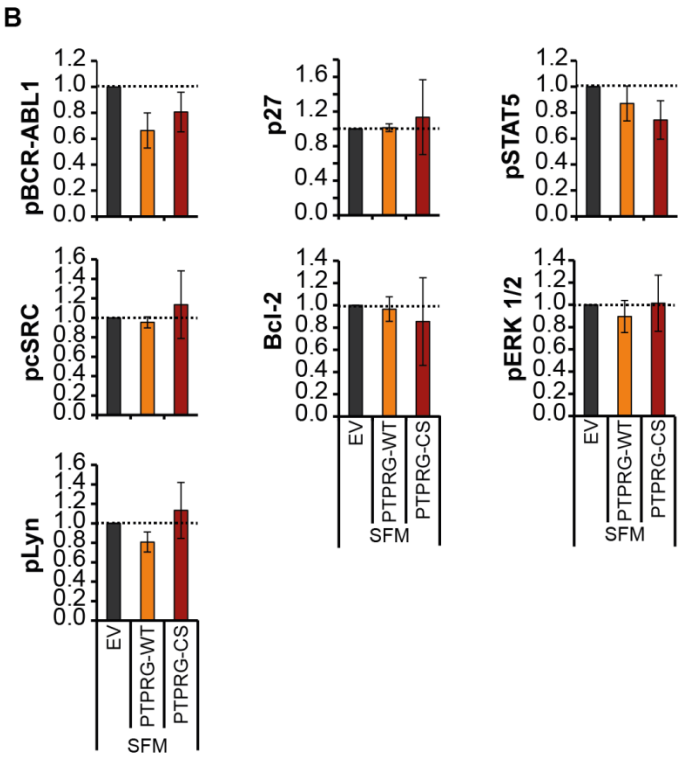

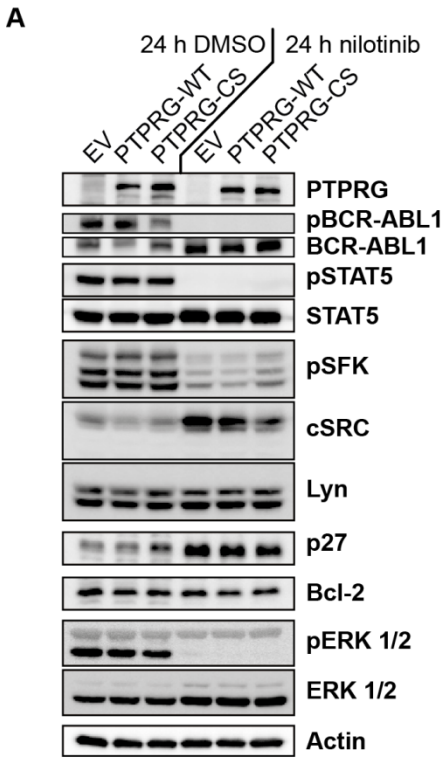

Figure 5-14. Nilotinib treatment and PTPRG over-expression affect BCR-ABL1 signal transduction in the same direction. (**A**) K562 cells over-expressing PTPRG-WT or PTPRG-CS were treated with nilotinib (1 µM, 24 h) or DMSO in presence of 10 % FCS. Cell lysates were prepared and subjected to SDS-PAGE and immunoblotting with the indicated antibodies. Total protein was detected after stripping off the respective phospho-specific antibodies. Representative blots of n=3 independent experiments are shown.
(**B**) Quantification of blots from n=3 independent experiments: For BCR-ABL1, cSRC, Lyn, STAT5, and ERK 1/2, the phospho-signal was divided by the respective total protein signal. For p27 and Bcl-2, the specific signal was divided by the actin signal. All signals are reported relative to the DMSO treated EV cell signals of the respective experiment. Shown is the mean relative intensity of n=3 independent experiments +/- standard deviation.

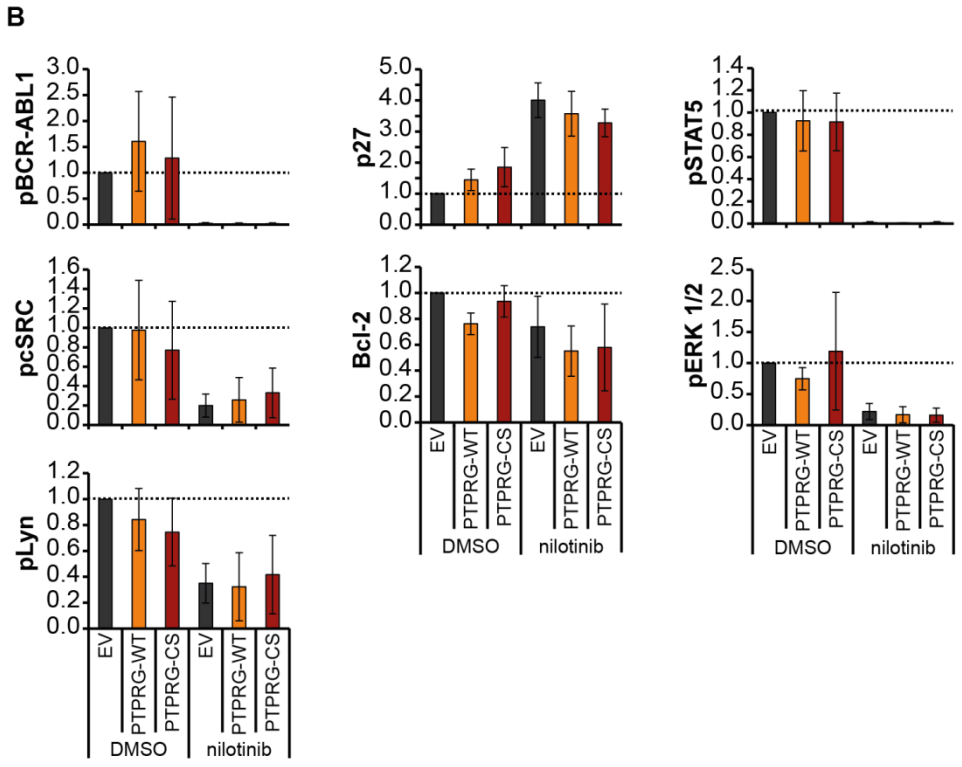

5.5 PTPRC decreases sensitivity to nilotinib and imatinib, increases the clonogenic capacity, and abrogates BCR-ABL1 signal transduction

In the shRNA-mediated knockdowns of PTPRC in K562 cells, a decrease of the IC_{50} for all tested TKI was seen, although the remaining mRNA expression of PTPRC was still around 60 % after knockdown. This observation suggested that PTPRC may in fact negatively affect the intrinsic sensitivity of CML cells to TKIs. In order to validate these findings, K562 cells with a CRISPR/Cas9-mediated PTPRC-knockout were created. Two single cell clones (KO A and B) were established, and one of them was additionally used to exogenously re-express PTPRC (KO A +PTPRC), or as control, was transduced with viral particles made from respective empty vector (KO A + EV). The cells were characterized for total protein expression by western blotting analysis (Figure 5-15, A). In the knockout cells, no PTPRC signal was detected, and the exogenous re-expression of PTPRC led to an expression level similar to that of the control cells, that were transduced with the CRISPR/Cas9 construct lacking a gRNA. The surface expression was analyzed by flow cytometry using a PTPRC specific antibody (Figure 5-15, B). The two knockout-cell lines, as well as the knockout cell line transduced with the empty vector did not have any PTPRC surface staining (comparable to unstained cells). The control- and PTPRC re-expressing cell lines expressed comparable PTPRC levels.

The PTPRC knockout- and re-expressing cells were subjected to the same analyses as described for the PTPRG over-expressing cells in chapter 5.4.

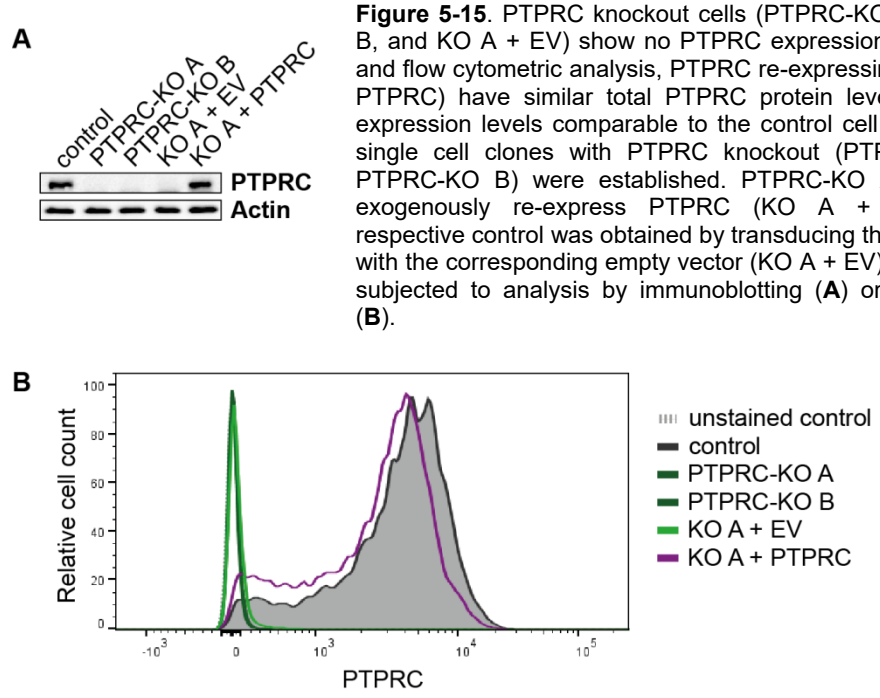

Figure 5-15. PTPRC knockout cells (PTPRC-KO A, PTPRC-KO B, and KO A + EV) show no PTPRC expression in total lysates and flow cytometric analysis, PTPRC re-expressing cells (KO A + PTPRC) have similar total PTPRC protein levels and surface expression levels comparable to the control cell line. Two K562 single cell clones with PTPRC knockout (PTPRC-KO A and PTPRC-KO B) were established. PTPRC-KO A was used to exogenously re-express PTPRC (KO A + PTPRC). The respective control was obtained by transducing the knockout cells with the corresponding empty vector (KO A + EV). The cells were subjected to analysis by immunoblotting (**A**) or flow cytometry (**B**).

First, the susceptibility of the engineered cell lines to TKI was tested using the IC_{50} assay. In Figure 5-16, A, representative fitted curves for IC_{50} assays carried out with nilotinib-treated cells show a shift to the left (lower nilotinib concentrations) of the PTPRC knockout cell lines. For two representative experiments carried out with 11 different nilotinib concentrations, the calculated IC_{50} values and their corresponding 95 % confidence intervals are shown in Table 5-6. The confidence intervals of the PTPRC expressing cells (control and KO A + PTPRC) are not overlapping with the intervals calculated from the PTPRC knockout cell lines (PTPRC-KO A, PTPRC-KO B, and KO A + EV). In Figure 5-16, B, C, and D, calculated IC_{50} values of six independent experiments for nilotinib, imatinib, and dasatinib are shown respectively. The IC_{50} values of nilotinib and imatinib were significantly lower in the cell lines lacking PTPRC. In the dasatinib-treated cells, the IC_{50} was affected to a lesser extent. A significant difference was observed only for one of the tested knockout cell lines. PTPRC knockout led to a mean nilotinib IC_{50} reduction of 23.2 – 27.6 % compared to the control cell line, and the re-expression of PTPRC led to an increase of the IC_{50} back to the levels of control cells (Table 5-7).

Similar to the analyses in PTPRG-expressing cells, we addressed the question, whether the PTPRC-KO does have an impact on the BCR-ABL1 driven transforming capacity, in absence of TKI. The control and PTPRC-KO cells were therefore analyzed for their colony forming capacity in methylcellulose. The PTPRC knockout cells formed significantly less colonies within 7 days of cultivation compared to the PTPRC expressing control cells (Figure 5-17, A). The transduction of the PTPRC knockout cells with the empty lentiviral control vector already led to an increase in colony formation of the KO A + EV cells probably caused by the required second round of lentiviral transduction. However, even this elevated colony formation could be moderately, but significantly further enhanced by PTPRC expression (Figure 5-17, B).

In order to analyze the signaling proteins that might be involved in the mediation of the described differences between PTPRC expressing and PTPRC knockout cells, we analyzed the cells by western blotting, under the two conditions already described for the PTPRG expressing cells. The cells were cultivated for 4 h in SFM (Figure 5-18), or for 24 h in presence of 10 % FCS and DMSO or nilotinib (Figure 5-19) and cell lysates were analyzed for the signaling molecules introduced in chapter 5.4.

The phosphorylation of BCR-ABL1 was moderately increased in the PTPRC knockout cells, both in presence and absence of serum. Absence of PTPRC led also to an increase in ERK 1/2 phosphorylation under both conditions, with even stronger phosphorylation signals in presence of serum (Figures 5-17 and 5-18).

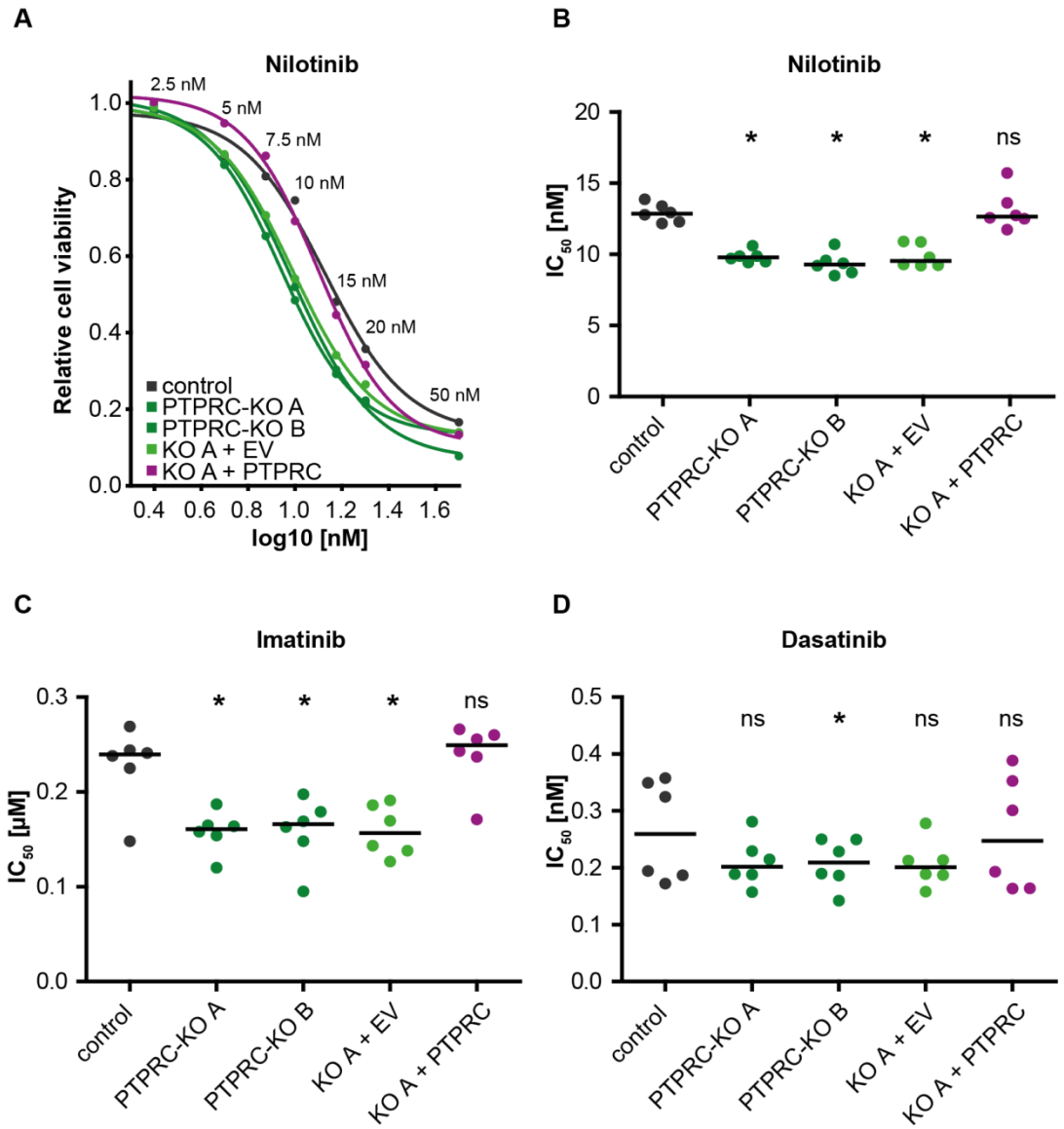

Figure 5-16. PTPRC modulates nilotinib and imatinib response in cell lines. (**A**) Fitted curves of one representative IC_{50} analysis carried out with 11 different nilotinib concentrations are shown. For more clarity, only dose ranges from 2.5 nM to 50 nM are presented.
IC_{50} analyses for nilotinib (**B**), imatinib (**C**), and dasatinib (**D**) were carried out with two individual clones (A and B) of K562 cells obtained by CRISPR/Cas9-mediated knockout of the *PTPRC* gene and corresponding control cells. Additionally, PTPRC-KO clone A was used to re-express PTPRC by lentiviral transduction (KO A + PTPRC; control: KO A + EV (empty vector)) PTPRC protein levels of engineered cells are shown in Figure 5-15. Each dot represents the IC_{50} value determined in one independent experiment with quadruplicate technical replicas, black bars show the median of n=6 independent experiments. Not significant (ns), if $p > 0.05$; * if $p < 0.05$. Comparison with the EV cells was performed with the Wilcoxon matched-pairs test.

Table 5-6. IC_{50}s for nilotinib of PTPRC knockout cell clones and re-expressing cells and respective 95 % confidence intervals of two representative experiments carried out with 11 nilotinib concentrations.

Nilotinib	Experiment A		Experiment B	
	IC_{50} [nM]	95 % confidence intervals	IC_{50} [nM]	95 % confidence intervals
control	13.39	12.11 to 14.8	12.29	11.08 to 13.62
PTPRC-KO A	9.706	9.25 to 10.18	9.87	8.985 to 10.84
PTPRC-KO B	8.726	8.522 to 8.934	8.51	8.052 to 8.995
KO A + EV	9.791	9.353 to 10.25	9.247	8.618 to 9.921
KO A + PTPRC	12.58	11.92 to 13.28	12.74	11.99 to 13.53

In nilotinib-treated cells, the BCR-ABL1 phosphorylation was completely abolished in all cell lines and also the ERK 1/2 signal was strongly reduced. The phosphorylation of the SFKs cSRC and Lyn was reduced in the PTPRC knockout cells, most prominently seen in absence of serum. The expression of the cell cycle inhibitor p27 was elevated in the engineered knockout cell lines, which was seen only in presence of serum (Figure 5-19, DMSO). This elevation was further promoted by nilotinib treatment. Importantly, all PTPRC knockout effects were rescued by the exogenous re-expression of PTPRC in one of the knockout clones.

Table 5-7. Relative nilotinib IC_{50} reductions compared to CRISPR/Cas9 control K562 cells for the experiments shown in Figure 5-16 B.

Nilotinib	IC_{50} % reduction control vs.			
	PTPRC-KO A	PTPRC-KO B	KO A + EV	KO A + PTPRC
Experiment 1	17.0	26.7	28.0	-23.0
Experiment 2	31.6	22.8	33.1	15.4
Experiment 3	27.1	26.0	16.0	-5.3
Experiment 4	19.0	24.3	10.4	-2.6
Experiment 5	27.5	34.8	26.9	6.0
Experiment 6	19.7	30.8	24.8	-3.7
Mean % reduction compared to control	**23.7**	**27.6**	**23.2**	**-2.2**

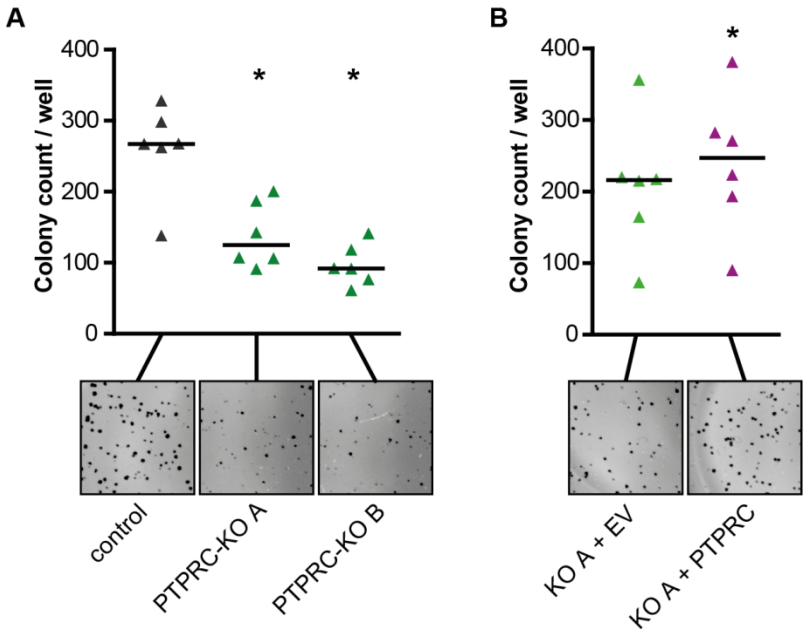

Figure 5-17. PTPRC promotes BCR-ABL1 dependent cell transformation. K562 *PTPRC* knockout clones A and B (**A**), or PTPRC re-expressing cells (KO A + PTPRC) (**B**) were analyzed for colony formation in methyl cellulose. Representative images of colonies are shown. Each triangle represents colony count per well (mean of duplicates of an individual experiment). Black bars represent the median of n=6 independent experiments. * if $p < 0.05$. Comparison with CRISPR/Cas9 control (**A**) or PTPRC KO A cells transduced with empty vector (KO A + EV) (**B**) was performed with the Wilcoxon matched-pairs test.

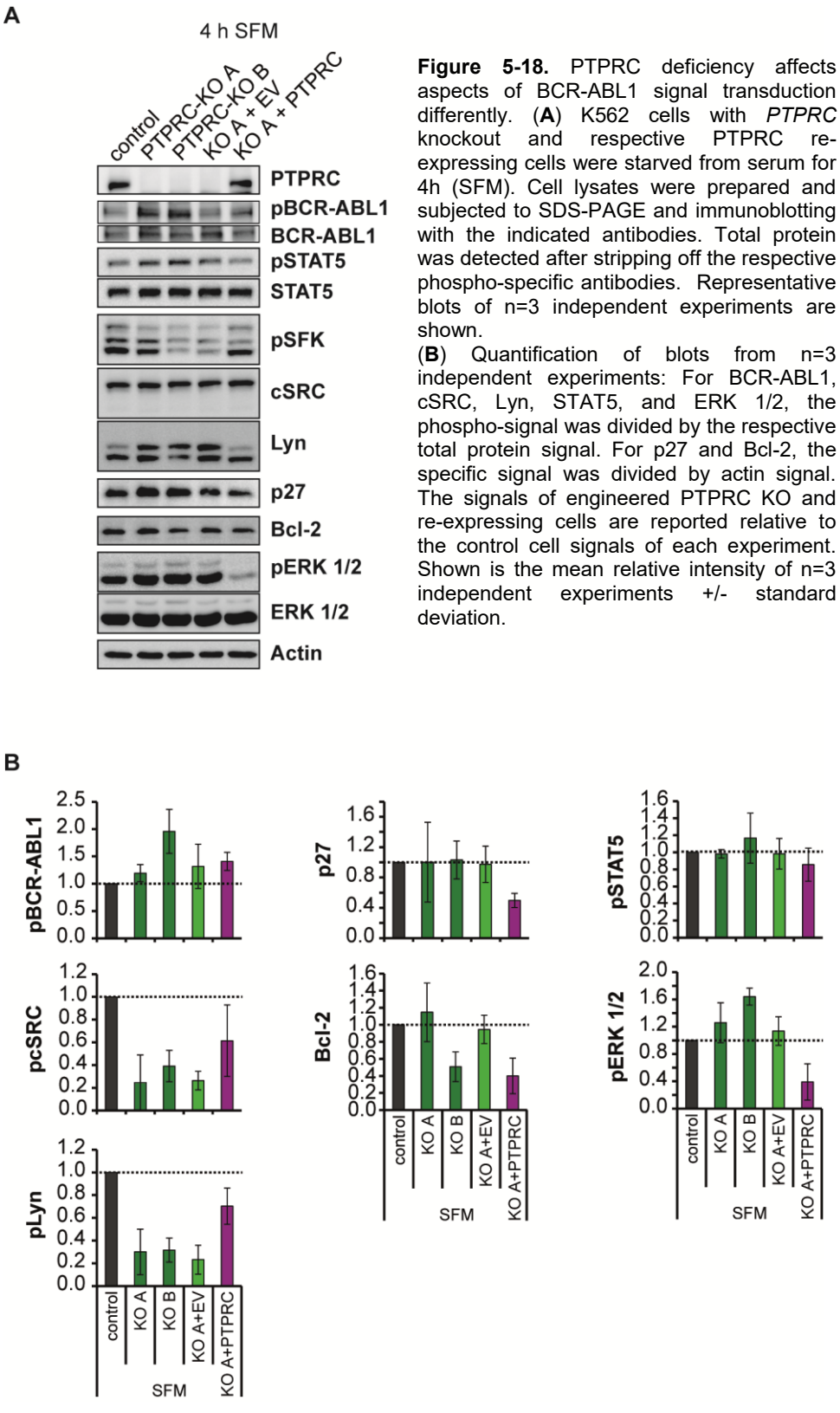

Figure 5-18. PTPRC deficiency affects aspects of BCR-ABL1 signal transduction differently. (**A**) K562 cells with *PTPRC* knockout and respective PTPRC re-expressing cells were starved from serum for 4h (SFM). Cell lysates were prepared and subjected to SDS-PAGE and immunoblotting with the indicated antibodies. Total protein was detected after stripping off the respective phospho-specific antibodies. Representative blots of n=3 independent experiments are shown.
(**B**) Quantification of blots from n=3 independent experiments: For BCR-ABL1, cSRC, Lyn, STAT5, and ERK 1/2, the phospho-signal was divided by the respective total protein signal. For p27 and Bcl-2, the specific signal was divided by actin signal. The signals of engineered PTPRC KO and re-expressing cells are reported relative to the control cell signals of each experiment. Shown is the mean relative intensity of n=3 independent experiments +/- standard deviation.

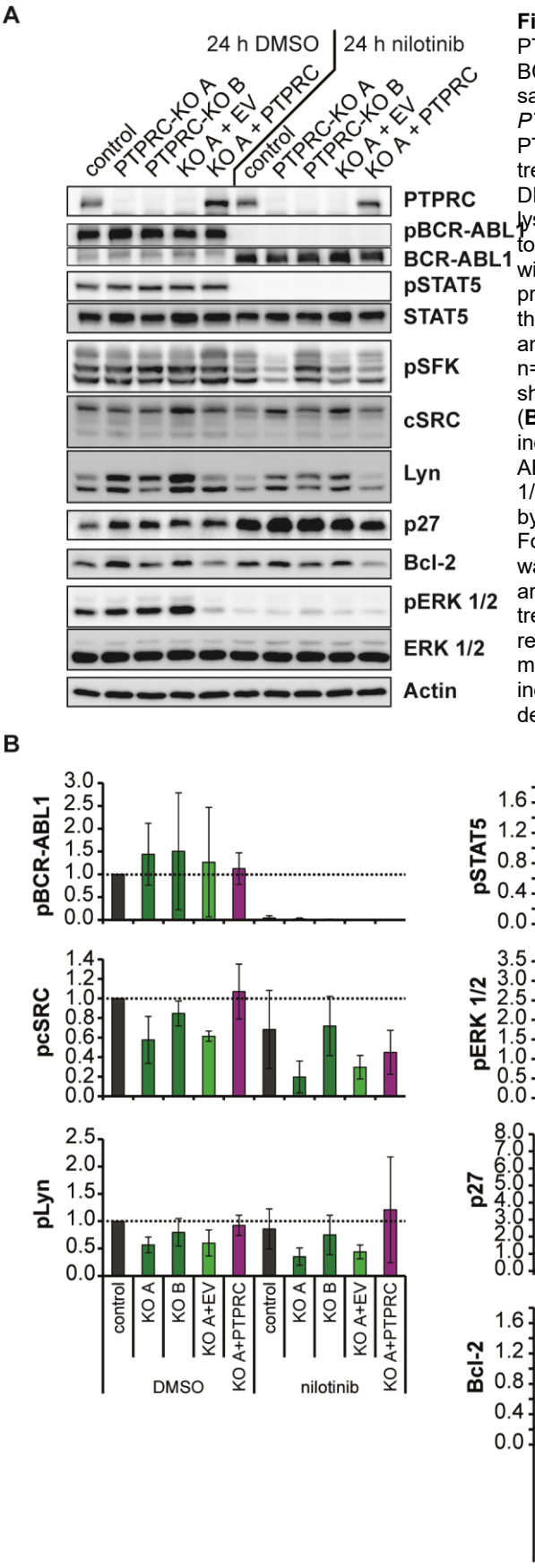

Figure 5-19. Nilotinib treatment and PTPRC deficiency affect aspects of BCR-ABL1 signal transduction in the same direction. (**A**) K562 cells with *PTPRC* knockout and respective PTPRC re-expressing cells were treated with nilotinib (1 µM, 24 h) or DMSO in presence of 10 % FCS. Cell lysates were prepared and subjected to SDS-PAGE and immunoblotting with the indicated antibodies. Total protein was detected after stripping off the respective phospho-specific antibodies. Representative blots of n=3 independent experiments are shown.
(**B**) Quantification of blots from n=3 independent experiments: For BCR-ABL1, cSRC, Lyn, STAT5, and ERK 1/2, the phospho-signal was divided by the respective total protein signal. For p27 and Bcl-2, the specific signal was divided by actin signal. All signals are reported relative to the DMSO treated control cell signals of the respective experiment. Shown is the mean relative intensity of n=3 independent experiments +/- standard deviation.

5.6 Combination-therapy approaches

The PTPRC knockout cells have an increased sensitivity to the TKI nilotinib (chapter 5.5) and these cells have a higher expression of p27 than the control cells (Figure 5-19). In addition, p27 levels increase upon nilotinib treatment. I therefore considered a combination-treatment of nilotinib with a p27-inducing agent might be beneficial to the treatment outcome.

P27 is known to be negatively regulated by PI3K (phosphoinositide 3-kinase) signaling (Crivellaro, 2016). An abundant PI3K in hematopoietic cells is PI3Kδ. The PI3Kδ inhibitor idelalisib (CAL-101, GS-1101) which is approved for treatment of B-cell leukemia/lymphoma, has recently been shown to cause elevation of p27 in CML cells (Chen, 2016). In this thesis, a combination approach of the TKI nilotinib together with the PI3Kδ inhibitor idelalisib was tested in the IC_{50} assay for parental K562 cells. The IC_{50} assay was carried out with the 7 standard concentrations of nilotinib in presence of either DMSO (vehicle), 1 µM, or 10 µM idelalisib for 72 hours. The combination of these two inhibitors resulted in an idelalisib-dose-dependent reduction of IC_{50} for nilotinib (Figure 5-20, A). In western blot analyses it was shown, that the treatment of K562 cells resulted in the expected dose-dependent decrease of AKT phosphorylation, and a slight increase in p27 levels (Figure 5-20, B).

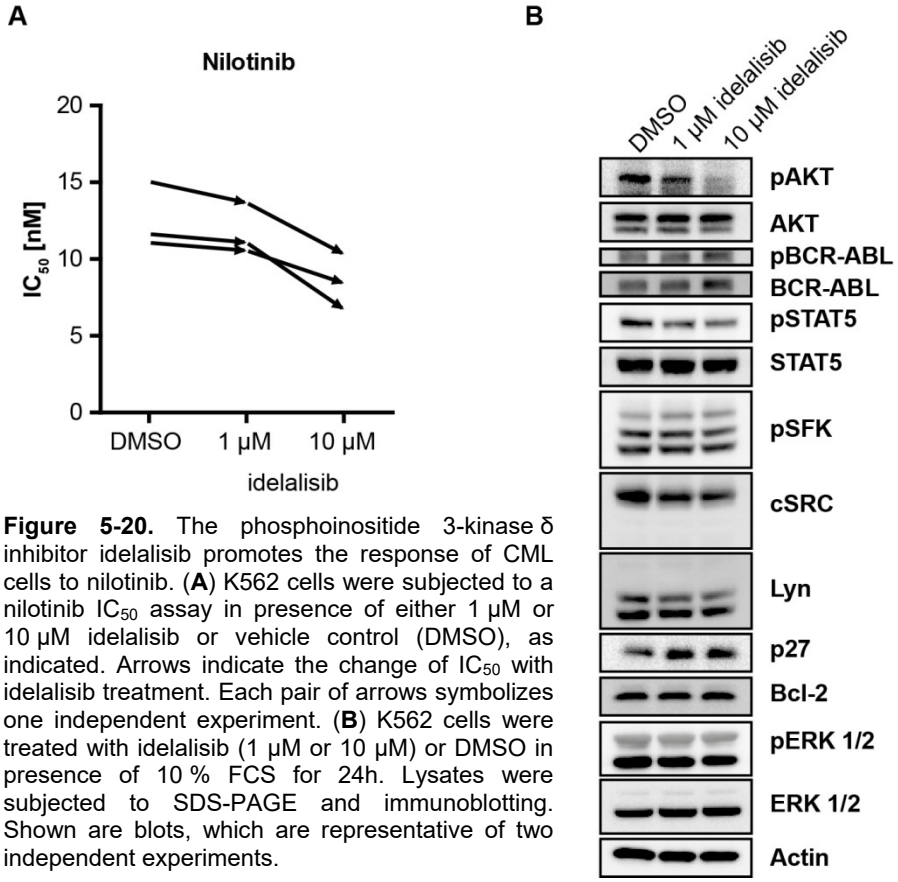

Figure 5-20. The phosphoinositide 3-kinase δ inhibitor idelalisib promotes the response of CML cells to nilotinib. (**A**) K562 cells were subjected to a nilotinib IC_{50} assay in presence of either 1 µM or 10 µM idelalisib or vehicle control (DMSO), as indicated. Arrows indicate the change of IC_{50} with idelalisib treatment. Each pair of arrows symbolizes one independent experiment. (**B**) K562 cells were treated with idelalisib (1 µM or 10 µM) or DMSO in presence of 10 % FCS for 24h. Lysates were subjected to SDS-PAGE and immunoblotting. Shown are blots, which are representative of two independent experiments.

6 Discussion

6.1 CML treatment response to nilotinib correlates with PTP mRNA expression

In the study presented in this thesis, a comprehensive analysis of the potential influence of PTPs on the treatment outcome of CML patients was carried out. In this screen, we found the expression of PTPRA, PTPRC, PTPRG, PTPRM, and PTPN13 to be positively correlated to nilotinib treatment efficiency. In contrast to other reports describing effects of PTPs on imatinib treatment (Shimizu, 2004; Koyama, 2006; Esposito, 2011; Mitra, 2013; Kok, 2014; Papadopoulou, 2016), our study was designed to investigate the influence of PTPs on the more potent second-generation TKI nilotinib. Such analyses have previously not been performed. For PTPRA, PTPRC, and PTPRM, no reports on a possible role in CML exist. Our study identifies them as interesting candidates for studies in CML background. The current aim of CML treatment has developed to the point, that not only the control of the disease by lifelong TKI treatment is desirable, but to optimize therapy, so that patients can safely stop their TKI treatment, and still remain in TFR. In order to do so, a fast and continuing achievement of a deep molecular response is required (Mahon, 2002; Mahon, 2010). Taking this into account, we chose having a MR^4 (*BCR-ABL1*^{IS} ≤ 0.01 %) after 9 months of nilotinib treatment as a particularly stringent cutoff point. The ELN guidelines define the achievement of MMR (*BCR-ABL1*^{IS} ≤ 0.1 %) after 12 months of TKI treatment as optimal response. In our study, we analyzed the mRNA expression status of 38 PTPs in total peripheral blood leukocytes of 66 newly diagnosed CML patients. To correlate the influence of a single PTP to the course of disease, two patient groups were defined according to whether or not a patient had reached a *BCR-ABL1*^{IS} ≤ 0.01 % (MR^4) after 9 months of nilotinib treatment. It is remarkable, that the pronounced effect of nilotinib appears still modulated by the PTP-status.

Interestingly, we could not find correlations with response for PTPN1 (Koyama, 2006), PTPN2 (Shimizu, 2004; Mitra, 2013), or PTPN6 (Esposito, 2011). These PTPs were previously reported to have an influence on imatinib treatment. However, contradictory findings were published for PTPN2 (Shimizu, 2004; Mitra, 2013; Kok, 2014) and PTPN6 (Esposito, 2011; Papadopoulou, 2016). One reason for the lack of association in our study might be that the more potent inhibitor nilotinib overcomes influences of those PTPs. Nevertheless, PTPN6 was still included in functional analyses (see below).

The selection of the 66 CML patient samples was done, not knowing the characteristics of the patients, or their treatment outcome, to enable a completely

blinded analysis. The only selection criterion was the active participation in the TIGER study. After the mRNA analyses had been finished, the patient characteristics were analyzed in more detail. Since the TIGER study protocol allowed certain pretreatments (TKI, HU), and the actual nilotinib dosing was allowed to be adjusted according to the patient's needs (side effects, adverse events), all available data for each patient were re-assessed after unblinding. Two cohorts with sub-sets of patients (n=54 and n=35 patients) were defined (chapter 5.1), with the n=35 patient sub-group literally having no pretreatments, and only minor nilotinib drug dose reductions. In these stringently selected sub-sets, the correlation to treatment outcome of the 5 PTPs (found in the initial analysis of the n=66 patients cohort) was re-evaluated. Doing so, we aimed to exclude influences of the pretreatment that might have already changed the PTP mRNA expression level in our analyzed samples, or insufficient treatment responses caused by nilotinib dose reductions, that both would compromise our results. PTPRA, PTPRC, and PTPRG could be confirmed to be significantly associated to MR^4 achievement after 9 months of study treatment in all sub-groups, supporting the initial finding, that these PTPs might play a role in modulating nilotinib treatment response. The significance for PTPRM was lost in one of the sub-groups, and for PTPN13, no significance could be confirmed in the newly defined patient sub-sets (Figure 5-2, Table 5-2).

Nevertheless, the smaller cohort sizes do limit the statistical power and significances could have been overlooked. If the identified PTPs should in the future be used as biomarkers for response, it would require additional analyses in larger patient cohorts.

PTPN13 was earlier described in 4 different publications by the same working group to be involved in the persistence of CML-leukemic stem cells (LSC) in the bone marrow (Huang, 2008; Huang, 2013a; Huang, 2013b; Huang, 2016). They describe PTPN13 as a factor contributing to treatment resistance of LSC. An inhibition of PTPN13 in their study reduced the LSC persistence (Huang, 2016). This would make PTPN13 a very interesting PTP to be followed up, but as the correlation with treatment response was lost in the more stringently selected patients, we did further analyze PTPN13 in our study. PTPRA, PTPRC, and PTPRG were still significantly associated with treatment outcome in all the analyzed patient cohorts, but we decided to continue the functional analyses only with PTPRC and PTPRG.

The analysis of PTP expression can be done using leukocytes of different origin *e. g.* bone marrow aspirates or peripheral blood, and these cells can either be used in total, or sub-populations can be selected, thereby focusing on specific cell types, but excluding others. Patient cDNA samples derived from peripheral blood were more

easily available than bone marrow aspirates. Therefore, we did not include bone marrow samples in our study, and focused on peripheral blood samples. A common sub-population of leukocytes are PBMCs (peripheral blood mononuclear cells), consisting of mainly lymphocytes and monocytes, but not including the multi-lobed nuclei-containing granulocytes. Since BCR-ABL1-mediated transformation affects the whole myeloid linage and granulocytes are an important and abundant group of CML cells, we did not want to exclude them from our study. Initially, all transformation in CML arises in HSCs. Therefore, analysis of only $CD34^+$ (a stem cell marker) cells would also be a relevant approach. The advantage of that would be to have a defined cell sub-set, more independent from the individual leukocyte composition of each patient. Moreover, eradication of CML stem cells is the ultimate aim of the therapy. Therefore these cells would be very relevant to assess response or resistance to therapy. There are only few $CD34^+$ cells in peripheral blood, thus isolation of sufficient cells for our mRNA analysis would have required bone-marrow samples. Therefore, these cells appeared not suitable for a large screening project, as they are not isolated in standard diagnostic procedures. Taken together, these reasons led us to choose total leukocytes from peripheral blood for our screen. As already indicated, the use of total leukocytes might lead to false positive or to the concealment of screening hits, since the individual percentage of different cell types with specifically high or low expression of PTPs might influence the result of our analysis. This was one of the reasons why functional, cell based analyses appeared mandatory to evaluate the intrinsic influence of selected PTPs on treatment response.

The PTP-status of the patients was determined only once at diagnosis and not again under TKI treatment, as the blood cell counts usually normalize within a few weeks of treatment (complete hematologic response), and then, no malignant cells would be present in the peripheral blood anymore. An additional analysis of PTP expression during nilotinib treatment would therefore reflect the status of a healthy donor and would not give any additional information with respect to a role of PTP levels for treatment response.

6.2 Experimental conditions to assess TKI responses in engineered CML cell lines

For the functional analyses, a direct assessment of the therapy response was chosen: the determination of nilotinib, imatinib, and dasatinib IC_{50} in cell lines with manipulated PTP levels. A similar approach was recently used by Chae *et al.* in an AML study (Chae, 2018). In our study, the engineered cells were treated with a

concentration range of the TKIs and the differences in the treatment susceptibility between the cell lines that express a specific PTP or not, were measured directly. For the specific configuration of these experiments, a number of considerations were important: As the compounds are not stable in aqueous solutions, the dilutions (1:200 from DMSO stock) had to be prepared fresh for every experiment. Small inaccuracies of these dilution steps would influence the resulting IC_{50}, therefore, all the experiments of one setup were strictly processed in parallel with the identical TKI dilution, to rule out differences caused by preparation of drug dilutions. To measure cell viability, the CellTiter Blue reagent was chosen, since it can directly be added to the cultured cells and the fluorescence signal can be measured directly without any further solubilization steps or medium changes. Mean values of measured fluorescence signals (quadruplicate replicas) were the base for the curve-fitting by Sigma Plot (chapter 4.12). The IC_{50} is then automatically calculated from this fitted curve. The curve-fitting is more accurate, the more values are used. Therefore, selected experiments were carried out with more TKI concentrations in the concentration range of the IC_{50}, and the corresponding 95% confidence intervals, as markers of the curve-fitting error were obtained. In these experiments, the confidence intervals were not overlapping between cell lines with different IC_{50}s (Tables 5-4 and 5-6). This proves that the reported differences are real, despite being relatively small. By using the Wilcoxon matched-pairs test for calculating the statistical significance of the differences between the engineered cells, we took into account that results obtained in the same experiment (identical dilutions) should be compared to each other, since the absolute values might have varied somewhat at different experimental days.

In order to get insight into the signaling changes that might be involved in the alterations of TKI response in PTPRG over-expressing and PTPRC knockout K562 cells, several signaling molecules were analyzed by western blotting analysis. First, BCR-ABL1 auto-phosphorylation (pY245- c-ABL1) was included in the analysis, since changes of that would hint on a direct impact of the PTP level change on BCR-ABL1 activity. STAT5 is constitutively activated by BCR-ABL1 and thereby contributes to the transformation of CML cell lines (*e. g.* K562) (de Groot, 1999). The analysis of the influence of PTPRG or PTPRC on pSTAT5 is therefore worth addressing. Since PTPRC is a known SFK-phosphatase (chapter 1.2.5), and BCR-ABL1 causes activation of SFK, the analysis of the activating phosphorylation of SFK (with an antibody detecting pY416-cSRC) was included in the study. The corresponding total proteins cSRC and Lyn were chosen since their size exactly matched the three bands visible in the phospho-SFK-blots. Lyn kinase has been shown to suppress apoptosis, specifically in BCR-ABL1-expressing cells, which makes Lyn an especially interesting

protein to study in our context (Ptasznik, 2004). PTPRG has earlier been described to reduce the phosphorylation of ERK 1/2 (Shu, 2010; Xiao, 2014). Also ERK-activation occurs constitutively downstream of BCR-ABL1 (Weisberg, 2007). Thus, ERK 1/2 was also included in the signaling analysis. In the study of Shu *et al.* it was also shown that the cell cycle inhibitor p27 was up-regulated in PTPRG expressing breast cancer cells (Shu, 2010). This made p27 an interesting candidate for playing a role for the observed changes in our analysis of the TKI sensitivity. The anti-apoptotic protein Bcl-2 can be successfully inhibited by the compound ABT-199 (venetoclax), which is approved by the FDA for treatment of some cases of CLL. As shown very recently by several groups, the combination of ABT-199 with TKI can lead to enhanced cell death in CML cells (Ko, 2014; Carter, 2016). In addition, BCR-ABL1 can positively regulate the Bcl-2 family proteins to support cell survival (Brown, 2017). We therefore included Bcl-2 in our analysis, to see whether the change in PTP levels would have an impact on Bcl-2 expression.

6.3 PTPRG promotes TKI responses of CML cells and attenuates BCR-ABL1-mediated transformation

PTPRG was previously reported to be down-regulated in CML patients (Della Peruta, 2010; Vezzalini, 2017), and has been described as a possible tumor suppressor in other cancer types (Stoker, 2016). In the study presented here we could show, that PTPRG is also important in the context of the CML treatment with the second-generation TKI nilotinib. The probability of reaching a MR^4 after 9 months of nilotinib treatment was significantly higher with higher PTPRG levels in the total leukocytes at diagnosis in all analyzed sub-cohorts. These differences were robust, despite the fact, that PTPRG was one of the PTPs with the lowest mean mRNA expression in the analyzed patient leukocytes (Figure 5-1). The mean mRNA expression in the analyzed healthy donors was the highest, the level in patients reaching an MR^4 at 9 months after study treatment was intermediate, and the lowest expression level was detected in patients not reaching an MR^4 at that timepoint. As mentioned above, the use of total peripheral blood leukocytes might lead to false positive findings, as the leukocyte composition of the individual blood cell sub-sets cannot be taken into account. Different cell types vary in PTPRG expression (Vezzalini, 2007; Vezzalini, 2017). The same laboratory also presented analyses of PTPRG expression (mRNA and flow cytometric analyses) of healthy controls and CML patients in bone marrow, PBMCs, peripheral blood, and CD34+ cells, and – interestingly - found a lower PTPRG expression in the CML patient samples in all cell populations (Della

Peruta, 2010). The flow cytometric analysis of peripheral blood was additionally carried out with samples taken from CML patients having a complete cytogenetic response, and these samples had, as expected, a similar expression of PTPRG as healthy controls, since all CML cells were eradicated by the TKI treatment. In our study, there was no substantial correlation of total leukocyte or thrombocyte count, or to the percentage of eosinophils, basophils, or blasts with PTPRG mRNA levels (PD Dr. M. Pfirrmann, Munich, personal communication). This observation argues against the possibility that changes in the leukocyte composition cause the association of PTPRG mRNA levels with treatment response.

In order to find out whether PTPRG does have a direct influence on TKI response, K562 cell lines stably over-expressing PTPRG either as the wild type protein, or as the phosphatase-dead PTPRG-CS mutant, were established. The over-expressed proteins were clearly detectable with a specific PTPRG antibody in western blots. The IC_{50}s of nilotinib, imatinib, and dasatinib were determined, and significant reductions of the IC_{50}s were found in the PTPRG-WT-expressing cell pools in case of nilotinib and imatinib treatment, but not in dasatinib-treated cells. The lowering of the IC_{50} was dependent on the phosphatase activity of PTPRG, because cells expressing PTPRG-CS did not show a significant reduction of the IC_{50}. The mean reduction of the IC_{50} in 6 different nilotinib experiments was 21.3 % for the PTPRG-WT cells compared to the empty vector-transduced cells. This change of roughly 20 % might at first sight appear small, but applied to the TKI dosing, a reduction of 20 % drug intake could improve side effects and diminish adverse events, thereby improve treatment compliance. In addition, a dose reduction for selected patients would definitely be an economic advantage, if the full therapeutic effect would be maintained. On the other hand, under standard dose, patients with high PTPRG level may more readily become eligible to stop TKI treatment and achieve a TFR.

The improved TKI response and earlier studies of PTPRG raise the question of possible effects of PTPRG expression on cell proliferation and other aspects of BCR-ABL1-mediated cell transformation. In our study, no obvious difference in the cell growth rate was seen under cultivation, but we did not directly measure cell proliferation rates. One other study in MCF-7 breast-cancer cells reported that cell growth, and anchorage-independent growth were inhibited dependent on PTPRG-levels (Liu, 2004). If this was also the case in our CML cell lines, the IC_{50} determination should nevertheless not have been biased, since it was done by calculating the individual maximum cell viability in each experiment, and should therefore not have been changed by differences in the absolute growth rate.

To assess effects of PTPRG on cell transformation, we evaluated the capacity of the engineered cells to form colonies in methylcellulose. We found a significant reduction (median reduction 35 %) of grown colonies in PTPRG-WT expressing - compared to empty vector-transduced cells. This finding is in line with previous reports in CML cells, where over-expression of PTPRG in different cell lines led to a colony reduction of 31 – 40 %. Also, PTPRG-expressing K562 cells had a reduced capacity to grow tumors in xenografted nude mice (Della Peruta, 2010).

To identify potential mechanisms for enhanced TKI sensitivity in PTPRG over-expressing cells, signaling analyses were carried out. They were performed in two different experimental setups: i) in absence of serum in order to get information on the influence of PTPRG on BCR-ABL1 signaling only, and ii) in presence of serum either with or without nilotinib treatment, similar to the conditions used in the IC_{50} assays. In the absence of serum, a clear reduction of BCR-ABL1 auto-phosphorylation by PTPRG over-expression can be detected. This is in line with previous reports (Della Peruta, 2010). This group also analyzed lysates of K562 cells transfected with full-length PTPRG by using total phospho-tyrosine detecting antibodies and found a strong reduction of phospho-signal in the lysates of the PTPRG-expressing cells. While the total phospho-tyrosine blots did not reveal such striking effects of PTPRG over-expression (data not shown), we found the phosphorylation of ERK 1/2 to be diminished in the PTPRG-WT-expressing cells, in presence, and to a lesser extent also in absence of serum. A reduced ERK 1/2 activation upon PTPRG over-expression has also been reported by others in a breast cancer cell line or in HEK293 cells expressing PTPRG (Shu, 2010; Xiao, 2014). An elevation of p27 as previously reported by Shu *et al.* was in our analysis only seen moderately in presence of serum. Our finding that the phosphorylation of the SFK Lyn is reduced in the PTPRG-WT expressing cells was not reported earlier. As shown in another study of K562 cells, the specific siRNA-mediated down-regulation of Lyn induced apoptosis, specifically in BCR-ABL1 positive cells (Ptasznik, 2004). It can be speculated, that the reduction in Lyn-activating phosphorylation could contribute to the lowering of the IC_{50} for nilotinib and imatinib, by induction of apoptosis in the PTPRG-WT expressing cells. If that really is the case, needs to be further addressed by apoptosis assays in our cell system. It may, however, be quite important for the improved TKI response. A simplified scheme, summarizing the main findings of PTPRG impact on the analyzed signal-transduction pathways, is provided in Figure 6-1.

As reviewed by Stoker, PTPRG is commonly deleted or down-regulated in different cancer entities suggesting that it is acting as a tumor suppressor (Stoker, 2016). The findings presented in this thesis argue in the same direction. One common mechanism

of PTPRG down-regulation appears to be promoter methylation. Several working groups have found *PTPRG* promoter methylation in different cancer types (Della Peruta, 2010; Stevenson, 2014; Xiao, 2014), and that the expression can be induced by the use of demethylating agents. Preliminary experiments by ourselves indicated that indeed, the combination of TKI with a demethylating agent can lower the IC_{50} for the respective TKI (data not shown). From that experiment alone, however, we cannot yet conclude that the induction of PTPRG is the underlying reason for this. To further address this question, it would be needed to specifically prevent induction of PTPRG expression by knockdown or knockout, and perform the combination-treatment with corresponding cell lines.

We have some evidence that the down-regulation of PTPRG is not a direct consequence of the oncogenic BCR-ABL1 signaling, but that BCR-ABL1 actually promotes PTPRG expression (data not shown). Long term continuous cultivation (> 6 months) of cell lines stably expressing BCR-ABL1 led to a decrease in PTPRG mRNA and protein expression compared to the starting level (data not shown). The low level of PTPRG expression in CML cells might therefore be a result of a long-term selection process in BCR-ABL1 addicted cells, potentially driven by a small growth advantage of the cells with lower PTPRG expression levels.

Taken together, we could confirm previous findings of Della Peruta *et al.* and Vezzalini *et al.*, who reported PTPRG to be down-regulated in CML cells and that over-expression in CML cell lines attenuated BCR-ABL1-mediated transformation (Della Peruta, 2010; Vezzalini, 2017). We could expand this knowledge with the finding, that PTPRG expression in peripheral blood at diagnosis does positively correlate to fast achievement of a deep molecular response in nilotinib-treated CML patients. We could additionally show that PTPRG expression directly influences the TKI susceptibility in case of nilotinib and imatinib in a phosphatase-activity dependent manner, possibly through elevating p27 levels and reducing the activity of Lyn and ERK 1/2.

6.4 PTPRC negatively influences treatment response and CML cell transformation

In our patient analyses, a higher expression of PTPRC was found to be correlated with the achievement of a *BCR-ABL1*^{IS} ≤ 0.01 % after 9 months of nilotinib study treatment in the initial analysis of the 66 patients cohort. This correlation was confirmed in the subsequent analyses of the more stringently selected patients (Figure 5-2, Table 5-2). As also seen for PTPRG, PTPRC expression was lowest in the patients not

reaching MR^4 after 9 months of study treatment, intermediate in the patients that did reach MR^4, and highest in the healthy donors (Figure 5-1).

Our study is the first report of PTPRC in the context of CML. In other leukemic entities, the role of PTPRC has been addressed but remains unclear. It was described as both, an oncogene and as a tumor suppressor. As an example, in T-cell ALL, PTPRC was reported to act as a tumor suppressor by negative regulation of Jak/STAT signaling (Porcu, 2012). Others found PTPRC expression to be negatively associated with survival rates in CLL or B-cell and T-cell ALL samples (Rizzo, 2013; Cario, 2014), but these two studies lack functional analyses.

We decided to include PTPRC in our functional analyses, to gain more information on the direct impact of PTPRC expression on the TKI sensitivity in CML cells. As all hematopoietic cells express PTPRC, we decided to reduce the expression level by shRNA-mediated knockdown. Initial experiments with such cells showed a possible influence of the PTPRC expression on the IC_{50}s for the used TKIs (Figure 5-5).

As the down-regulation by shRNA was not resulting in good knockdown efficiencies, we decided to establish CRISPR/Cas9-mediated knockout single cell clones. I was able to establish two clones, made by using two different gRNAs (A and B, see chapter 4.10.1). One of the used gRNAs (A) was covering a part of an intron sequence. This enables a successful cleavage of the sequence by the Cas9 nuclease on the genomic level, but as this sequence is not fully present in the mRNA of PTPRC we had the possibility, to exogenously re-express PTPRC in that particular knockout clone, without risking that the stable CRISPR/Cas9 machinery is targeting the introduced sequence. The gRNA sequence B is completely located within in the open reading frame. This might lead to disruption of the re-introduced PTPRC sequence, which made this clone unsuitable for the re-expression of PTPRC. As shown by immunoblots and flow cytometry, I was able to generate a cell pool from PTPRC-KO A with rescued PTPRC expression levels (KO A + PTPRC) comparable to the control K562 cells (Figure 5-15). As control, the PTPRC-KO A clone was transduced with the corresponding empty vector (KO A + EV). By using the cells with restored PTPRC levels, we can exclude that results obtained using the KO-clone might be clonal effects specific to the selected clone, rather than being related to the absence of PTPRC.

We found that the knockout of PTPRC in K562 cells led to a significant decrease of the IC_{50}s for nilotinib and imatinib, and to much lesser extent (not significant for two out of three tested cell clones), in dasatinib-treated cells. This effect of the PTPRC depletion could be reverted by exogenous re-expression of PTPRC in the PTPRC-KO A cells, strongly supporting, that the IC_{50} shift is a direct consequence of the absence of PTPRC. These findings indicate, that PTPRC would exert a resistance

promoting role, because the cells were more sensitive to nilotinib and imatinib treatment in absence of PTPRC.

The analysis of the BCR-ABL1 driven clonogenic capacity of the engineered cells showed that the absence of PTPRC significantly reduced the ability of the K562 cells to form colonies in methylcellulose. Unfortunately, the transduction of the empty vector to the PTPRC-KO A cells already led to an increased colony formation, but still, this elevated colony formation was significantly further increased in cells re-expressing PTPRC. This leads to the conclusion, that PTPRC absence diminishes the clonogenic capacity of this CML cell line.

As discussed above (chapter 6.2), an analysis of selected signaling proteins in immunoblotting experiments was carried out to find possible mediators of the described phenotypes. In the PTPRC-KO cells, a prominent reduction of the catalytic-site phosphorylation of cSRC (mean reduction 60 – 80 %) and Lyn (mean reduction 70 – 80 %) were seen in the absence of serum, and to a lesser extent also in presence of serum (Figures 5-18 and 5-19). PTPRC is known to regulate SFK-mediated signaling by direct de-phosphorylation of the inhibitory tyrosine residue (Y530 in human cSRC), and thereby facilitating the phosphorylation of the active-site tyrosine (see introduction 1.2.5) (Hermiston, 2009). The absence of PTPRC in our KO cells most likely leads to a sustained phosphorylation of the inhibitory tyrosine residue, hampering the full activation of the SFK. The re-introduction of PTPRC in the KO A clone led to a clear increase in the phosphorylation of the active-site tyrosine, supporting this mechanism. For further experiments, it would be of interest, to analyze the phosphorylation of the inhibitory tyrosine of these SFKs, to confirm the assumed direct action of PTPRC on that residue in our cell model. As already discussed for the PTPRG-WT-expressing cells, that also showed a reduced Lyn phosphorylation, we can speculate that this activity reduction contributes to the TKI treatment outcome, as the down-regulation of Lyn alone (without TKI treatment) already led to induction of apoptosis in K562 cells (Ptasznik, 2004).

In presence of serum, a basal elevation of the cell cycle inhibitor p27 was seen only in the PTPRC-KO cells. The treatment of the cell lines with 1 µM nilotinib led to an even further elevation of p27 levels. The basal increase of p27 up to about 2-fold in the KO cells might in presence of sub-optimal nilotinib concentrations contribute to the effects seen in the IC_{50} assays: the small difference in p27 levels might drive these cells into cell-cycle arrest already at lower nilotinib concentrations, compared to PTPRC expressing cells.

The absence of PTPRC slightly increased the phosphorylation of BCR-ABL1, indicating that BCR-ABL1 might be a direct target of PTPRC. PTPRC is described to

act as a negative regulator of Jak-mediated cytokine signaling by directly binding and de-phosphorylating Jaks (Irie-Sasaki, 2001). In our CML cell system, PTPRC might negatively regulate BCR-ABL1 auto-phosphorylation, kinase activity, and downstream signaling. The phosphorylations of the signaling molecules ERK 1 and 2, downstream of BCR-ABL1, were also elevated in absence of PTPRC, indicating that PTPRC might act as a negative regulator in this signaling pathway. Nevertheless, to establish BCR-ABL1 as PTPRC target, additional experiments would be needed: *e. g.* to show the direct interaction of these two proteins, and the PTPRC phosphatase-activity-dependent decrease of BCR-ABL1 phosphorylation.

Taken together, absence of PTPRC leads on the one hand to apparently tumor-promoting changes like increasing BCR-ABL1 auto-phosphorylation and ERK 1/2 activation, and on the other hand to tumor-suppressive changes by increasing p27 expression and decreasing SFK activation. In our here-presented cell line model, these pathways integrate to an enhancement of TKI sensitivity in absence of PTPRC, identifying PTPRC expression as tumor-supporting event. As the SFK inhibition, in absence of PTPRC, appears contributing to the treatment sensitization, it is not surprising, that the down-regulation of PTPRC does not have such a strong impact on the treatment with dasatinib as this TKI also inhibits the SFK. Using this TKI might therefore be an advantage for some of the patients that do not have an optimal response to nilotinib or imatinib. In Figure 6-1, the here identified actions of PTPRC on BCR-ABL1 and its signaling are summarized.

As it seems favorable to inhibit PTPRC in the CML cells, the use of specific inhibitors might be advantageous. Perron *et al.* introduced a PTPRC selective allosteric inhibitor that was able to repress T-cell receptor signals (Perron, 2014). It would be very interesting to test this compound in our cell system for the influence on the IC_{50}s of the TKIs.

The results of the functional analyses in PTPRC-KO cells are contrasting to the finding in our patient analysis, where a high PTPRC expression-level was correlated to a better treatment response. As already mentioned before, the use of total peripheral blood leukocytes with unknown cell composition of the individual blood sample might lead to correlations which reflect cellular composition rather than intrinsic roles of PTPs for treatment response. PTPRC is especially highly expressed in *e. g.* T-cell-lymphocytes (Arimura & Yagi, 2010), consequently, a patient sample containing more lymphocytes would result in higher PTPRC expression in our analysis. In our study, the PTPRC expression level was neither substantially correlated to the patients´ leukocyte or thrombocyte counts, nor to the percentage of eosinophils, basophils, or blasts (PD Dr. Markus Pfirrmann, Munich, personal communication), but an effect of different

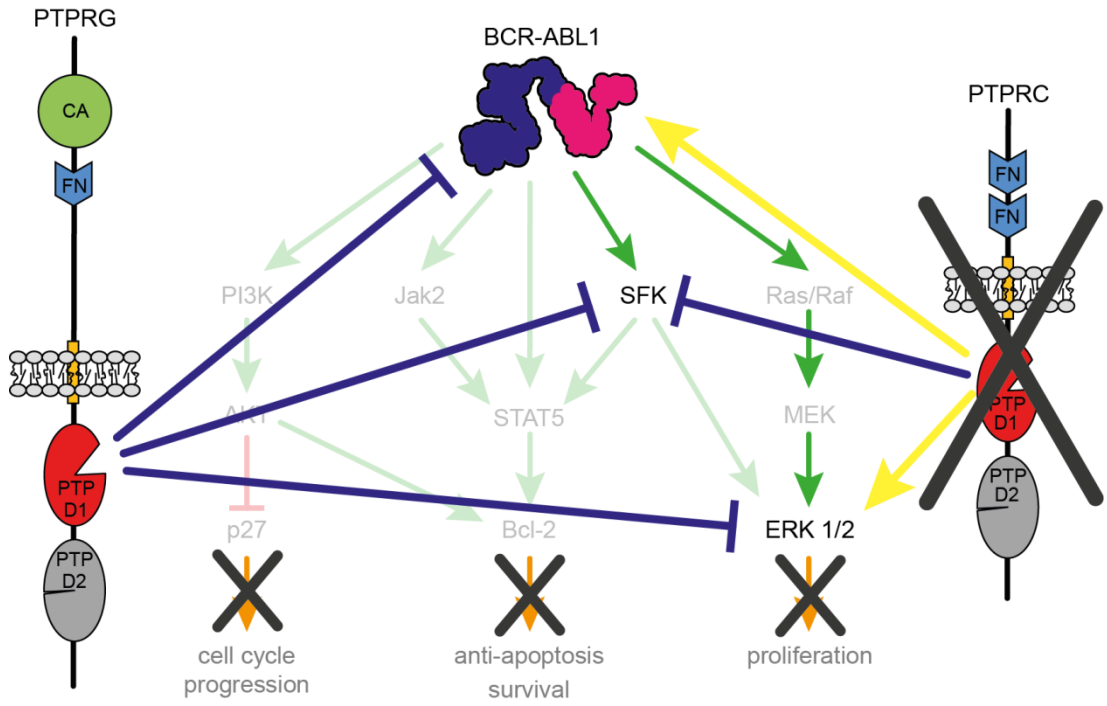

Figure 6-1. PTPRG activity and absence of PTPRC attenuate the BCR-ABL1 driven signal-transduction pathways. Shown here is a summary of the identified actions of either PTPRG over-expression, or CRISPR/Cas9-mediated knockout of PTPRC on the signaling cascades introduced in Figure 1-2. (**Left**) PTPRG expression leads to an inhibition of BCR-ABL1 auto-phosphoryation, a diminished SFK activation, and a reduction of ERK 1/2 phosphorylation. All these effects are attenuating the BCR-ABL1 driven transformation. (**Right**) The absence of PTPRC has a negative effect on SFK activation. Although the absence of PTPRC also promotes the activity of BCR-ABL1 and ERK 1/2, the net result of the signaling changes in absence of PTPRC is a promotion of therapy response.
Yellow arrows: activation, blue marks: inhibition / inactivation.

cellular composition cannot be ruled out. One other possibility to explain this discrepancy is the possibility, that not only the expression level *per se* is important, but the localization of PTPRC within the cells. A study of Saint-Paul *et al*. reported PTPRC to be mis-localized to lipid rafts in AML cells. This led to an increased cytokine signaling, that contributed to AML development and maintenance. They found that both, down-regulation of PTPRC, or the disruption of the lipid rafts using a pharmacologic approach, led to a reduction of leukemia formation in cell lines and mouse models (Saint-Paul, 2016). One might speculate that the large amounts of PTPRC in primary CML cells are largely mis-localized and therefore unrelated to the affects of PTPRC found in the cell line experiments. To investigate a possible role of such a localization effect in CML cells, further experiments would be needed.

PTPRC activity was described to be inhibited by dimer-formation, and that a specific PTPRC point- mutation that prevented inhibition by dimer-formation could cause lymphoproliferation and autoimmunity (Majeti, 2000). Taking this into account, it might be possible that the higher expression level of PTPRC (the PTP with the second highest expression in the primary samples of all 38 analyzed PTPs) might lead to an

increased inactivation of PTPRC in cells with higher expression, and that might favor the treatment outcome, just as shown in the functional analyses. A direct comparison of the PTPRC level per cell in primary samples and K562 cells was not carried out, but the mean relative mRNA level in the primary samples was much higher than in the K562 cells (Figures 5-1 and 5-3). If an inactivation by dimerization would hold true in the patient samples, it may be beneficial to the treatment outcome to further enhance or stabilize this state by use of PTPRC dimerization-inducing antibodies, similar to previous studies (Spertini, 2004), in addition to TKI treatment.

6.5 PTPN6 does not influence treatment sensitivity in our cell models

Several research groups have found a decreasing level of PTPN6 expression during CML progression from CP to BC (Amin, 2007; Li, 2014; Wang, 2017). One additional group has investigated a KCL-22 cell line derivative, which was resistant to imatinib (KCL-22-R) and found PTPN6 expression to be down-regulated in the resistant cells when compared to the imatinib-sensitive (KCL-22-S) counterpart. They exogenously over-expressed PTPN6 in the resistant cells, and found a restoration of imatinib, nilotinib, and dasatinib sensitivity (Esposito, 2011). A similar phenotype was obtained by shRNA-mediated knockdown of the close relative of PTPN6, PTPN11 (SHP2) in the KCL-22-R cells: the sensitivity was restored. These two PTPs are very similar in structure, but in general have opposing effects on signal transduction (Poole & Jones, 2005). Therefore it is not surprising that the over-expression of PTPN6 or the down-regulation of PTPN11 result in similar phenotypes. Unfortunately, these investigators did not present an experiment with knockdown of PTPN6 in the sensitive cell line, which would support their statement of PTPN6 being the main factor for resistance development. Nevertheless, we decided to follow up on this concept and included PTPN6 in our cell analyses. This was done although we did not find a correlation of PTPN6 expression with treatment outcome in our patient samples. However, PTPN6 is relatively abundantly expressed, and silencing of gene expression in different hematopoietic cancers had been reported (Hendriks & Böhmer, 2016). The first experiments we carried out employing shRNA-mediated knockdowns of PTPN6 in the parental KCL-22 cells, followed by the analysis of IC_{50} changes as discussed above. Using two different shRNAs, we obtained knockdown efficiencies of 50 – 70 %, but the IC_{50} analyses did not give a clear cut result, they varied in different experiments. Therefore, we decided to knockout the *PTPN6* gene to obtain more reliable results. Two established KO clones were again analyzed, but still, no obvious difference in TKI

sensitivity was found. Then K562 cells, that are expressing very little PTPN6, were used to over-express PTPN6-wild type or the phosphatase-dead PTPN6-CS mutant. Despite good over-expression levels of PTPN6, again no substantial changes in the TKI sensitivity of the engineered cells were seen.

An earlier study of Papadopoulou *et al.* tried to find a prognostic relevance of PTPN6 in CML patient samples (Papadopoulou, 2016). They observed a trend of a lower PTPN6 expression in non-responding CML patients, but could not find significant correlations of PTPN6 level with treatment outcome, similar to our findings presented in this thesis.

We can conclude from our experiments that PTPN6 is not directly responsible for the TKI sensitivity in the CML background. The fact that the KCL-22-R cell line investigated by Esposito *et al.* had a lower PTPN6 level may therefore rather present an alteration caused by the clonal selection of the resistant cells than being the cause of the resistance itself. The key experiment (knockdown of PTPN6 in the sensitive cell line) was not shown in their work, but was now provided in this thesis. It revealed that the absence of PTPN6 alone does not substantially influence the TKI sensitivity. Since PTPN6 is a known negative regulator of cytokine signaling (Hendriks & Böhmer, 2016), it can be speculated, that an abrogation of cytokine signaling caused by the lack or the over-expression of PTPN6 in those cells causes the described phenotypes. PTPN6 down-regulation in advanced stages of CML might indicate that the abrogation of the cytokine signaling is contributing to the progression of the disease, but as our experiments have shown, presumably not because of a direct influence on the inhibitor sensitivity.

6.6 Implications for therapy optimization and combination-treatments

The cell cycle inhibitor p27 is stabilized and thereby up-regulated by the inhibition of the PI3K-signaling pathway. Idelalisib, a specific inhibitor of PI3Kδ was approved for the treatment of CLL. Chen *et al.* have used idelalisib in combination with imatinib to treat K562 cells (Chen, 2016) and found an accumulation of p27. We have combined the PI3K-inhibitor idelalisib with the TKI nilotinib and assessed the influence of this combination on the IC_{50} for nilotinib in K562 cells (Figure 5-20). As expected, the combination of the two drugs led to a reduction of the IC_{50} for nilotinib. This is a proof of principle that the findings presented in this thesis may help to find new therapy approaches, or find co-treatments that support and complement the standard TKI treatments. The results obtained in this thesis revealed several possible starting points

for therapy optimization. These include the induction of PTPRG expression using demethylating agents, the inhibition PTPRC by cross-linking antibodies or inhibitors, the elevation of p27 (*e. g.* by treatment with idelalisib), as well as the inhibition of SFK (*e. g.* by using dasatinib). All this might prove helpful in order to further optimize TKI treatment response in CML patients and thereby improving the chances of some CML patients to reach a functional cure of the disease. Moreover, findings in this thesis may in the future be used to either establish new prognostic markers, or help to identify patients that are eligible to safely reduce TKI dosage.

7 Referenzen

Alaiya AA, Aljurf M, Shinwari Z, Almohareb F, Malhan H, Alzahrani H, Owaidah T, Fox J, Alsharif F, Mohamed SY, Rasheed W, Aldawsari G, Hanbali A, Ahmed SO, Chaudhri N (2016) Protein signatures as potential surrogate biomarkers for stratification and prediction of treatment response in chronic myeloid leukemia patients. *International journal of oncology* **49:** 913-933

Albert BV (2017) Effect of protein-tyrosine phosphatase gamma (PTPRG) on cell transformation and tyrosine kinase inhibitor (TKI) response in CML cell lines. Institute of Molecular Cell Biology, Jena University Hospital,

Alonso A, Pulido R (2016) The extended human PTPome: a growing tyrosine phosphatase family. *FEBS Journal* **283:** 1404-1429

Alonso A, Sasin J, Bottini N, Friedberg I, Osterman A, Godzik A, Hunter T, Dixon J, Mustelin T (2004) Protein tyrosine phosphatases in the human genome. *Cell* **117:** 699-711

Amin HM, Hoshino K, Yang H, Lin Q, Lai R, Garcia-Manero G (2007) Decreased expression level of SH2 domain-containing protein tyrosine phosphatase-1 (Shp1) is associated with progression of chronic myeloid leukaemia. *The Journal of pathology* **212:** 402-410

Arimura Y, Yagi J (2010) Comprehensive expression profiles of genes for protein tyrosine phosphatases in immune cells. *Science signaling* **3:** rs1

Baccarani M, Deininger MW, Rosti G, Hochhaus A, Soverini S, Apperley JF, Cervantes F, Clark RE, Cortes JE, Guilhot F, Hjorth-Hansen H, Hughes TP, Kantarjian HM, Kim DW, Larson RA, Lipton JH, Mahon FX, Martinelli G, Mayer J, Muller MC, Niederwieser D, Pane F, Radich JP, Rousselot P, Saglio G, Saussele S, Schiffer C, Silver R, Simonsson B, Steegmann JL, Goldman JM, Hehlmann R (2013) European LeukemiaNet recommendations for the management of chronic myeloid leukemia: 2013. *Blood* **122:** 872-884

Brown LM, Hanna DT, Khaw SL, Ekert PG (2017) Dysregulation of BCL-2 family proteins by leukemia fusion genes. *Journal of Biological Chemistry* **292:** 14325-14333

Bruecher-Encke B, Griffin JD, Neel BG, Lorenz U (2001) Role of the tyrosine phosphatase SHP-1 in K562 cell differentiation. *Leukemia* **15:** 1424-1432

Burmeister T, Reinhardt R (2008) A multiplex PCR for improved detection of typical and atypical BCR-ABL fusion transcripts. *Leukemia research* **32:** 579-585

Cale CM, Klein NJ, Novelli V, Veys P, Jones AM, Morgan G (1997) Severe combined immunodeficiency with abnormalities in expression of the common leucocyte antigen, CD45. *Archives of disease in childhood* **76:** 163-164

Cario G, Rhein P, Mitlohner R, Zimmermann M, Bandapalli OR, Romey R, Moericke A, Ludwig WD, Ratei R, Muckenthaler MU, Kulozik AE, Schrappe M, Stanulla M, Karawajew L (2014) High CD45 surface expression determines relapse risk in children with precursor B-cell and T-cell acute lymphoblastic leukemia treated according to the ALL-BFM 2000 protocol. *Haematologica* **99:** 103-110

Carter BZ, Mak PY, Mu H, Zhou H, Mak DH, Schober W, Leverson JD, Zhang B, Bhatia R, Huang X, Cortes J, Kantarjian H, Konopleva M, Andreeff M (2016) Combined targeting of BCL-2 and BCR-ABL tyrosine kinase eradicates chronic myeloid leukemia stem cells. *Science translational medicine* **8:** 355ra117

Chae H-D, Cox N, Dahl GV, Lacayo NJ, Davis KL, Capolicchio S, Smith M, Sakamoto KM (2018) Niclosamide suppresses acute myeloid leukemia cell proliferation through inhibition of CREB-dependent signaling pathways. *Oncotarget* **9:** 4301-4317

Chen Y, Zhou Q, Zhang L, Wang R, Jin M, Qiu Y, Kong D (2016) Idelalisib induces G1 arrest and apoptosis in chronic myeloid leukemia K562 cells. *Oncology reports* **36:** 3643-3650

Cheung AK, Lung HL, Hung SC, Law EW, Cheng Y, Yau WL, Bangarusamy DK, Miller LD, Liu ET, Shao JY, Kou CW, Chua D, Zabarovsky ER, Tsao SW, Stanbridge EJ, Lung ML (2008) Functional analysis of a cell cycle-associated, tumor-suppressive gene, protein tyrosine phosphatase receptor type G, in nasopharyngeal carcinoma. *Cancer research* **68:** 8137-8145

Cramer K, Nieborowska-Skorska M, Koptyra M, Slupianek A, Penserga ET, Eaves CJ, Aulitzky W, Skorski T (2008) BCR/ABL and other kinases from chronic myeloproliferative disorders stimulate single-strand annealing, an unfaithful DNA double-strand break repair. *Cancer research* **68:** 6884-6888

Crivellaro S, Carra G, Panuzzo C, Taulli R, Guerrasio A, Saglio G, Morotti A (2016) The non-genomic loss of function of tumor suppressors: an essential role in the pathogenesis of chronic myeloid leukemia chronic phase. *BMC cancer* **16:** 314

Cross NC, Hochhaus A, Muller MC (2015) Molecular monitoring of chronic myeloid leukemia: principles and interlaboratory standardization. *Annals of hematology* **94 Suppl 2:** S219-225

Daley GQ, Van Etten RA, Baltimore D (1990) Induction of chronic myelogenous leukemia in mice by the P210bcr/abl gene of the Philadelphia chromosome. *Science* **247:** 824-830

Danhauser-Riedl S, Warmuth M, Druker BJ, Emmerich B, Hallek M (1996) Activation of Src kinases p53/56lyn and p59hck by p210bcr/abl in myeloid cells. *Cancer research* **56:** 3589-3596

de Groot RP, Raaijmakers JA, Lammers JW, Jove R, Koenderman L (1999) STAT5 activation by BCR-Abl contributes to transformation of K562 leukemia cells. *Blood* **94:** 1108-1112

de Klein A, van Kessel AG, Grosveld G, Bartram CR, Hagemeijer A, Bootsma D, Spurr NK, Heisterkamp N, Groffen J, Stephenson JR (1982) A cellular oncogene is translocated to the Philadelphia chromosome in chronic myelocytic leukaemia. *Nature* **300:** 765-767

Della Peruta M, Martinelli G, Moratti E, Pintani D, Vezzalini M, Mafficini A, Grafone T, Iacobucci I, Soverini S, Murineddu M, Vinante F, Tecchio C, Piras G, Gabbas A, Monne M, Sorio C (2010) Protein tyrosine phosphatase receptor type {gamma} is a functional tumor suppressor gene specifically downregulated in chronic myeloid leukemia. *Cancer research* **70:** 8896-8906

den Hertog J, Ostman A, Bohmer FD (2008) Protein tyrosine phosphatases: regulatory mechanisms. *FEBS Journal* **275:** 831-847

Drube J, Ernst T, Pfirrmann M, Albert BV, Drube S, Reich D, Kresinsky A, Halfter K, Sorio C, Fabisch C, Hochhaus A, Böhmer F-D (2018) PTPRG and PTPRC modulate nilotinib response in chronic myeloid leukemia cells. *Oncotarget* **9:** 9442-9455

Druker BJ, Tamura S, Buchdunger E, Ohno S, Segal GM, Fanning S, Zimmermann J, Lydon NB (1996) Effects of a selective inhibitor of the Abl tyrosine kinase on the growth of Bcr-Abl positive cells. *Nature Medicine* **2:** 561-566

Ernst T, Hochhaus A (2012) Chronic myeloid leukemia: clinical impact of BCR-ABL1 mutations and other lesions associated with disease progression. *Seminars in oncology* **39:** 58-66

Esposito N, Colavita I, Quintarelli C, Sica AR, Peluso AL, Luciano L, Picardi M, Del Vecchio L, Buonomo T, Hughes TP, White D, Radich JP, Russo D, Branford S, Saglio G, Melo JV, Martinelli R, Ruoppolo M, Kalebic T, Martinelli G, Pane F (2011) SHP-1 expression accounts for resistance to imatinib treatment in Philadelphia chromosome-positive cells derived from patients with chronic myeloid leukemia. *Blood* **118:** 3634-3644

Godfrey R, Arora D, Bauer R, Stopp S, Muller JP, Heinrich T, Bohmer SA, Dagnell M, Schnetzke U, Scholl S, Ostman A, Bohmer FD (2012) Cell transformation by FLT3 ITD in acute myeloid leukemia involves oxidative inactivation of the tumor suppressor protein-tyrosine phosphatase DEP-1/ PTPRJ. *Blood* **119:** 4499-4511

Groffen J, Stephenson JR, Heisterkamp N, de Klein A, Bartram CR, Grosveld G (1984) Philadelphia chromosomal breakpoints are clustered within a limited region, bcr, on chromosome 22. *Cell* **36:** 93-99

Gu S, Sayad A, Chan G, Yang W, Lu Z, Virtanen C, Van Etten RA, Neel BG (2018) SHP2 is required for BCR-ABL1-induced hematologic neoplasia. *Leukemia* **32:** 203-213

Hanfstein B, Muller MC, Hehlmann R, Erben P, Lauseker M, Fabarius A, Schnittger S, Haferlach C, Gohring G, Proetel U, Kolb HJ, Krause SW, Hofmann WK, Schubert J, Einsele H, Dengler J, Hanel M, Falge C, Kanz L, Neubauer A, Kneba M, Stegelmann F, Pfreundschuh M, Waller CF, Branford S, Hughes TP, Spiekermann K, Baerlocher GM, Pfirrmann M, Hasford J, Saussele S, Hochhaus A, Sakk, German CMLSG (2012) Early molecular and cytogenetic response is predictive for long-term progression-free and overall survival in chronic myeloid leukemia (CML). *Leukemia* **26:** 2096-2102

Hanfstein B, Shlyakhto V, Lauseker M, Hehlmann R, Saussele S, Dietz C, Erben P, Fabarius A, Proetel U, Schnittger S, Krause SW, Schubert J, Einsele H, Hanel M, Dengler J, Falge C, Kanz L, Neubauer A, Kneba M, Stegelmann F, Pfreundschuh M, Waller CF, Spiekermann K, Baerlocher GM, Pfirrmann M, Hasford J, Hofmann WK, Hochhaus A, Muller MC, Sakk, the German CMLSG (2014) Velocity of early BCR-ABL transcript elimination as an optimized predictor of outcome in chronic myeloid leukemia (CML) patients in chronic phase on treatment with imatinib. *Leukemia* **28:** 1988-1992

Hantschel O, Nagar B, Guettler S, Kretzschmar J, Dorey K, Kuriyan J, Superti-Furga G (2003) A myristoyl/phosphotyrosine switch regulates c-Abl. *Cell* **112:** 845-857

Hantschel O, Warsch W, Eckelhart E, Kaupe I, Grebien F, Wagner KU, Superti-Furga G, Sexl V (2012) BCR-ABL uncouples canonical JAK2-STAT5 signaling in chronic myeloid leukemia. *Nature chemical biology* **8:** 285-293

Hasford J, Baccarani M, Hoffmann V, Guilhot J, Saussele S, Rosti G, Guilhot F, Porkka K, Ossenkoppele G, Lindoerfer D, Simonsson B, Pfirrmann M, Hehlmann R (2011) Predicting complete cytogenetic response and subsequent progression-free survival in 2060 patients with CML on imatinib treatment: the EUTOS score. *Blood* **118:** 686-692

Hasford J, Pfirrmann M, Hehlmann R, Allan NC, Baccarani M, Kluin-Nelemans JC, Alimena G, Steegmann JL, Ansari H (1998) A new prognostic score for survival of patients with chronic myeloid leukemia treated with interferon alfa. Writing Committee for the Collaborative CML Prognostic Factors Project Group. *Journal of the National Cancer Institute* **90:** 850-858

Hehlmann R, Berger U, Hochhaus A (2005) Chronic myeloid leukemia: a model for oncology. *Annals of hematology* **84:** 487-497

Hendriks WJ, Böhmer F-D (2016) Non-transmembrane PTPs in Cancer. In *Protein Tyrosine Phosphatases in Cancer*, Neel BG, Tonks NK (eds). Springer Science+Business Media

Hendriks WJ, Elson A, Harroch S, Pulido R, Stoker A, den Hertog J (2013) Protein tyrosine phosphatases in health and disease. *FEBS Journal* **280:** 708-730

Hermiston ML, Zikherman J, Zhu JW (2009) CD45, CD148, and Lyp/Pep: critical phosphatases regulating Src family kinase signaling networks in immune cells. *Immunological reviews* **228:** 288-311

Hochhaus A, Kreil S, Corbin AS, La Rosee P, Muller MC, Lahaye T, Hanfstein B, Schoch C, Cross NC, Berger U, Gschaidmeier H, Druker BJ, Hehlmann R (2002) Molecular and chromosomal mechanisms of resistance to imatinib (STI571) therapy. *Leukemia* **16:** 2190-2196

Hochhaus A, Larson RA, Guilhot F, Radich JP, Branford S, Hughes TP, Baccarani M, Deininger MW, Cervantes F, Fujihara S, Ortmann CE, Menssen HD, Kantarjian H, O'Brien SG, Druker BJ, Investigators I (2017) Long-Term Outcomes of Imatinib Treatment for Chronic Myeloid Leukemia. *The New England journal of medicine* **376:** 917-927

Hochhaus A, Saglio G, Hughes TP, Larson RA, Kim DW, Issaragrisil S, le Coutre PD, Etienne G, Dorlhiac-Llacer PE, Clark RE, Flinn IW, Nakamae H, Donohue B, Deng W, Dalal D, Menssen HD, Kantarjian HM (2016) Long-term benefits and risks of frontline nilotinib vs imatinib for chronic myeloid leukemia in chronic phase: 5-year update of the randomized ENESTnd trial. *Leukemia* **30:** 1044-1054

Hoffbrand AV, Pettit JE, Moss PAH, Hoelzer D (2002) *Grundkurs Hämatologie, ISBN: 3-89412-514-4*, Blackwell Verlag.

Hosmer DW, Lemeshow S (1989) *Applied Logistic Regression*: John Wiley & Sons, Inc.

Huang W, Bei L, Eklund EA (2013a) Fas-associated phosphatase 1 (Fap1) influences betacatenin activity in myeloid progenitor cells expressing the Bcr-abl oncogene. *Journal of Biological Chemistry* **288:** 12766-12776

Huang W, Bei L, Eklund EA (2013b) Fas-associated phosphatase 1 mediates Fas resistance in myeloid progenitor cells expressing the Bcr-abl oncogene. *Leukemia & lymphoma* **54:** 619-630

Huang W, Luan CH, Hjort EE, Bei L, Mishra R, Sakamoto KM, Platanias LC, Eklund EA (2016) The role of Fas-associated phosphatase 1 in leukemia stem cell persistence during tyrosine kinase inhibitor treatment of chronic myeloid leukemia. *Leukemia* **30:** 1502-1509

Huang W, Zhu C, Wang H, Horvath E, Eklund EA (2008) The interferon consensus sequence-binding protein (ICSBP/IRF8) represses PTPN13 gene transcription in differentiating myeloid cells. *Journal of Biological Chemistry* **283:** 7921-7935

Hughes TP, Kaeda J, Branford S, Rudzki Z, Hochhaus A, Hensley ML, Gathmann I, Bolton AE, van Hoomissen IC, Goldman JM, Radich JP, International Randomised Study of Interferon versus STISG (2003) Frequency of major molecular responses to imatinib or interferon alfa plus cytarabine in newly diagnosed chronic myeloid leukemia. *The New England journal of medicine* **349:** 1423-1432

Irie-Sasaki J, Sasaki T, Matsumoto W, Opavsky A, Cheng M, Welstead G, Griffiths E, Krawczyk C, Richardson CD, Aitken K, Iscove N, Koretzky G, Johnson P, Liu P, Rothstein DM, Penninger JM (2001) CD45 is a JAK phosphatase and negatively regulates cytokine receptor signalling. *Nature* **409:** 349-354

Jain P, Kantarjian H, Patel KP, Gonzalez GN, Luthra R, Kanagal Shamanna R, Sasaki K, Jabbour E, Romo CG, Kadia TM, Pemmaraju N, Daver N, Borthakur G, Estrov Z, Ravandi F, O'Brien S, Cortes J (2016) Impact of BCR-ABL transcript type on outcome in patients with chronic-phase CML treated with tyrosine kinase inhibitors. *Blood* **127:** 1269-1275

Jayavelu AK, Muller JP, Bauer R, Bohmer SA, Lassig J, Cerny-Reiterer S, Sperr WR, Valent P, Maurer B, Moriggl R, Schroder K, Shah AM, Fischer M, Scholl S, Barth J, Oellerich T, Berg T, Serve H, Frey S, Fischer T, Heidel FH, Bohmer FD (2016) NOX4-driven ROS formation mediates PTP inactivation and cell transformation in FLT3ITD-positive AML cells. *Leukemia* **30:** 473-483

Julien SG, Dube N, Hardy S, Tremblay ML (2011) Inside the human cancer tyrosine phosphatome. *Nature Reviews Cancer* **11:** 35-49

Ko TK, Chuah CT, Huang JW, Ng KP, Ong ST (2014) The BCL2 inhibitor ABT-199 significantly enhances imatinib-induced cell death in chronic myeloid leukemia progenitors. *Oncotarget* **5:** 9033-9038

Kok CH, Leclercq T, Watkins DB, Saunders V, Wang J, Hughes TP, White DL (2014) Elevated PTPN2 expression is associated with inferior molecular response in de-novo chronic myeloid leukaemia patients. *Leukemia* **28:** 702-705

Koyama N, Koschmieder S, Tyagi S, Portero-Robles I, Chromic J, Myloch S, Nurnberger H, Rossmanith T, Hofmann WK, Hoelzer D, Ottmann OG (2006) Inhibition of phosphotyrosine phosphatase 1B causes resistance in BCR-ABL-positive leukemia cells to the ABL kinase inhibitor STI571. *Clinical Cancer Research* **12:** 2025-2031

Kumar V, Cheng P, Condamine T, Mony S, Languino LR, McCaffrey JC, Hockstein N, Guarino M, Masters G, Penman E, Denstman F, Xu X, Altieri DC, Du H, Yan C, Gabrilovich DI (2016) CD45 Phosphatase Inhibits STAT3 Transcription Factor Activity in Myeloid Cells and Promotes Tumor-Associated Macrophage Differentiation. *Immunity* **44:** 303-315

Kung C, Pingel JT, Heikinheimo M, Klemola T, Varkila K, Yoo LI, Vuopala K, Poyhonen M, Uhari M, Rogers M, Speck SH, Chatila T, Thomas ML (2000)

Mutations in the tyrosine phosphatase CD45 gene in a child with severe combined immunodeficiency disease. *Nature Medicine* **6:** 343-345

La Rosee P, Deininger MW (2010) Resistance to imatinib: mutations and beyond. *Seminars in hematology* **47:** 335-343

Li Y, Liu X, Guo X, Liu X, Luo J (2017) DNA methyltransferase 1 mediated aberrant methylation and silencing of SHP-1 gene in chronic myelogenous leukemia cells. *Leukemia research* **58:** 9-13

Li Y, Yang L, Pan Y, Yang J, Shang Y, Luo J (2014) Methylation and decreased expression of SHP-1 are related to disease progression in chronic myelogenous leukemia. *Oncology reports* **31:** 2438-2446

Liedtke M, Pandey P, Kumar S, Kharbanda S, Kufe D (1998) Regulation of Bcr-Abl-induced SAP kinase activity and transformation by the SHPTP1 protein tyrosine phosphatase. *Oncogene* **17:** 1889-1892

Liu S, Sugimoto Y, Sorio C, Tecchio C, Lin YC (2004) Function analysis of estrogenically regulated protein tyrosine phosphatase gamma (PTPgamma) in human breast cancer cell line MCF-7. *Oncogene* **23:** 1256-1262

Mahon FX, Delbrel X, Cony-Makhoul P, Faberes C, Boiron JM, Barthe C, Bilhou-Nabera C, Pigneux A, Marit G, Reiffers J (2002) Follow-up of complete cytogenetic remission in patients with chronic myeloid leukemia after cessation of interferon alfa. *Journal of clinical oncology : official journal of the American Society of Clinical Oncology* **20:** 214-220

Mahon FX, Rea D, Guilhot J, Guilhot F, Huguet F, Nicolini F, Legros L, Charbonnier A, Guerci A, Varet B, Etienne G, Reiffers J, Rousselot P, Intergroupe Francais des Leucemies Myeloides C (2010) Discontinuation of imatinib in patients with chronic myeloid leukaemia who have maintained complete molecular remission for at least 2 years: the prospective, multicentre Stop Imatinib (STIM) trial. *The Lancet Oncology* **11:** 1029-1035

Majeti R, Xu Z, Parslow TG, Olson JL, Daikh DI, Killeen N, Weiss A (2000) An inactivating point mutation in the inhibitory wedge of CD45 causes lymphoproliferation and autoimmunity. *Cell* **103:** 1059-1070

McNeill L, Salmond RJ, Cooper JC, Carret CK, Cassady-Cain RL, Roche-Molina M, Tandon P, Holmes N, Alexander DR (2007) The differential regulation of Lck kinase phosphorylation sites by CD45 is critical for T cell receptor signaling responses. *Immunity* **27:** 425-437

Mitra A, Sasikumar K, Parthasaradhi BV, Radha V (2013) The tyrosine phosphatase TC48 interacts with and inactivates the oncogenic fusion protein BCR-Abl but not cellular Abl. *Biochimica et biophysica acta* **1832:** 275-284

Naldini L, Stacchini A, Cirillo DM, Aglietta M, Gavosto F, Comoglio PM (1986) Phosphotyrosine antibodies identify the p210c-abl tyrosine kinase and proteins

phosphorylated on tyrosine in human chronic myelogenous leukemia cells. *Molecular and Cellular Biology* **6:** 1803-1811

Nowell PC, Hungerford DA (1960a) Chromosome studies on normal and leukemic human leukocytes. *Journal of the National Cancer Institute* **25:** 85-109

Nowell PC, Hungerford DA (1960b) A minute chromosome in human chronic granulocytic leukemia. *Science* **132:** 1488-1501

Oka T, Ouchida M, Koyama M, Ogama Y, Takada S, Nakatani Y, Tanaka T, Yoshino T, Hayashi K, Ohara N, Kondo E, Takahashi K, Tsuchiyama J, Tanimoto M, Shimizu K, Akagi T (2002) Gene silencing of the tyrosine phosphatase SHP1 gene by aberrant methylation in leukemias/lymphomas. *Cancer research* **62:** 6390-6394

Okutani Y, Kitanaka A, Tanaka T, Kamano H, Ohnishi H, Kubota Y, Ishida T, Takahara J (2001) Src directly tyrosine-phosphorylates STAT5 on its activation site and is involved in erythropoietin-induced signaling pathway. *Oncogene* **20:** 6643-6650

Ostman A, Frijhoff J, Sandin A, Bohmer FD (2011) Regulation of protein tyrosine phosphatases by reversible oxidation. *Journal of Biochemistry* **150:** 345-356

Ostman A, Hellberg C, Bohmer FD (2006) Protein-tyrosine phosphatases and cancer. *Nature Reviews Cancer* **6:** 307-320

Papadopoulou V, Kontandreopoulou E, Panayiotidis P, Roumelioti M, Angelopoulou M, Kyriazopoulou L, Diamantopoulos PT, Vaiopoulos G, Variami E, Kotsianidis I, Athina Viniou N (2016) Expression, prognostic significance and mutational analysis of protein tyrosine phosphatase SHP-1 in chronic myeloid leukemia. *Leukemia & lymphoma* **57:** 1182-1188

Perron MD, Chowdhury S, Aubry I, Purisima E, Tremblay ML, Saragovi HU (2014) Allosteric noncompetitive small molecule selective inhibitors of CD45 tyrosine phosphatase suppress T-cell receptor signals and inflammation in vivo. *Molecular pharmacology* **85:** 553-563

Pfirrmann M, Baccarani M, Saussele S, Guilhot J, Cervantes F, Ossenkoppele G, Hoffmann VS, Castagnetti F, Hasford J, Hehlmann R, Simonsson B (2016) Prognosis of long-term survival considering disease-specific death in patients with chronic myeloid leukemia. *Leukemia* **30:** 48-56

Poole AW, Jones ML (2005) A SHPing tale: perspectives on the regulation of SHP-1 and SHP-2 tyrosine phosphatases by the C-terminal tail. *Cellular signalling* **17:** 1323-1332

Porcu M, Kleppe M, Gianfelici V, Geerdens E, De Keersmaecker K, Tartaglia M, Foa R, Soulier J, Cauwelier B, Uyttebroeck A, Macintyre E, Vandenberghe P, Asnafi V, Cools J (2012) Mutation of the receptor tyrosine phosphatase PTPRC (CD45) in T-cell acute lymphoblastic leukemia. *Blood* **119:** 4476-4479

Ptasznik A, Nakata Y, Kalota A, Emerson SG, Gewirtz AM (2004) Short interfering RNA (siRNA) targeting the Lyn kinase induces apoptosis in primary, and drug-resistant, BCR-ABL1(+) leukemia cells. *Nature Medicine* **10:** 1187-1189

Reckel S, Gehin C, Tardivon D, Georgeon S, Kukenshoner T, Lohr F, Koide A, Buchner L, Panjkovich A, Reynaud A, Pinho S, Gerig B, Svergun D, Pojer F, Guntert P, Dotsch V, Koide S, Gavin AC, Hantschel O (2017) Structural and functional dissection of the DH and PH domains of oncogenic Bcr-Abl tyrosine kinase. *Nature communications* **8:** 2101

Rhee I, Veillette A (2012) Protein tyrosine phosphatases in lymphocyte activation and autoimmunity. *Nature immunology* **13:** 439-447

Rizzo D, Lotay A, Gachard N, Marfak I, Faucher JL, Trimoreau F, Guerin E, Bordessoule D, Jaccard A, Feuillard J (2013) Very low levels of surface CD45 reflect CLL cell fragility, are inversely correlated with trisomy 12 and are associated with increased treatment-free survival. *American journal of hematology* **88:** 747-753

Rowley JD (1973) Letter: A new consistent chromosomal abnormality in chronic myelogenous leukaemia identified by quinacrine fluorescence and Giemsa staining. *Nature* **243:** 290-293

Roy A, Banerjee S (2015) p27 and leukemia: cell cycle and beyond. *Journal of cellular physiology* **230:** 504-509

Saint-Paul L, Nguyen CH, Buffiere A, Pais de Barros JP, Hammann A, Landras-Guetta C, Filomenko R, Chretien ML, Johnson P, Bastie JN, Delva L, Quere R (2016) CD45 phosphatase is crucial for human and murine acute myeloid leukemia maintenance through its localization in lipid rafts. *Oncotarget* **7:** 64785-64797

Sanjana NE, Shalem O, Zhang F (2014) Improved vectors and genome-wide libraries for CRISPR screening. *Nature methods* **11:** 783-784

Schmidt S, Wolf D (2009) Role of gene-expression profiling in chronic myeloid leukemia. *Expert review of hematology* **2:** 93-103

Shimizu T, Miyakawa Y, Iwata S, Kuribara A, Tiganis T, Morimoto C, Ikeda Y, Kizaki M (2004) A novel mechanism for imatinib mesylate (STI571) resistance in CML cell line KT-1: role of TC-PTP in modulating signals downstream from the BCR-ABL fusion protein. *Experimental Hematology* **32:** 1057-1063

Shu ST, Sugimoto Y, Liu S, Chang HL, Ye W, Wang LS, Huang YW, Yan P, Lin YC (2010) Function and regulatory mechanisms of the candidate tumor suppressor receptor protein tyrosine phosphatase gamma (PTPRG) in breast cancer cells. *Anticancer research* **30:** 1937-1946

Sokal JE, Cox EB, Baccarani M, Tura S, Gomez GA, Robertson JE, Tso CY, Braun TJ, Clarkson BD, Cervantes F, et al. (1984) Prognostic discrimination in "good-risk" chronic granulocytic leukemia. *Blood* **63:** 789-799

Spertini F, Perret-Menoud V, Barbier N, Chatila T, Barbey C, Corthesy B (2004) Epitope-specific crosslinking of CD45 down-regulates membrane-associated tyrosine phosphatase activity and triggers early signalling events in human activated T cells. *Immunology* **113:** 441-452

Stevenson WS, Best OG, Przybylla A, Chen Q, Singh N, Koleth M, Pierce S, Kennedy T, Tong W, Kuang SQ, Garcia-Manero G (2014) DNA methylation of membrane-bound tyrosine phosphatase genes in acute lymphoblastic leukaemia. *Leukemia* **28:** 787-793

Stoker A (2016) RPTPs and Cancer. In *Protein Tyrosine Phosphatases in Cancer*, Neel BG, Tonks NK (eds). Springer Science+Business Media

Tauchi T, Ohyashiki K, Yamashita Y, Sugimoto S, Toyama K (1997) SH2-containing phosphotyrosine phosphatase SHP-1 is involved in BCR-ABL signal transduction pathways. *International journal of oncology* **11:** 471-475

Tchilian EZ, Wallace DL, Wells RS, Flower DR, Morgan G, Beverley PC (2001) A deletion in the gene encoding the CD45 antigen in a patient with SCID. *Journal of immunology* **166:** 1308-1313

Tonks NK (2013) Protein tyrosine phosphatases--from housekeeping enzymes to master regulators of signal transduction. *FEBS Journal* **280:** 346-378

Vezzalini M, Mafficini A, Tomasello L, Lorenzetto E, Moratti E, Fiorini Z, Holyoake TL, Pellicano F, Krampera M, Tecchio C, Yassin M, Al-Dewik N, Ismail MA, Al Sayab A, Monne M, Sorio C (2017) A new monoclonal antibody detects downregulation of protein tyrosine phosphatase receptor type gamma in chronic myeloid leukemia patients. *Journal of hematology & oncology* **10:** 129

Vezzalini M, Mombello A, Menestrina F, Mafficini A, Della Peruta M, van Niekerk C, Barbareschi M, Scarpa A, Sorio C (2007) Expression of transmembrane protein tyrosine phosphatase gamma (PTPgamma) in normal and neoplastic human tissues. *Histopathology* **50:** 615-628

Wang J, Hua L, Guo M, Yang L, Liu X, Li Y, Shang X, Luo J (2017) Notable roles of EZH2 and DNMT1 in epigenetic dormancy of the SHP1 gene during the progression of chronic myeloid leukaemia. *Oncology letters* **13:** 4979-4985

Weisberg E, Manley PW, Cowan-Jacob SW, Hochhaus A, Griffin JD (2007) Second generation inhibitors of BCR-ABL for the treatment of imatinib-resistant chronic myeloid leukaemia. *Nature Reviews Cancer* **7:** 345-356

Wylie AA, Schoepfer J, Jahnke W, Cowan-Jacob SW, Loo A, Furet P, Marzinzik AL, Pelle X, Donovan J, Zhu W, Buonamici S, Hassan AQ, Lombardo F, Iyer V, Palmer M, Berellini G, Dodd S, Thohan S, Bitter H, Branford S, Ross DM, Hughes TP, Petruzzelli L, Vanasse KG, Warmuth M, Hofmann F, Keen NJ,

Sellers WR (2017) The allosteric inhibitor ABL001 enables dual targeting of BCR-ABL1. *Nature* **543:** 733-737

Xiao J, Lee ST, Xiao Y, Ma X, Houseman EA, Hsu LI, Roy R, Wrensch M, de Smith AJ, Chokkalingam A, Buffler P, Wiencke JK, Wiemels JL (2014) PTPRG inhibition by DNA methylation and cooperation with RAS gene activation in childhood acute lymphoblastic leukemia. *International journal of cancer* **135:** 1101-1109

Zhang F, Wen Y, Guo X (2014) CRISPR/Cas9 for genome editing: progress, implications and challenges. *Human molecular genetics* **23:** R40-46

8 Abkürzungsverzeichnis

ABL1	Abelson Murine Leukemia Viral Oncogene Homolog 1
AKT	v-akt murine thymoma viral oncogene homolog, identical to PKB
ALL	acute lymphoblastic leukemia
AML	acute myeloid leukemia
AP	accelerated phase
BC	blast crisis
Bcl-2	B-cell lymphoma 2
BCR	breakpoint cluster region
BCR-ABL1	oncogenic fusion protein of BCR and ABL1
CA domain	carbonic anhydrase-like domain
CCyR	complete cytogenetic remission
CLL	chronic lymphocytic leukemia
CML	chronic myeloid leukemia
CP	chronic phase
CRISPR/Cas	clustered regularly interspaced short palindromic repeats/CRISPR-associated protein
crRNA	CRISPR RNA
CS	mutation of the catalytically active cysteine to serine
Csk	C-terminal SRC kinase
cSRC	cellular homologue to v-src expressed by Rous **S**a**rc**oma virus
DSB	double-strand DNA break
dsRNA	double-stranded RNA
e. g.	*exempli gratia*, for example
ELN	European LeukemiaNET
ERK	extracellular signal-regulated kinase
et al.	*et alii*, and others
FCS	fetal calf serum
FDA	US Food and Drug Administration
FISH	fluorescence in situ hybridization
FLT3-ITD	Fms-like tyrosine kinase 3 with internal tandem duplication
FN domain	fibronectin-like domain
gRNA	guide RNA
HDR	homology-directed repair
HIV	human immunodeficiency virus
HSC	hematopoietic stem cell
HU	hydroxyurea
IC_{50}	half-maximal inhibitory concentration
IFN-α	interferon-α
IQR	interquartile range
IS	international scale
Jak2	Janus kinase 2
KO	knockout
Lck	lymphocyte-specific protein tyrosine kinase, p56Lck, a SFK
LSC	leukemic stem cell

Lyn	Lck/Yes related novel tyrosine kinase, a SFK
MEK	MAP- and ERK kinase
MR^4	deep molecular response with a $BCR\text{-}ABL1^{IS} \leq 0.01$ %
mRNA	messenger RNA
NHEJ	Non-homologous end-joining
P/S	penicillin/streptomycin
p27	CDKN1B, cyclin-dependent kinase inhibitor 1B, also $p27^{Kip1}$
p56	identical to the SFK Lck
PCR	Polymerase-chain reaction
PEG-IFN-2αb	pegylated interferon α2b
PI3K	phosphatidylinositol-3-kinase
PKB	protein kinase B, identical to AKT
PTK	protein-tyrosine kinase
PTP	protein-tyrosine phosphatase
pY	phospho-tyrosine
RISC	RNAi –induced silencing complex
RNAi	RNA interference
ROS	reactive-oxygen-species
RPTP	receptor-like protein-tyrosine phosphatase
RT-qPCR	reverse transcription- quantitative PCR
SCID	severe combined immunodeficiency
SFK	SRC-family kinases
SFM	serum-free medium
SH2 domain	SRC homology 2 domain
shRNA	small hairpin RNA
siRNA	small interfering RNA
TFR	treatment-free remission
TKI	tyrosine-kinase inhibitor
WT	wild type

9 Wissenschaftliche Publikationen

PTPRG and PTPRC modulate nilotinib response in chronic myeloid leukemia cells
J. Drube, T. Ernst, M. Pfirrmann, B. V. Albert, S. Drube, D. Reich, A. Kresinsky, K. Halfter, C. Sorio, C. Fabisch, A. Hochhaus, and F.-D. Böhmer, *Oncotarget*, 2018,
DOI: 10.18632/oncotarget.24253

The Neurobeachin-Like 2 Protein Regulates Mast Cell Homeostasis
S. Drube, R. Grimlowski, C. Deppermann, J. Frobel, F. Kraft, N. Andreas, D. Stegner, J. Dudeck, F. Weber, M. Rodiger, C. Gopfert, J. Drube, D. Reich, B. Nieswandt, A. Dudeck, and T. Kamradt, *Journal of Immunology*, 199 (2017), 2948-2957.

Protein-Tyrosine Phosphatase Dep-1 Controls Receptor Tyrosine Kinase Flt3 Signaling
D. Arora, S. Stopp, S. A. Böhmer, J. Schons, R. Godfrey, K. Masson, E. Razumovskaya, L. Ronnstrand, S. Tanzer, R. Bauer, F. D. Böhmer, and J. P. Müller, *Journal of Biological Chemistry*, 286 (2011), 10918-29.

The Receptor Tyrosine Kinase C-Kit Controls IL-33 Receptor Signaling in Mast Cells
S. Drube, S. Heink, S. Walter, T. Lohn, M. Grusser, A. Gerbaulet, L. Berod, J. Schons, A. Dudeck, J. Freitag, S. Grotha, D. Reich, O. Rudeschko, J. Norgauer, K. Hartmann, A. Roers, and T. Kamradt, *Blood*, 115 (2010), 3899-906.

Vorträge

Protein-tyrosine phosphatase expression analysis in chronic myeloid leukemia (CML)-patient samples and cell lines
6th POSTGRADUATE SYMPOSIUM on Cancer Research, April 2014, Dornburg, Deutschland

Das Phosphorylierungsmuster von FLT3, einer AML-assoziierten Tyrosinkinase
5. Tag der Nachwuchswissenschaftler des FZL, Juni 2008, Jena, Deutschland*
* Auszeichnung: 1. Vortragspreis

Poster

Protein Tyrosin Phosphatasen modulieren das Therapieansprechen in CML Zellen
Protein-tyrosine phosphatases modulate therapy response in CML cells
J. Drube, B. V. Albert, M. Pfirrmann, T. Ernst, A. Hochhaus, and F.-D. Böhmer
Jahrestagung der Deutschen, Österreichischen und Schweizerischen Gesellschaften für Hämatologie und Medizinische Onkologie (DGHO), Oktober 2016, Leipzig, Deutschland

Protein-tyrosine phosphatase expression and therapy response in CML cells
J. Drube, T. Ernst, A. Hochhaus, and F.-D. Böhmer
Signal Transduction Society (STS), 19th Joint Meeting Signal Transduction, Receptors, Mediators and Genes, November 2015, Weimar, Deutschland

Protein-tyrosine phosphatase expression and therapy response in CML cells
J. Drube, B. V. Albert, T. Ernst, A. Hochhaus, and F.-D. Böhmer
7th POSTGRADUATE SYMPOSIUM on Cancer Research, April 2015, Dornburg, Deutschland

Influence of PTP1B, SHP-1, and SHP-2 on the phosphorylation pattern of FLT3
J. Schons, J. P. Müller, E. Razumovskaya, K. Masson, L. Rönnstrand, C. Stocking , F.-D. Böhmer
Tyrosine Kinase Signaling meeting, “Tyrosine kinases in tumorigenesis”, Ludwig Institute for Cancer Research, August 2008, Uppsala, Schweden

10 Ehrenwörtliche Erklärung

Hiermit versichere ich,

(1) dass mir die Promotionsordnung der Fakultät für Biowissenschaften bekannt ist,

(2) dass ich die vorliegende Dissertation selbständig angefertigt habe, und alle verwendeten Quellen, Hilfsmittel und persönlichen Informationen als solche gekennzeichnet habe,

(3) dass mich Prof. Dr. Frank-D. Böhmer bei der Auswahl und Anfertigung des Materials sowie Manuskriptes unterstützt hat,

(4) dass ich weder die Hilfe eines Promotionsberaters in Anspruch genommen habe, noch andere Personen unmittelbare oder mittelbare geldwerte Leistungen von mir erhalten haben, die im Zusammenhang mit dem Inhalt der vorgelegten Dissertation stehen,

(5) dass ich die Dissertation noch nicht als Prüfungsarbeit für eine staatliche oder andere wissenschaftliche Prüfung eingereicht habe

(6) dass ich zu keinem Zeitpunkt die gleiche, eine in wesentlichen Teilen ähnliche oder eine andere Abhandlung als Dissertation an einer anderen Hochschule eingereicht habe.

Jena, 30.01.2018

_____

Julia Drube